ADAPTATION AND DEVELOPMENT OF NCHRP 350 TL-2 LOW-PROFILE, CONCRETE BRIDGE RAILING SYSTEM FOR AASHTO MASH TL-1 CONCRETE BRIDGE DECKS

Submitted by

Russell Masterson, B.S.C.E.
Graduate Research Assistant

Ronald Faller, Ph.D., P.E.
Research Professor & MwRSF Director

Joshua Steelman, Ph.D., P.E
Associate Professor

Scott Rosenbaugh, M.S.C.E.
Research Engineer

Robert Bielenberg, M.S.M.E.
Research Engineer

Tewodros Yosef, Ph.D.
Post-Doctoral Research Associate

MIDWEST ROADSIDE SAFETY FACILITY
Nebraska Transportation Center
University of Nebraska-Lincoln

Main Office
Prem S. Paul Research Center at Whittier School
Room 130, 2200 Vine Street
Lincoln, Nebraska 68583-0853
(402)472-0965

Outdoor Test Site
4630 N.W. 36th Street
Lincoln, Nebraska 68524

Submitted to

United States Department of Agriculture – Forest Service
National Technology and Development Program
5785 Hwy 10 West
Missoula, Montana 59808

MwRSF Research Report No. TRP-03-470-23

July 12, 2023

TECHNICAL REPORT DOCUMENTATION PAGE

1. Report No. TRP-03-470-23	**2. Government Accession No.**	**3. Recipient's Catalog No.**
4. Title and Subtitle Adaptation and Development of NCHRP 350 TL-2 Low-Profile, Concrete Bridge Railing System for AASHTO MASH TL-1 Concrete Bridge Decks		**5. Report Date** July 12, 2023 **6. Performing Organization Code**
7. Author(s) Masterson, R.W., Faller, R.K., Steelman, J.S., Rosenbaugh, S.K, Bielenberg, R.W., and Yosef, T.Y.		**8. Performing Organization Report No.** TRP-03-470-23
9. Performing Organization Name and Address Midwest Roadside Safety Facility (MwRSF) Nebraska Transportation Center University of Nebraska-Lincoln Main Office: Prem S. Paul Research Center at Whittier School Room 130, 2200 Vine Street Lincoln, Nebraska 68583-0853 Outdoor Test Site: 4630 N.W. 36th Street Lincoln, Nebraska 68524		**10. Work Unit No.** **11. Contract** 12318720C0009 WBS or UNL # 25-1113-0012-010
12. Sponsoring Agency Name and Address United States Department of Agriculture – Forest Service National Technology and Development Program 5785 Hwy 10 West Missoula, MT 59808		**13. Type of Report and Period Covered** Final Report: 2020 - 2023 **14. Sponsoring Agency Code**

15. Supplementary Notes

Prepared in cooperation with U.S. Department of Transportation, Federal Highway Administration

16. Abstract

In 2002, the Midwest Roadside Safety Facility (MwRSF), in partnership with the Midwest Pooled Fund Program (MPFP), developed, crash tested, and evaluated a low-height, reinforced concrete bridge railing to meet the TL-2 impact safety standards published in the National Cooperative Highway Research Program (NCHRP) Report No. 350. The 20-in. tall bridge railing was configured with a top width of 14 in. and base width of 11 in., which resulted in a crashworthy system. The low-height, concrete bridge railing system was also configured with a sloped end treatment.

More recently, the United States Department of Agriculture - Forest Service – National Technology and Development Program expressed interest in adapting the NCHRP Report No. 350 TL-2 bridge railing for use on reinforced concrete bridge decks where it would be deemed crashworthy according to the American Association of State Highway and Transportation Officials (AASHTO) *Manual for Assessing Safety Hardware* (MASH) TL-1 impact safety standards.

The modification process involved determining the capacity of the NCHRP Report No. 350 TL-2 bridge railing using yield-line and punching shear analytical methods published in the AASHTO *Load Resistance Factored Design (LRFD) Bridge Design Specifications*. Appropriate modifications were incorporated into the bridge railing, which included changes in width and steel reinforcement to ensure that it would withstand MASH TL-1 impacts scenarios but provide MASH TL-2 structural capacity. A literature review was conducted to obtain common design parameters for bridge deck overhangs, and different combinations of overhangs were evaluated for compatibility with the modified bridge railing system using three design cases corresponding to extreme limit state and strength limit state load combinations. Based on this analysis and design effort, a recommended bridge railing configuration was provided along with example designs for the transverse steel reinforcement used within bridge deck overhangs ranging from 6 to 10 in. thick.

17. Key Words USDA-FS, NDTP, Bridge Rail, MASH 2016, Crashworthy, AASHTO, Yield-Line, Punching Shear, Redirective Capacity, Bridge Deck		**18. Distribution Statement** No restrictions. This document is available through the National Technical Information Service. 5285 Port Royal Road Springfield, VA 22161	
19. Security Classification (of this report) Unclassified	**20. Security Classification (of this page)** Unclassified	**21. No. of Pages** 80	**22. Price**

Form DOT F 1700.7 (8-72) Reproduction of completed page authorized

DISCLAIMER STATEMENT

The contents of this report reflect the views and opinions of the authors who are responsible for the facts and the accuracy of the data presented herein. The contents do not necessarily reflect the official views or policies of the United States Department of Agriculture – Forest Service (USDA-FS) and National Technology and Development Program (NTDP). This report does not constitute a standard, specification, or regulation. Trade or manufacturers' names, which may appear in this report, are cited only because they are considered essential to the objectives of the report. The United States (U.S.) government and the USDA-FS and NTDP do not endorse products or manufacturers.

ACKNOWLEDGEMENTS

The authors wish to acknowledge the USDA-FS and MTDD for sponsoring this project. Acknowledgement is also given to the following individuals who contributed to the completion of this research project.

Midwest Roadside Safety Facility
J.C. Holloway, M.S.C.E., Research Engineer & Assistant Director –Physical Testing Division
K.A. Lechtenberg, M.S.M.E., Research Engineer
C.S. Stolle, Ph.D., Research Assistant Professor
M. Asadollahi Pajouh, Ph.D., P.E., Research Assistant Professor
B.J. Perry, M.E.M.E., Research Associate Engineer
A.T. Russell, B.S.B.A., Testing and Maintenance Technician II
E.W. Krier, B.S., Former Engineering Testing Technician II
D.S. Charroin, Engineering Testing Technician II
R.M. Novak, Engineering Testing Technician II
S.M. Tighe, Engineering Testing Technician I
T.C. Donahoo, Engineering Testing Technician I
J.T. Jones, Engineering Testing Technician I
C. Charroin, Temporary Engineering Construction Testing Technician I
T. Shapland, Temporary Engineering Construction Testing Technician I
E.L. Urbank, B.A., Research Communication Specialist
Z.Z. Jabr, Engineering Technician
J. Oliver, Solidworks Drafting Coordinator
Undergraduate and Graduate Research Assistants

USDA-FS and National Technology and Development Program (NTDP)
Josh Connors, P.E, Supervisory Program Manager
Jacob Ormes, P.E., Assistant National Bridge Program Manager
Barrett McMurtry, National Bridge Program Manager
Christopher Murphy, Engineer, Acting FAM-NRM Group Leader and Project Manager
Marlee Okeefe, Contract Specialist
Matthew Cox, Contract Specialist

SI* (MODERN METRIC) CONVERSION FACTORS

APPROXIMATE CONVERSIONS TO SI UNITS

Symbol	When You Know	Multiply By	To Find	Symbol
		LENGTH		
in.	inches	25.4	millimeters	mm
ft	feet	0.305	meters	m
yd	yards	0.914	meters	m
mi	miles	1.61	kilometers	km
		AREA		
in^2	square inches	645.2	square millimeters	mm^2
ft^2	square feet	0.093	square meters	m^2
yd^2	square yard	0.836	square meters	m^2
ac	acres	0.405	hectares	ha
mi^2	square miles	2.59	square kilometers	km^2
		VOLUME		
fl oz	fluid ounces	29.57	milliliters	mL
gal	gallons	3.785	liters	L
ft^3	cubic feet	0.028	cubic meters	m^3
yd^3	cubic yards	0.765	cubic meters	m^3
		NOTE: volumes greater than 1,000 L shall be shown in m^3		
		MASS		
oz	ounces	28.35	grams	g
lb	pounds	0.454	kilograms	kg
T	short ton (2,000 lb)	0.907	megagrams (or “metric ton”)	Mg (or "t")
		TEMPERATURE (exact degrees)		
°F	Fahrenheit	5(F-32)/9 or (F-32)/1.8	Celsius	°C
		ILLUMINATION		
fc	foot-candles	10.76	lux	lx
fl	foot-Lamberts	3.426	candela per square meter	cd/m^2
		FORCE & PRESSURE or STRESS		
lbf	poundforce	4.45	newtons	N
lbf/in^2	poundforce per square inch	6.89	kilopascals	kPa

APPROXIMATE CONVERSIONS FROM SI UNITS

Symbol	When You Know	Multiply By	To Find	Symbol
		LENGTH		
mm	millimeters	0.039	inches	in.
m	meters	3.28	feet	ft
m	meters	1.09	yards	yd
km	kilometers	0.621	miles	mi
		AREA		
mm^2	square millimeters	0.0016	square inches	in^2
m^2	square meters	10.764	square feet	ft^2
m^2	square meters	1.195	square yard	yd^2
ha	hectares	2.47	acres	ac
km^2	square kilometers	0.386	square miles	mi^2
		VOLUME		
mL	milliliter	0.034	fluid ounces	fl oz
L	liters	0.264	gallons	gal
m^3	cubic meters	35.314	cubic feet	ft^3
m^3	cubic meters	1.307	cubic yards	yd^3
		MASS		
g	grams	0.035	ounces	oz
kg	kilograms	2.202	pounds	lb
Mg (or "t")	megagrams (or “metric ton”)	1.103	short ton (2,000 lb)	T
		TEMPERATURE (exact degrees)		
°C	Celsius	1.8C+32	Fahrenheit	°F
		ILLUMINATION		
lx	lux	0.0929	foot-candles	fc
cd/m^2	candela per square meter	0.2919	foot-Lamberts	fl
		FORCE & PRESSURE or STRESS		
N	newtons	0.225	poundforce	lbf
kPa	kilopascals	0.145	poundforce per square inch	lbf/in^2

*SI is the symbol for the International System of Units. Appropriate rounding should be made to comply with Section 4 of ASTM E380.

TABLE OF CONTENTS

LIST OF FIGURES

LIST OF TABLES

1 INTRODUCTION

1.1 Background

In 2002, the Midwest Roadside Safety Facility (MwRSF), in partnership with the Midwest Pooled Fund Program (MPFP), developed, crash tested, and evaluated a low-height, reinforced concrete bridge railing to meet the TL-2 impact safety standards published in the National Cooperative Highway Research Program (NCHRP) Report No. 350 [1-2]. The 20-in. tall bridge railing was configured with a top width of 14 in. and base width of 11 in., which resulted in a crashworthy system. The bridge railing utilized a rectangular shape as the upper beam and a narrow, lower vertical wall to support the beam. Overall, the bridge railing generally appeared to be an upside-down "L" shape with the top section extending forward from the vertical wall, which was intended to reduce wheel climb during impact events. One full-scale vehicle crash test was conducted with a 2000P pickup truck. Basic details of the original MPFP concrete bridge railing system are depicted in Figure 1, while Figure 2 shows the bridge railing system as constructed for the full-scale vehicle crash testing program. Table 1 summarizes the dimensions and material properties used in the bridge railing [2].

The low-height, concrete bridge railing system was also configured with a sloped end treatment. For the end treatment, the 20-in. tall, reinforced-concrete bridge railing was configured to slope downward to the roadway surface using the same vertical slope that was utilized for the TTI sloped concrete end treatment [3-4]. The sloped, reinforced-concrete end treatment was 15 ft long with an upstream height of 4 in. and width of 14 in. Using the noted configuration and geometry, MwRSF researchers deemed it unnecessary to conduct additional crash testing on the sloped concrete end treatment beyond that testing already conducted by TTI researchers [3-4].

More recently, the United States Department of Agriculture - Forest Service – National Technology and Development Program expressed interest in adapting the NCHRP Report No. 350 TL-2 bridge railing for use on reinforced concrete bridge decks where it would be deemed crashworthy according to the American Association of State Highway and Transportation Officials (AASHTO) *Manual for Assessing Safety Hardware* (MASH) TL-1 impact safety standards [5]. For this effort, consideration was given toward reducing the overall footprint, utilizing less material, and lowering the cost of construction, while still maintaining a satisfactory level of roadside safety for motorists using the USDA-FS-NTDP's roadways.

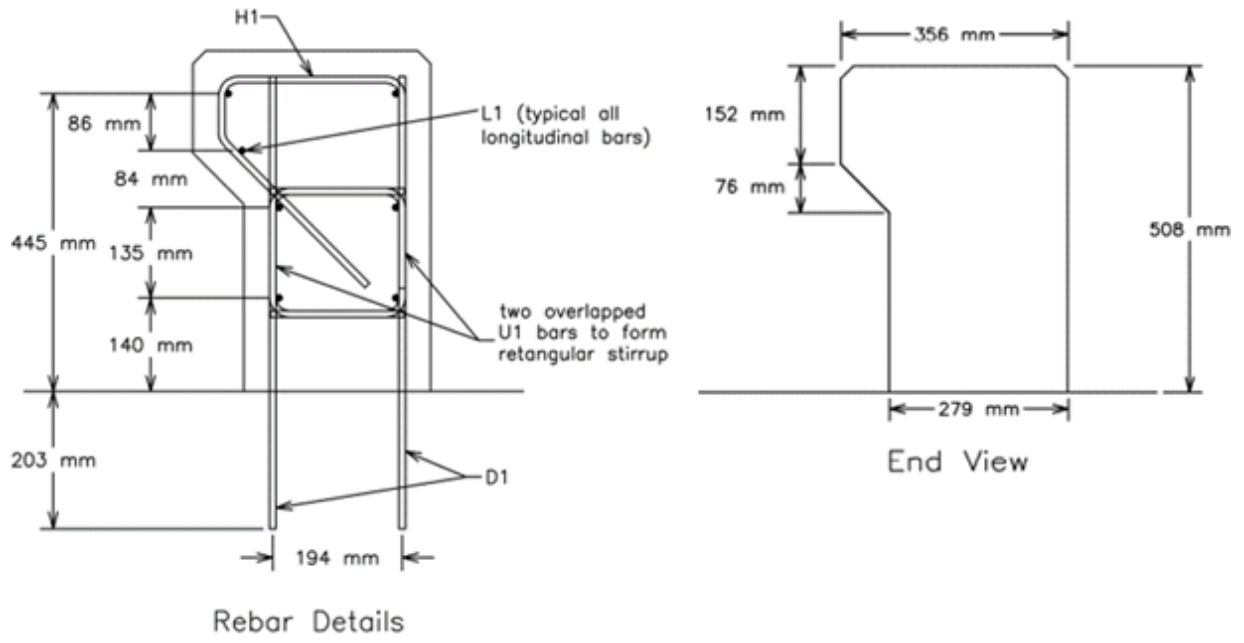

Figure 1. Cross Section Design Drawings of NCHRP Report No. 350 NDOT TL-2 Low-Profile, Concrete Bridge Rail System [2]

Figure 2. Constructed TL-2 Low-Profile, Concrete Bridge Rail System for Full-Scale Crash Testing [2]

Table 1. Dimensions and Material Properties of TL-2 Low-Profile, Concrete Bridge Rail System [2]

Item	Description	Value
Dimensions	Top Width (in.)	14
	Bottom Width (in.)	11
	Overall Height (in.)	20
	Vertical Rebar Spacing (in.)	24
	Concrete Clear Cover (in.)	1.5
	Vertical & Horizontal Rebar Size	3
Material Properties	Steel Yield Strength (ksi)	60
	Specified Concrete Compressive Strength (ksi)	4.5

1.2 Objectives

The objectives of the research project were to: (1) develop the necessary details to adapt the NCHRP Report No. 350 TL-2 low-profile, concrete bridge rail system for use on a typical United States Department of Agriculture - Forest Service – National Technology and Development Program (USDA-FS-NTDP) concrete bridge deck and (2) perform engineering analysis and evaluation of the NCHRP Report No. 350 TL-2 low-profile, concrete bridge railing to confirm its use on a USDA-FS-NTDP concrete bridge decks using the American Association of State Highway and Transportation Officials (AASHTO) *Manual for Assessing Safety Hardware (MASH) 2016* [5] Test Level 1 (TL-1) impact safety standards without component testing or full-scale vehicle crash testing.

1.3 Research Approach

A literature review was conducted to determine prior research pertaining to the development, construction, testing, and evaluation of the NCHRP Report No. 350 TL-2 low-profile, concrete bridge rail as well as to identify typical design configurations utilized when constructing low-volume, concrete bridge deck and rail overhang sections. As a result, a range of bridge deck design details for overhangs were obtained. Next, the low-height, concrete bridge rail in question was analyzed theoretically using the equations outlined in Section 13 of the AASHTO Load Resistance Factored Design (LRFD) Bridge Design Specifications [6] for yield-line and punching shear failure modes at interior and end sections of the barrier.

After determining the strength of the original TL-2 low-profile, bridge railing system, the appropriate modifications were made to provide a design capable of accommodating MASH 2016 TL-1 impact events. The bridge railing's performance was analyzed when mounted to a concrete deck overhang. Using the sample design drawings obtained during the literature review process, design ranges were determined for deck thickness and number of steel mats for a corresponding deck thickness, bar sizing, and spacings in the deck, as well as cantilever overhang length. The deck thicknesses ranged from 6 in. to 10 in., the transverse deck bar sizes ranged between No. 4 and No. 5, and the spacing of the transverse bars varied between 6 in. and 24 in. The deck overhang lengths varied between 1 ft and 5 ft. Because a wide range of possible deck overhangs could be utilized in conjunction with the USDA-FS-NTDP bridge railing, deck designs were developed accounting for Design Cases 1, 2, and 3 in AASHTO LRFD BDS.

2 LITERATURE REVIEW

2.1 Introduction

Historically, limited research has been performed on the development, crash testing, and evaluation of low-profile, concrete bridge railing systems. This section documents the literature that was obtained and deemed noteworthy.

To adapt the original NCHRP Report No. 350 TL-2 concrete bridge railing system for use as a AASHTO MASH TL-1 bridge railing for concrete deck overhangs, a list of commonly-used deck parameters and their practical ranges were investigated. Examples of USDA-FS-NTDP bridge deck overhangs with relevant details were reviewed. From these drawings, details such as the steel reinforcement patterns used in the bridge rail and deck, the overhang length of the bridge deck, the deck thickness, and the clear cover of the bridge deck were obtained. Additional bridge deck details were gathered during the literature review from studies conducted by MwRSF and TTI, as well as bridge deck design provisions outlined in the Nebraska DOT's Bridge Office Policies and Procedures (BOPP) manual [7]. The ranges of typical deck parameters used with bridges found on low-volume roads are tabulated in Table 2.

Table 2. Summary of Deck Parameters [2,7]

Deck Parameter		**Range of Values**
Deck Thickness	Single Steel Mat (in.)	6 - 6.5
	Double Steel Mat (in.)	7 - 10
Transverse Rebar Size		No. 4 and 5 Bars
Transverse Rebar Spacing (in.)		6 – 24
Cantilever Length (ft)		1 - 5

2.2 USDA-FS-NTDP Bridge Deck and Rail Example Drawings

2.2.1 Hellroaring Creek Culvert Replacement Design

The first drawing set provided by USDA-FS-NTDP is shown in Figures 3 and 4. These details depict the bridge deck and rail developed to replace the bridge rail and deck system that spanned Hellroaring Creek [8]. The replacement bridge deck had a uniform thickness of 6 in. and an overhang length of 11¾ in., as measured from the centerline of the exterior-most inverted-T girder to the edge of the deck. The barrier itself was 18 in. tall and had a tapered thickness. The bridge rail was 12 in. thick at the base and 9½ in. thick at the top. The low-height concrete bridge rail was reinforced with six longitudinal No. 4 bars placed into two columns. The No. 4 longitudinal bars were surrounded by No. 4 stirrups placed at a 12-in. spacing along the length of the barrier. The clear cover for the bridge railing was 2 in. To connect the bridge rail to the deck, the vertical steel on the traffic and non-traffic facing side of the barrier was anchored into the deck, utilizing an L-shaped bend, as shown in Figure 4. Details concerning the deck steel were not provided for this USDA-FS-NTDP deck design.

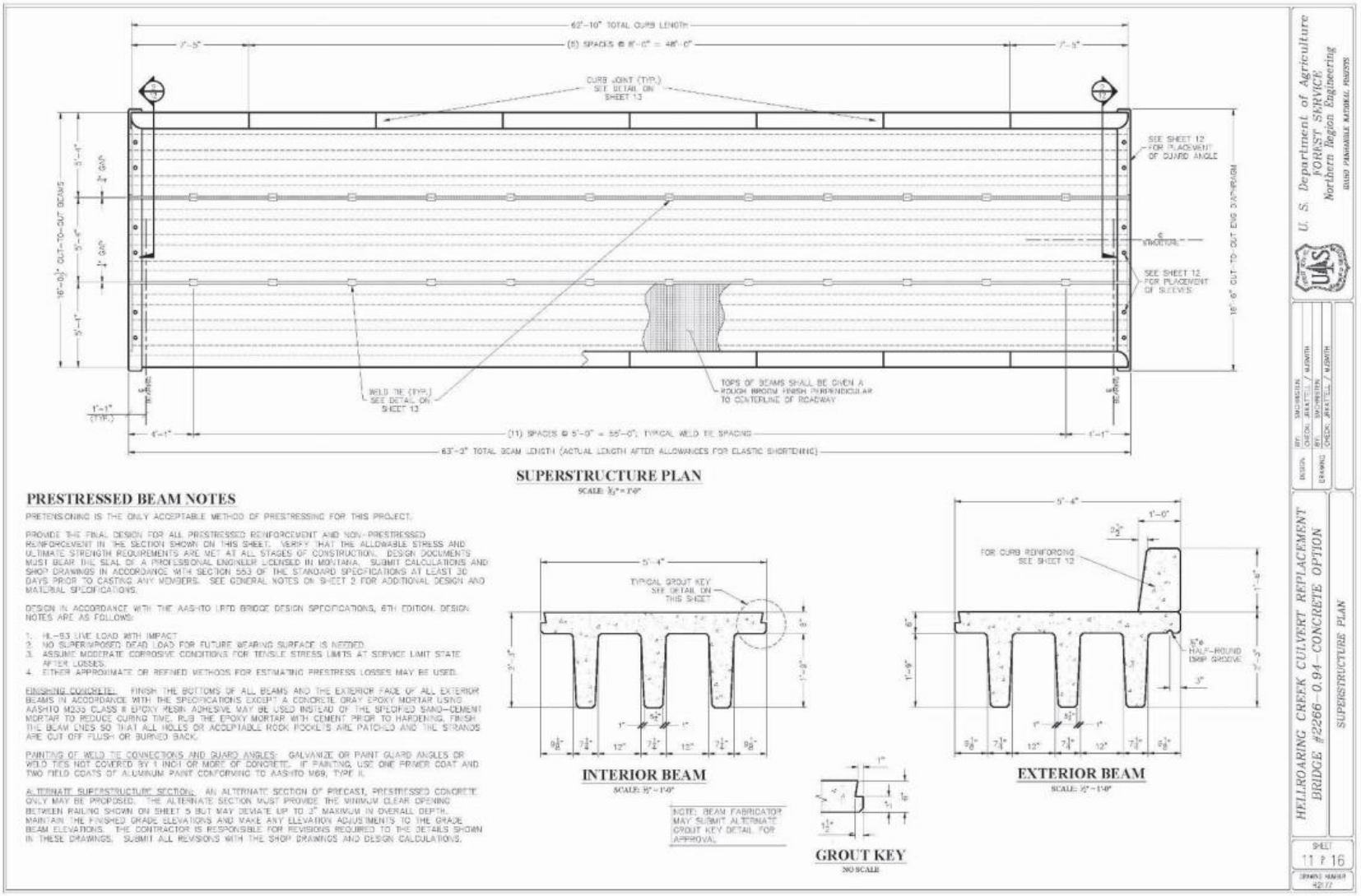

Figure 3. Hellroaring Creek Culvert Replacement Design Plans [8]

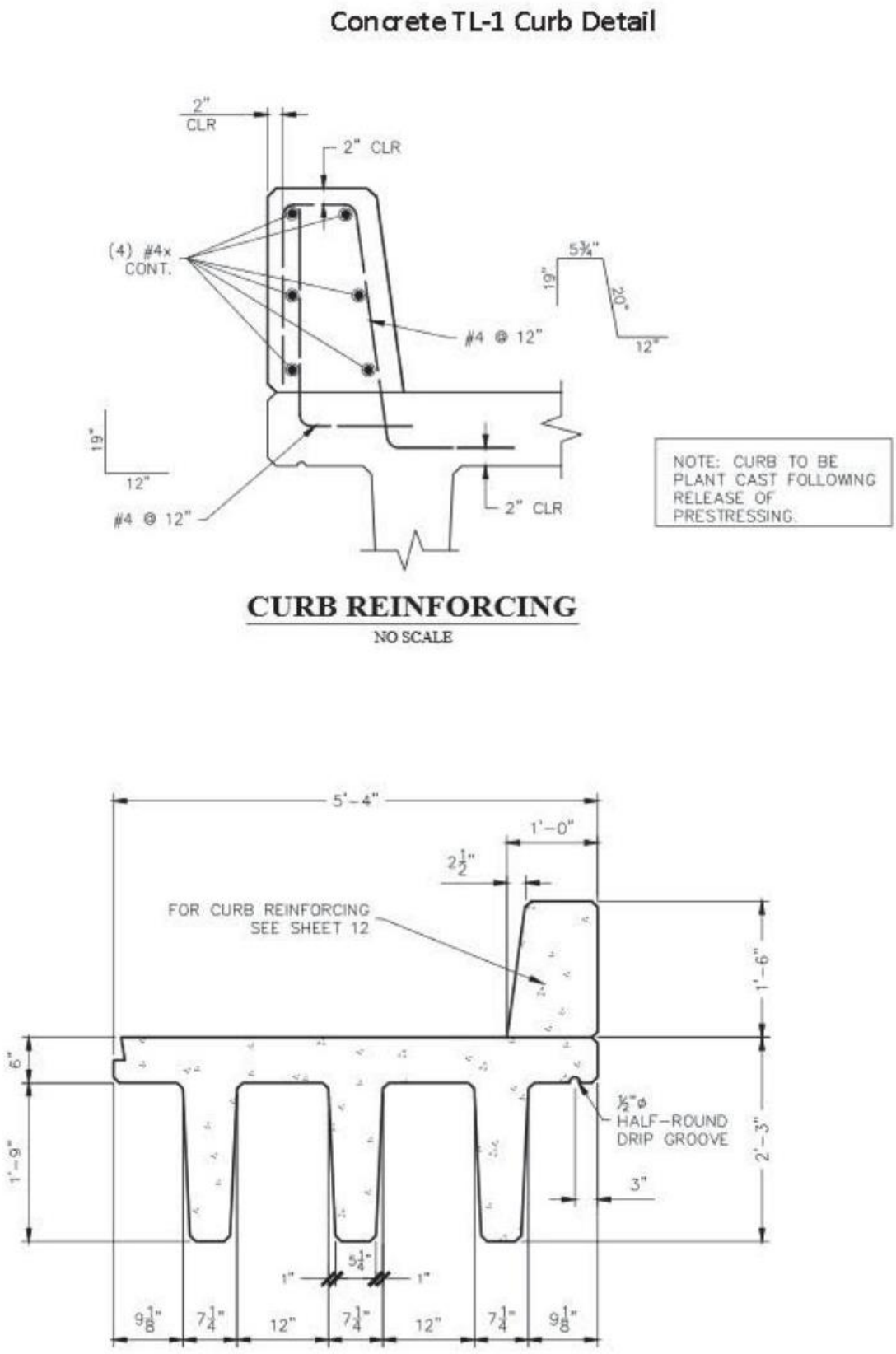

Figure 4. Hellroaring Creek Culvert Replacement Bridge Rail Connection Details [8]

2.2.2 White Mountain National Forest Bridge Deck and Rail System

The USDA-FS-NTDP drawing for a bridge deck constructed for use in the White Mountain National Forest is shown in Figure 5. While the deck was constructed using reinforced concrete, the bridge rail was built using primarily timber material [8]. As the system being examined for this study was to be constructed from reinforced concrete, the timber bridge rail was not considered for design details. The deck's top and bottom clear covers were 2½ in. and 1 in., respectively. Additionally, the deck thickness was 8½ in. at the interior sections and 9 in. at the deck edges. The deck overhang length was 2 ft, as measured from the centerline of the exterior girder to the deck. Lastly, to reinforce the deck, two steel mats were utilized. The top mat was constructed with transverse steel above the longitudinal steel. The transverse steel was located beneath the longitudinal steel in the bottom mat.

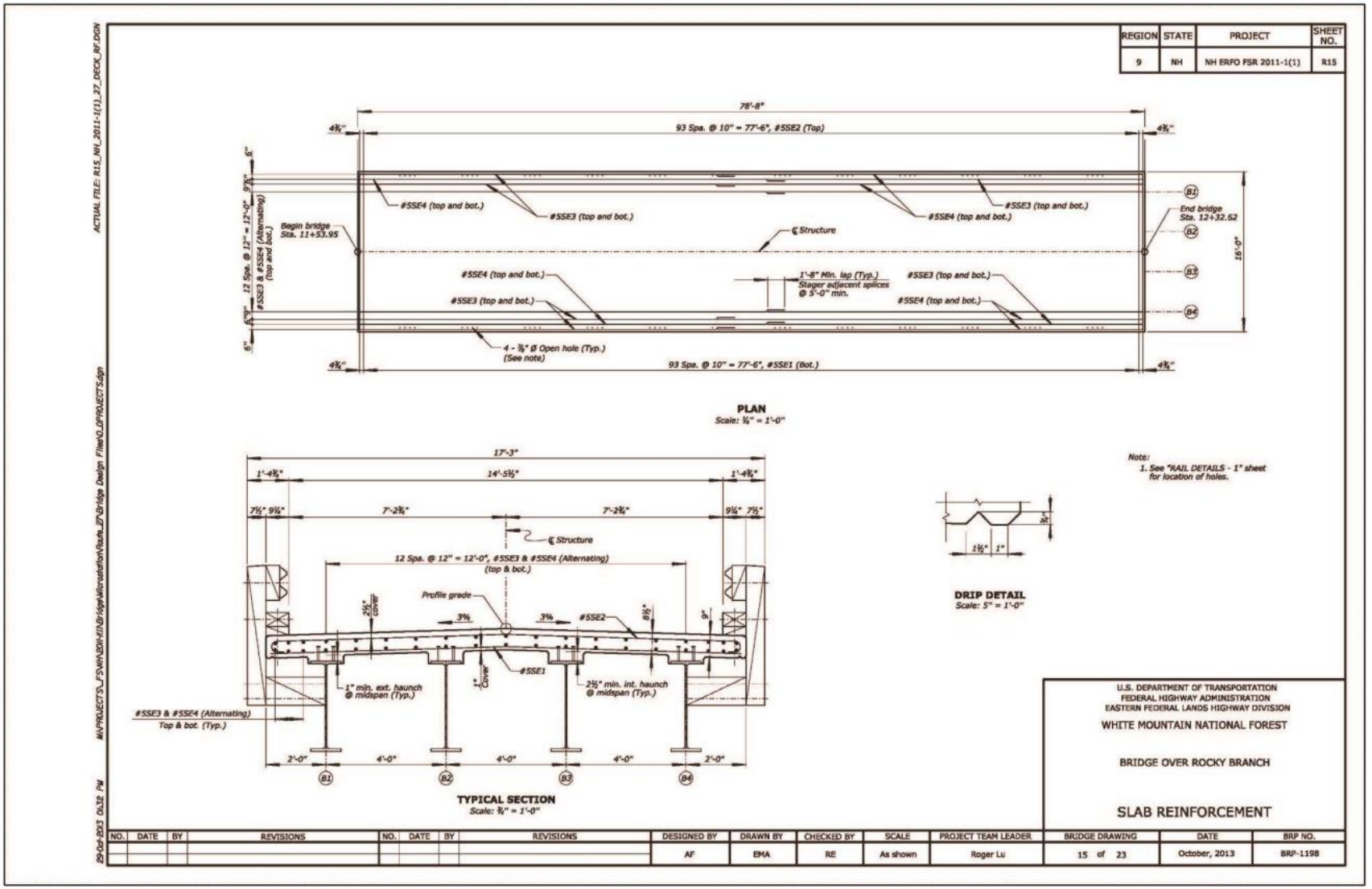

Figure 5. White Mountain National Forest Bridge Deck Design Drawings [8]

2.2.3 Gifford Pinchot National Forest Bridge Deck and Rail System

The final drawing set provided by USDA-FS-NTDP, as shown in Figures 6 and 7, was created to construct the bridge spanning the East Fork Lewis River in Gifford Pinchot National Forest [8]. The bridge had an overhang length of 4 ft and a deck edge thickness of 10 in. While the bar size in the deck was not shown in the drawings, it was observed that two mats were used to reinforce the deck. The top clear cover was 2 in., and the bottom clear cover was 1 in. Next, the bridge rail connected to the deck was reviewed. The guardrail system consisted of a 12-in. tall x 14-in. thick reinforced concrete curb with a clear cover of 1½ in. A steel post mounted to the top of the curb was used to attach the bridge rail. Because the post and railing were not constructed from concrete, only the reinforced concrete curb and its connection details to the deck were further examined. The reinforcement utilized on the non-traffic facing side of the curb was anchored into the deck, but it was not tied to any of the deck's reinforcing steel. The traffic-facing reinforcement from the curb was also anchored into the deck and bent into an L-shape, allowing for 12 in. of lap length to be developed between the reinforcing steel in the curb and the bottom mat of transverse steel in the deck.

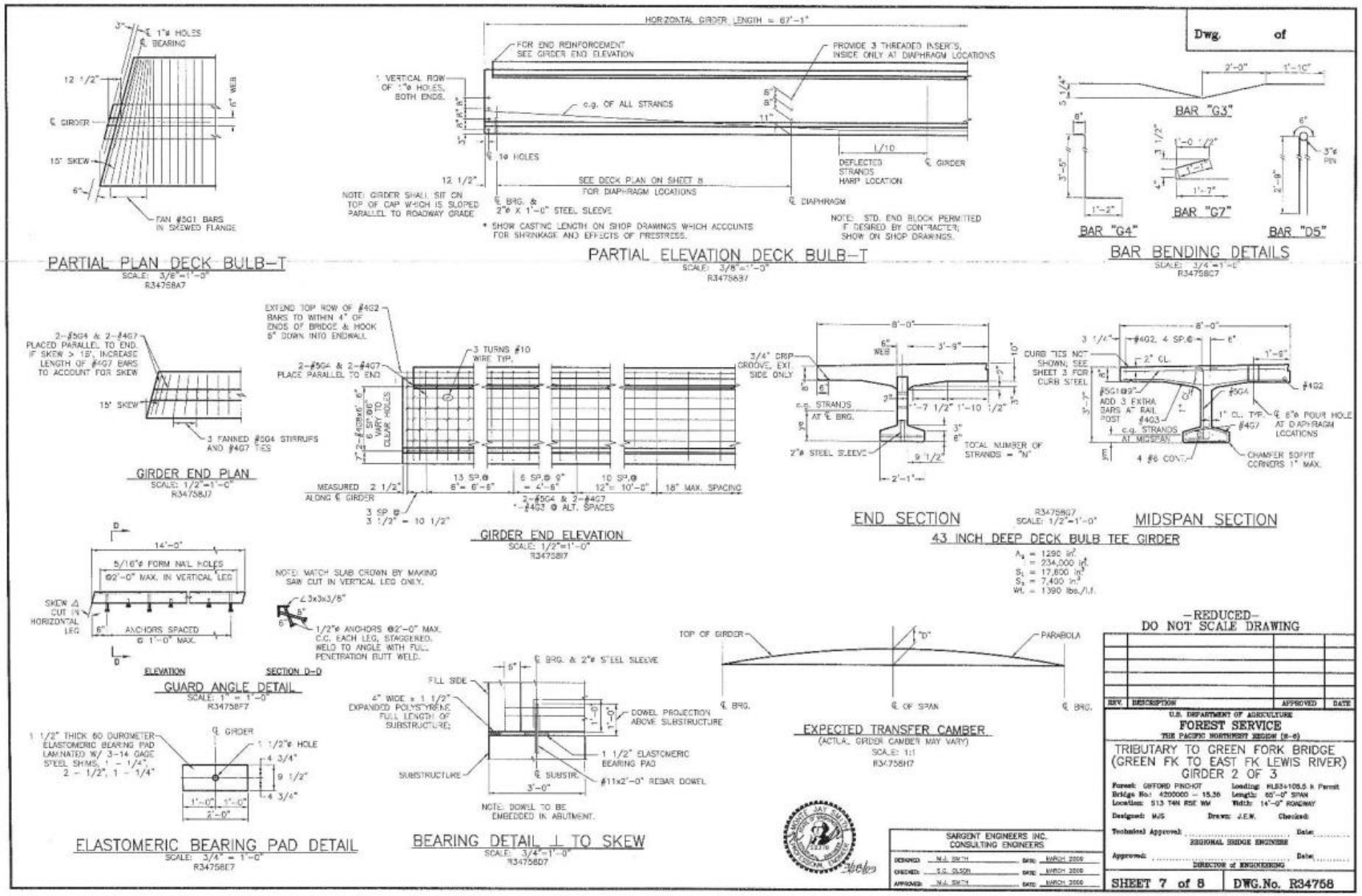

Figure 6. Bridge Deck Design Drawing for Gifford Pinchot National Forest, Girder 1 [8]

July 12, 2023
MwRSF Report No. TRP-03-470-23

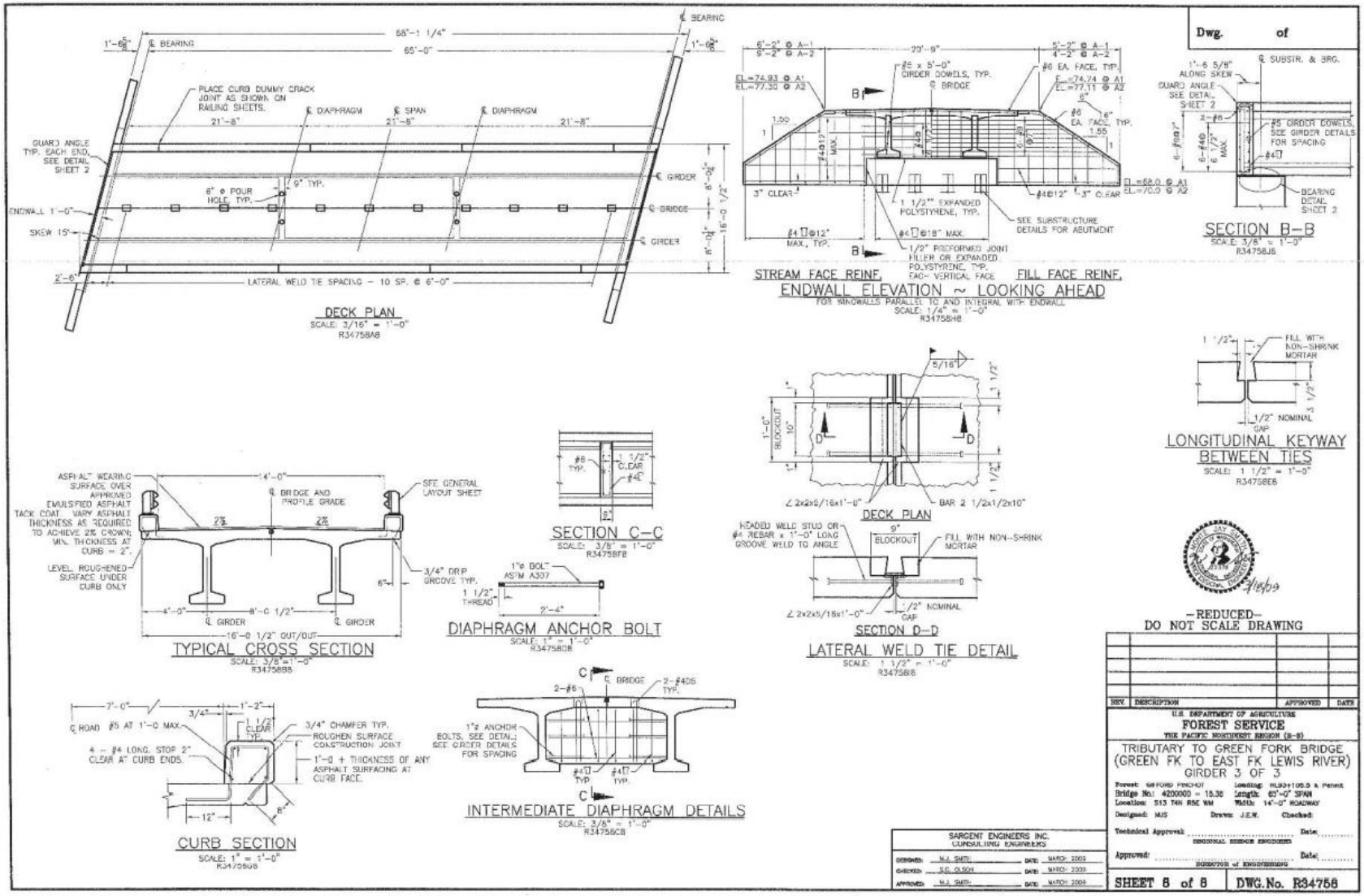

Figure 7. Bridge Deck Design Drawing for Gifford Pinchot National Forest, Girder 2 [8]

2.3 Supplementary Bridge Deck and Rail Example Drawings

2.3.1 NDOT Open Concrete Bridge Rail

This subsection summarizes the bridge deck and rail designs developed by MwRSF. The first MwRSF design to be evaluated was the NDOT Open Concrete Bridge Rail (OCBR) system [9]. The bridge rail had a top beam measuring 14 in. wide by 16 in. deep, with a post width of 11 in. The overall height of the bridge rail was 29 in. To tie the barrier to the deck, four No. 6 bars were used on the traffic facing and four No. 4 bars were used on the non-traffic facing sides of the barrier were bent into L-shaped hooks and were then tied into the transverse reinforcement in the deck. A cross-section view of the bridge deck and rail system is provided in Figure 8 and the bill of bars corresponding to the bridge rail is shown in Figure 9. From the design drawing, it was determined that the NDOT Open Concrete Bridge Rail had a thickness of 6 in. and used a single mat as reinforcement. The cross-sectional design drawing showed that the transverse bars were placed below the longitudinal bars in the deck. By placing the longitudinal steel above the transverse steel, the longitudinal bars could resist any downward prying action of the deck and rail if the bridge rail system fractured.

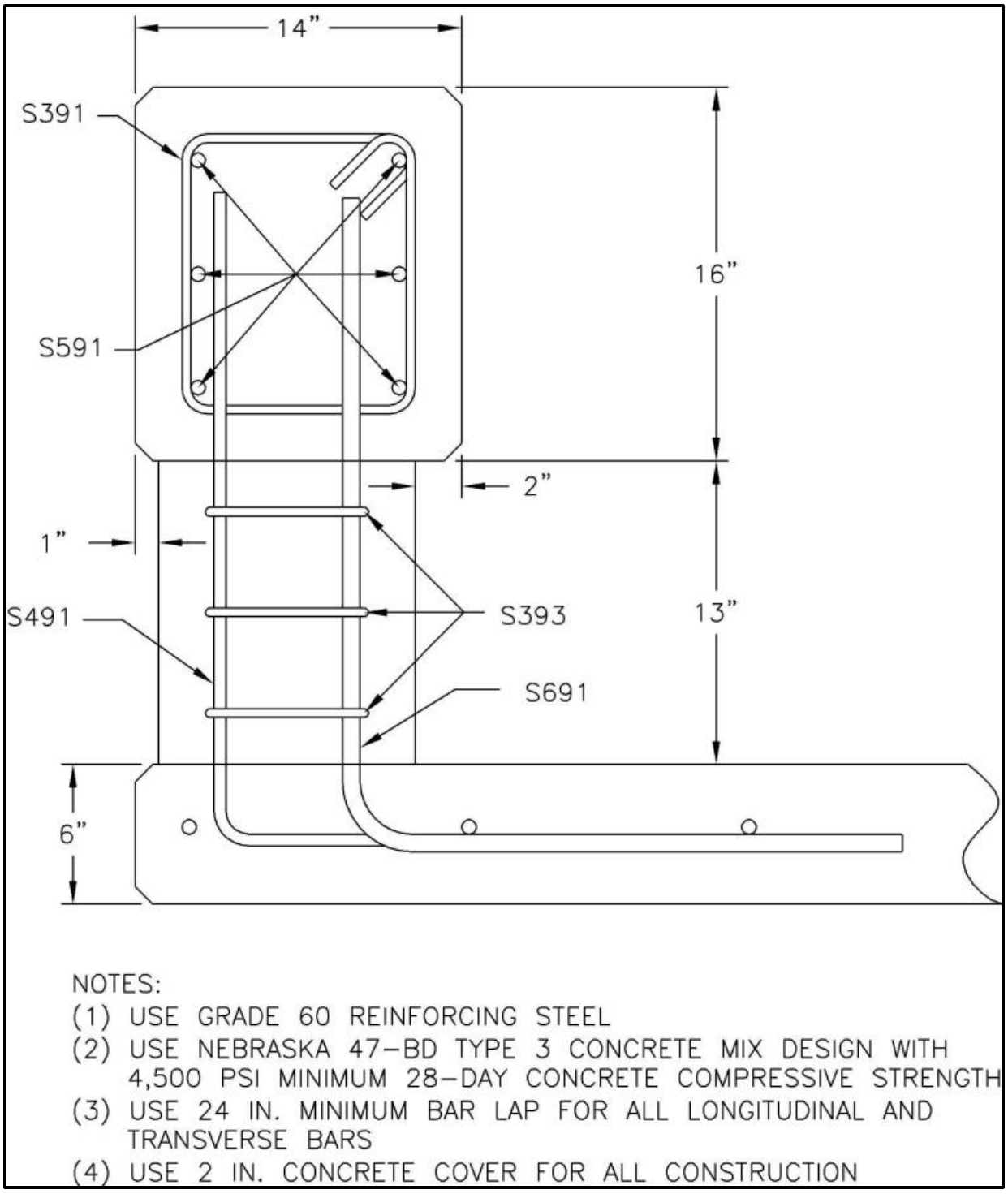

Figure 8 Cross Section of NDOT Open Concrete Bridge Rail on Thin Bridge Deck [9]

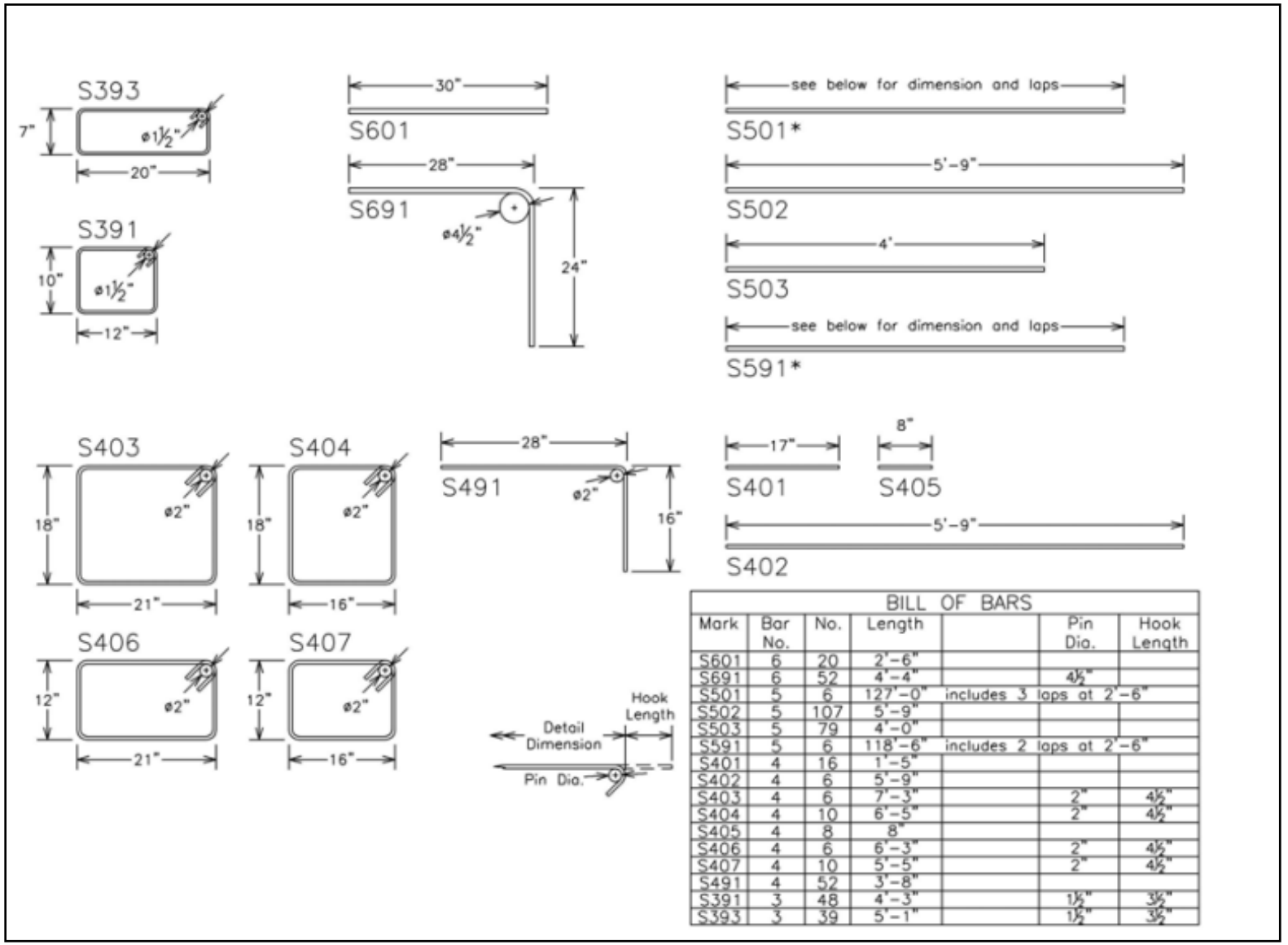

BILL OF BARS

Mark	Bar No.	No.	Length		Pin Dia.	Hook Length
S601	6	20	2'-6"			
S691	6	52	4'-4"		4½"	
S501	5	6	127'-0"	includes 3 laps at 2'-6"		
S502	5	107	5'-9"			
S503	5	79	4'-0"			
S591	5	6	118'-6"	includes 2 laps at 2'-6"		
S401	4	16	1'-5"			
S402	4	6	5'-9"			
S403	4	6	7'-3"		2"	4½"
S404	4	10	6'-5"		2"	4½"
S405	4	8	8"			
S406	4	6	6'-3"		2"	4½"
S407	4	10	5'-5"		2"	4½"
S491	4	52	3'-8"			
S391	3	48	4'-3"		1½"	3½"
S393	3	39	5'-1"		1½"	3½"

Figure 9. Bill of Bars for NDOT Open Concrete Bridge Rail [9]

2.3.2 NDOT TL-2 Bridge Rail

Design drawings from the NDOT TL-2 steel bridge rail were also evaluated in order to provide insights into design details typically used in concrete deck overhang sections [10]. While the bridge railing system was configured with only steel components, the research results provided insights into the reinforcement of thin decks that are used with lower performance concrete barriers and bridge railings. The reinforced concrete deck was 7 in. thick and utilized two mats of steel reinforcement, as shown in Figure 10. In the bottom steel mat, the transverse steel was located beneath the longitudinal steel. In the top mat, the transverse steel was above the longitudinal steel. Compared to the other bridge rail and deck systems that were reviewed, this system was the thinnest deck with two mats of steel reinforcement. As a result, a deck thickness of 7 in. was selected as the lower bound requirement for double mats of steel reinforcement in decks considered herein for compatibility with the attached bridge rail.

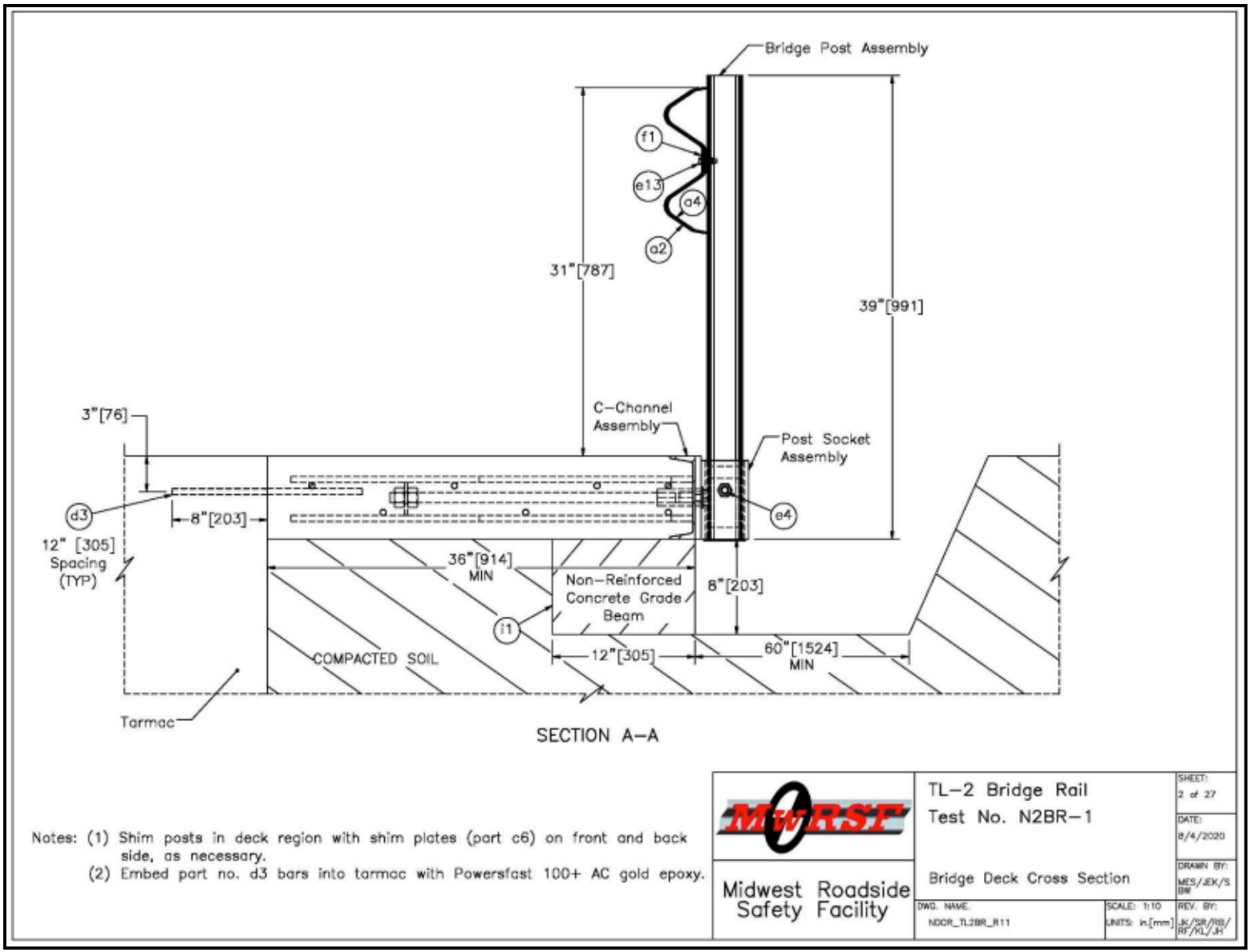

Figure 10. Cross Section View of NDOR TL-2 Bridge Rail [10]

2.3.3 WVDOT TL-1 Glulam Timber Bridge Rail

The final bridge deck and rail design to be reviewed was the WVDOT TL-1 glulam timber bridge rail [11-12]. This bridge rail system consisted of two scupper blocks stacked on top of one another with a glulam bridge railing mounted to the top of the scupper blocks, resulting in a total bridge rail height of 19¾ in. The bridge rail was then mounted to the edge of a nail-laminated timber deck using four 30-in. long timber bolts, which were inserted through the railing and scupper blocks and into the deck. Figure 11 provides a design drawing of the cross-section view of the bridge rail attached to the edge of the nail-laminated deck.

One full-scale vehicle crash test was successfully performed with a 2270P, ½-ton, Quad cab, Dodge pickup truck. The low-height, curb-type, timber bridge rail attached to a transverse, nail-laminated, timber bridge deck was deemed acceptable according to the AASHTO MASH TL-1. Given that the 19¾-in. height was proven sufficient for containing TL-1 impacts, the implication for the bridge railing being adapted in this project was that a 20 in. height was also adequate for MASH TL-1 vehicle containment.

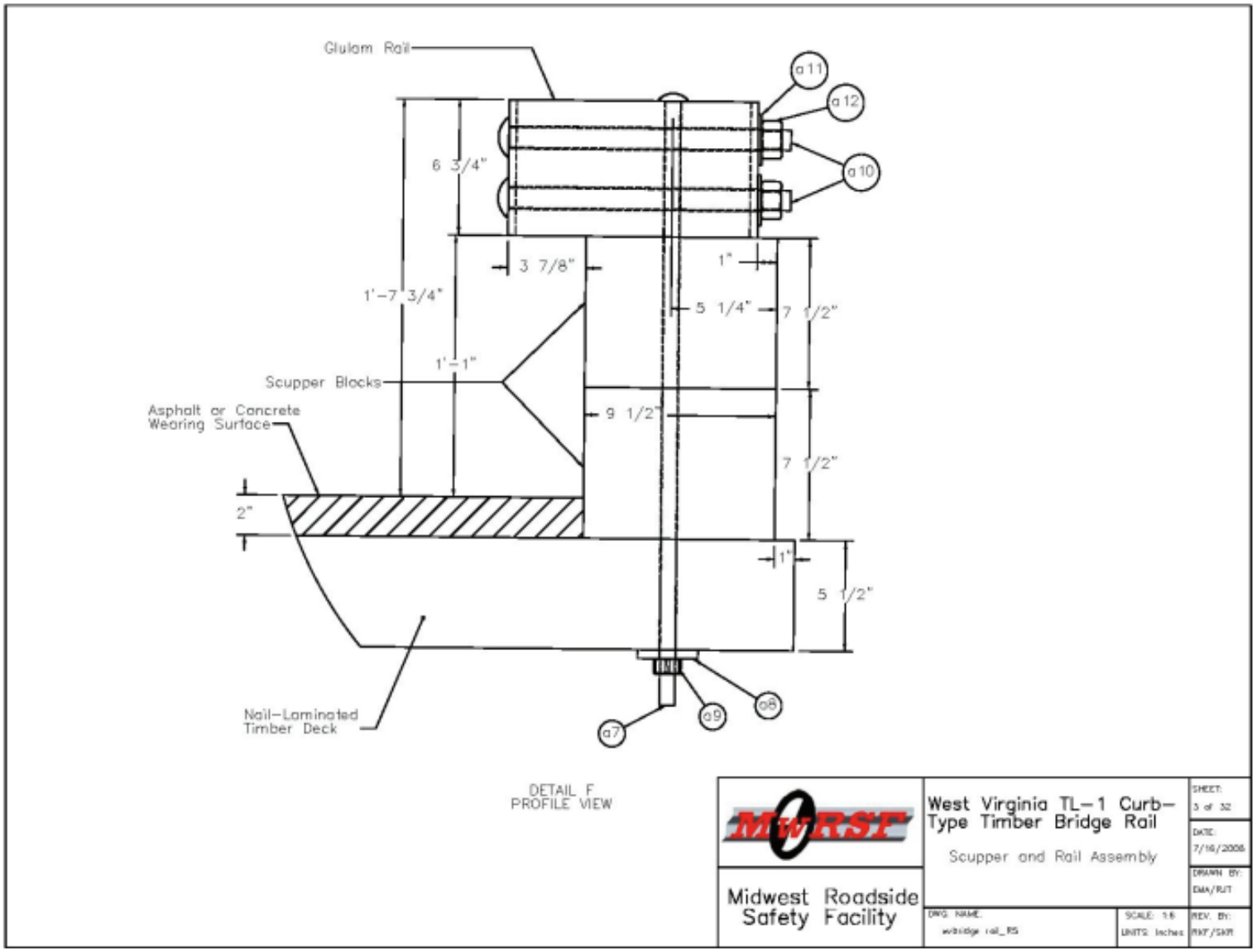

Figure 11. Design Drawing of WVDOT Timber Bridge Rail [11-12]

2.3.4 TTI Design Drawings

Bridge Rail and deck design drawings from TTI were also examined to gain additional insight into bridge deck overhang design for low-height, bridge rail systems [13-15]. The TTI designs are shown in Figures 12 to 15. Figures 12 and 13 show TTI's MASH TL-3 Single Slope Bridge Rail developed for TxDOT. While the bridge rail in this design is too tall to provide relevant design details for the low-height, bridge rail being investigated in this project, the bridge deck thickness is in line with what would be typically used for a low-height bridge rail. The deck had a uniform thickness of 6 in., and a single mat of steel was utilized. While the longitudinal bars are not shown in the design details, the transverse bars in the steel mat are shown to be No. 4 bars spaced 18¼ in. from one another along the length of the deck edge.

The MASH TL-4 T2P Retrofit Bridge Rail was another TTI configuration, which is shown in Figure 14. Similar to the TxDOT Single Slope Bridge Rail, the guardrail attached to the bridge deck was too tall to provide design details applicable to the low-height bridge rail analyzed in this study. Therefore, only the design details of the bridge deck were examined. The overhang length was 40 in., as measured from the outside face of the exterior deck support to the deck edge. The deck thickness was 6 in., and a single mat of steel was used to reinforce the deck. The longitudinal bars were placed within the steel mat above the transverse steel. By placing the longitudinal steel above the transverse steel, the longitudinal bars could resist any downward prying action of the deck and rail in the event that the bridge rail system fractured.

The final TTI design that was examined included the MASH TL-3 T223 Concrete Beam-and-Post Bridge Rail. A cross section of this system is shown in Figure 15. Similar to the bridge rail being examined in this study, the T223 concrete beam and box post bridge rail consisted of two distinct uniform bridge thicknesses. Due to the similarities between this system and the NDOT concrete beam and post bridge railing and deck system, the research team reviewed the reinforcement patterns in the bridge railing, the connection details between the barrier and the deck, as well as the deck reinforcement. In the top rail section of the barrier, eight No. 4 longitudinal bars were placed into two columns and tied together with stirrups with an unspecified bar size. To attach the bridge rail to the deck, the rebar on the traffic facing side of the barrier was bent into an L-shaped hook and was then inserted into the 5-in. thick deck. On the non-traffic facing side of the bridge rail, the rebar was inserted into the deck without any bends. Within the deck, a single mat was utilized in which the longitudinal reinforcement was placed below the transverse steel. While the placement of the longitudinal steel relative to the transverse steel would not prevent an upward prying action from the deck, the box beam used to support the deck provided enough stiffness to eliminate any prying concerns.

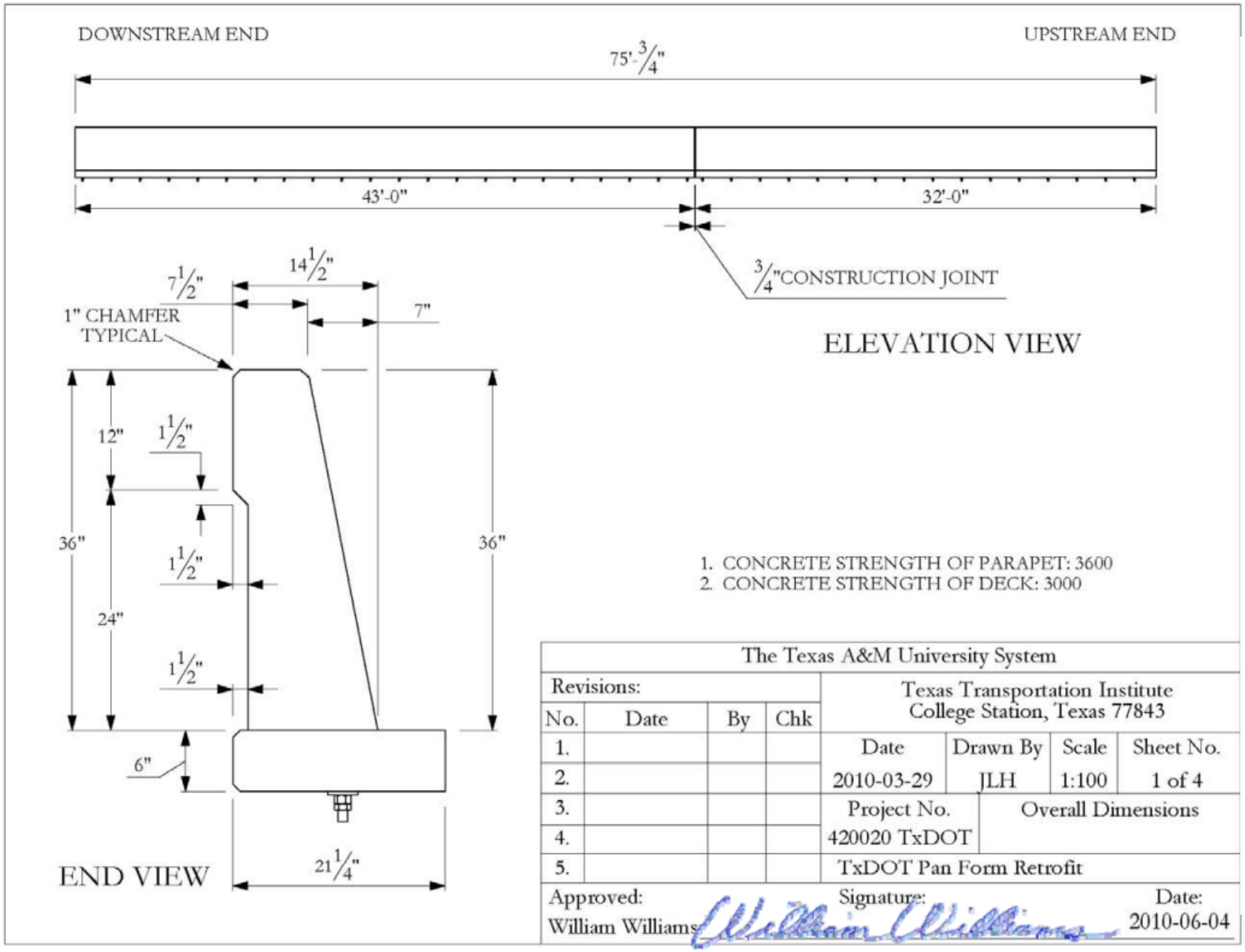

Figure 12. Design Drawings for TxDOT Pan Form Retrofit Bridge Rail [13]

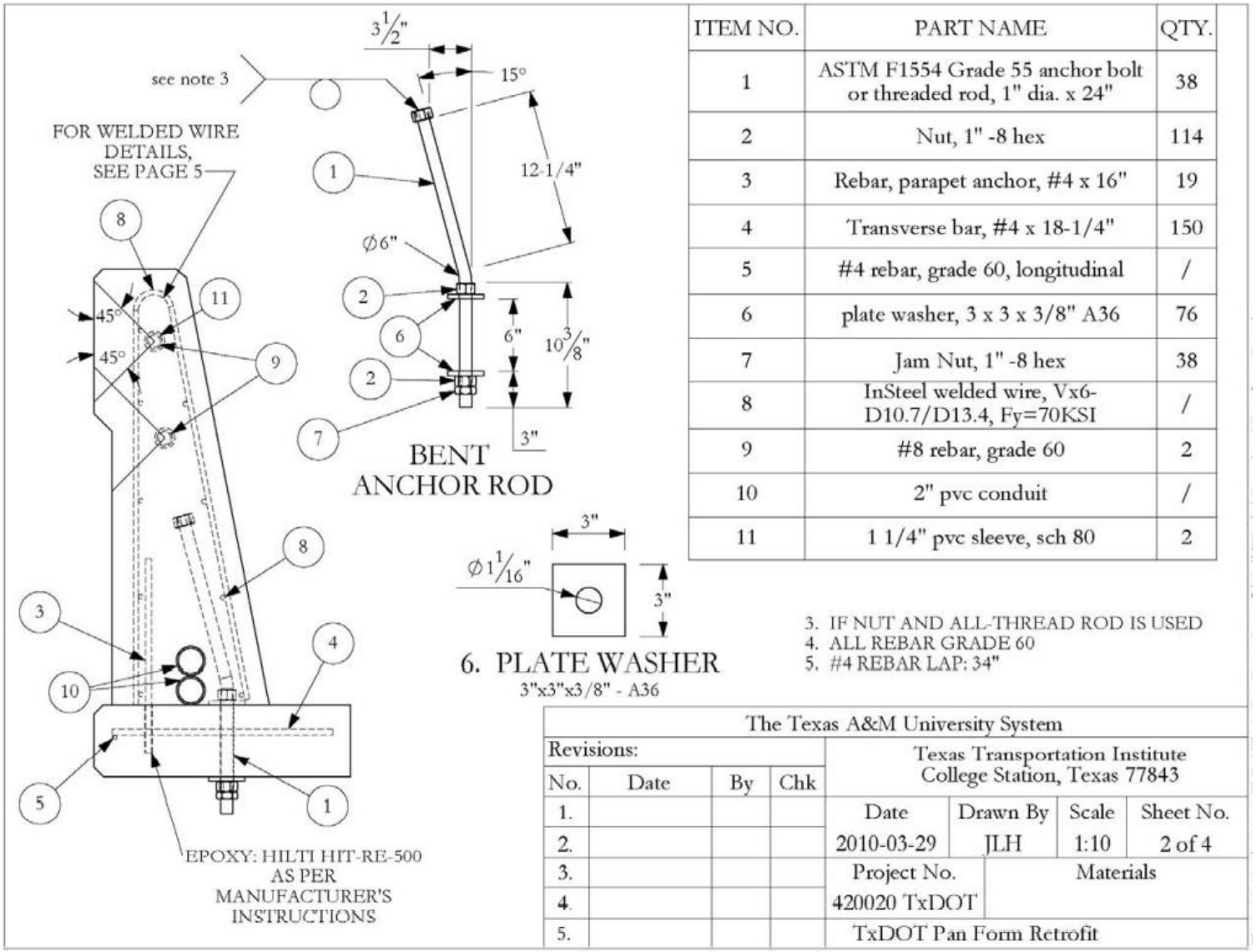

ITEM NO.	PART NAME	QTY.
1	ASTM F1554 Grade 55 anchor bolt or threaded rod, 1" dia. x 24"	38
2	Nut, 1" -8 hex	114
3	Rebar, parapet anchor, #4 x 16"	19
4	Transverse bar, #4 x 18-1/4"	150
5	#4 rebar, grade 60, longitudinal	/
6	plate washer, 3 x 3 x 3/8" A36	76
7	Jam Nut, 1" -8 hex	38
8	InSteel welded wire, Vx6-D10.7/D13.4, Fy=70KSI	/
9	#8 rebar, grade 60	2
10	2" pvc conduit	/
11	1 1/4" pvc sleeve, sch 80	2

Figure 13. Design Drawings for TxDOT Pan Form Retrofit Bridge Rail [13]

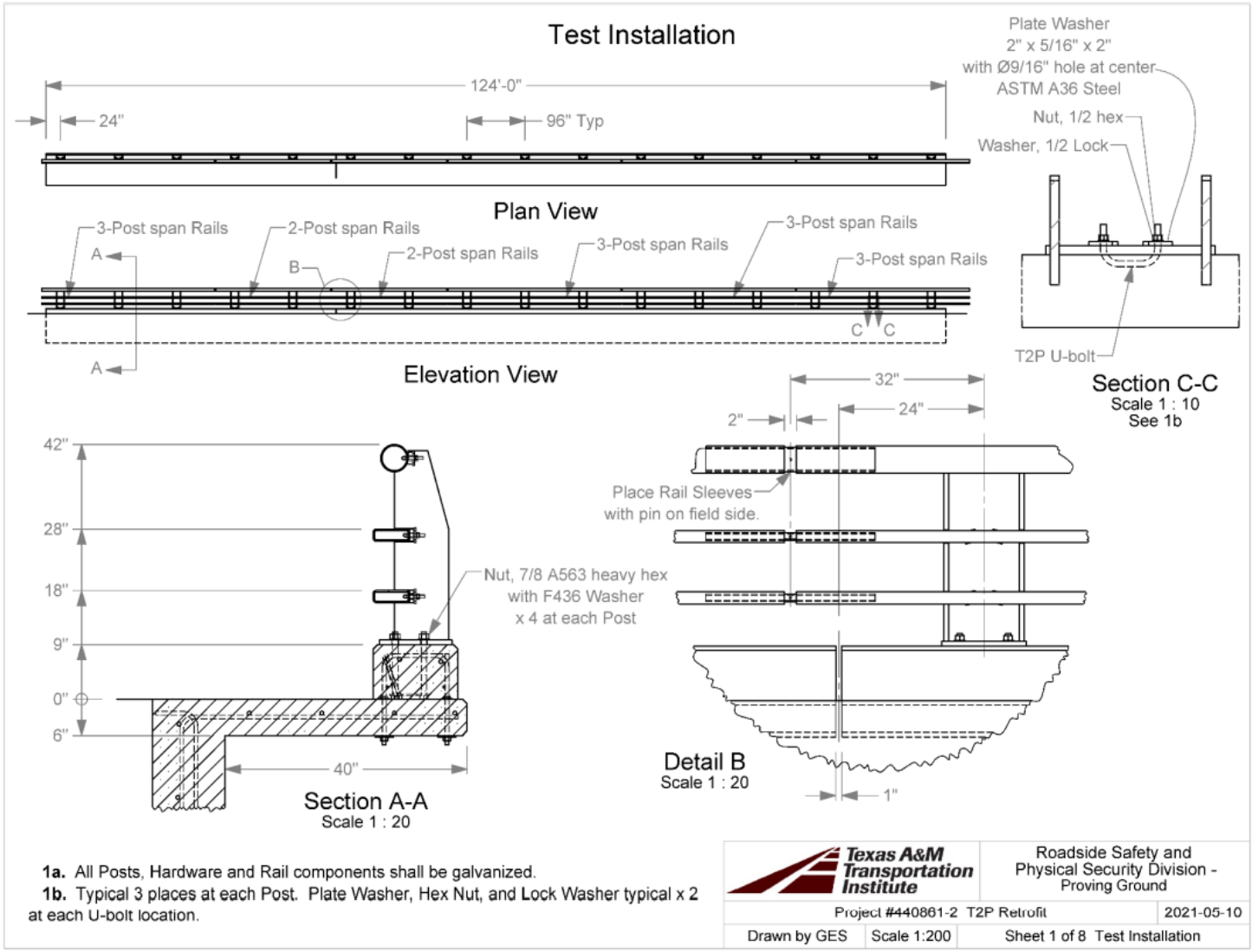

Figure 14. Design Drawings for T2P Retrofit Bridge Rail [14]

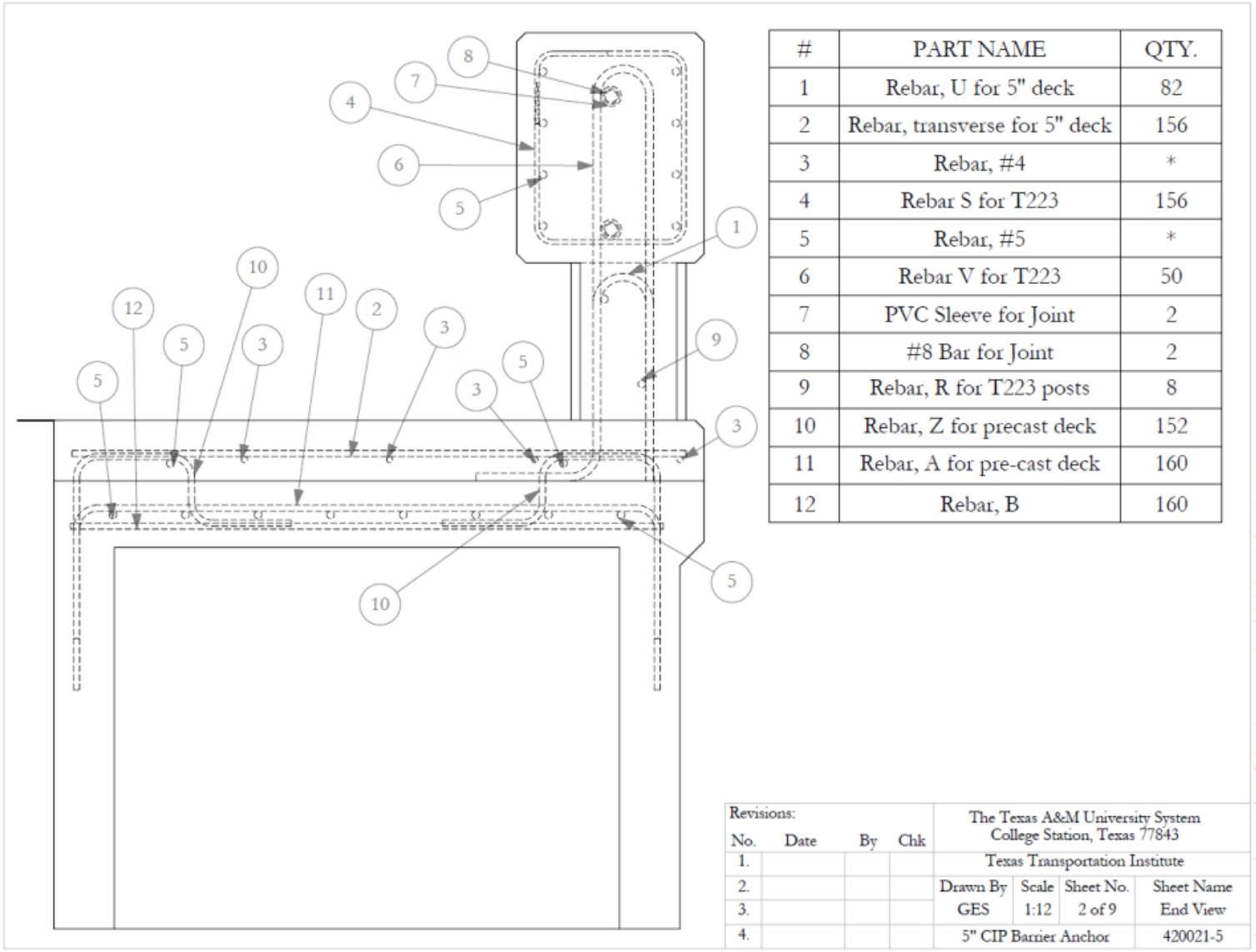

#	PART NAME	QTY.
1	Rebar, U for 5" deck	82
2	Rebar, transverse for 5" deck	156
3	Rebar, #4	*
4	Rebar S for T223	156
5	Rebar, #5	*
6	Rebar V for T223	50
7	PVC Sleeve for Joint	2
8	#8 Bar for Joint	2
9	Rebar, R for T223 posts	8
10	Rebar, Z for precast deck	152
11	Rebar, A for pre-cast deck	160
12	Rebar, B	160

Revisions:				The Texas A&M University System College Station, Texas 77843			
No.	Date	By	Chk				
1.				Texas Transportation Institute			
2.				Drawn By	Scale	Sheet No.	Sheet Name
3.				GES	1:12	2 of 9	End View
4.				5" CIP Barrier Anchor			420021-5

Figure 15. Design Drawings for T223 Concrete Beam-and-Post Bridge Rail [15]

2.4 BOPP Manual

In addition to the design drawings discussed in Sections 2.2 and 2.3, NDOT's BOPP manual was consulted. Section 3.3.3 of the BOPP manual outlines the common design practices for bridge decks utilizing prestressed inverted-tee girders [7]. Therefore, it was deemed relevant as several deck designs in Sections 2.2 and 2.3 utilized inverted tee girders. BOPP section 3.3.3 states that cast-in-place slabs must have a minimum deck thickness of 6 in. and noted that for the minimum 6-in. thick slab, No. 5 longitudinal bars at 10 in. spacing should be used in conjunction with No. 5 transverse bars at 6-in. spacing. With this reinforcement pattern, no additional steel is required to strengthen overhang sections of the deck. If the above-described design guidance is followed, a 19-in. maximum overhang length is allowed.

2.5 Sloped End Treatments for Low-Height Barriers

2.5.1 TTI Concrete End Treatment

In 1998, the Texas A&M Transportation Institute (TTI) developed a sloped concrete end treatment for use with a low-height, concrete work-zone barrier [3]. The sloped end treatment had an upstream end configured with a 4-in. tall blunt end measuring 14.4 in. wide, while its downstream end measured 20 in. tall and 28 in. wide. Additionally, the overall length of the treatment was 15 ft. The concrete end treatment was anchored to the road surface using seven steel pins spaced 24 in. apart from one another and inserted through the segment and road surface at its centerline. The end treatment was crash tested using four small cars and three pickup trucks in accordance with Test Level 2 safety performance criteria found in the NCHRP Report No. 350 impact safety standards [1]. The seven crash test designation nos. and associated impact conditions used for the concrete end treatment are provided in Table 3. Following the completion of the full-scale crash testing program, the concrete end treatment was deemed crashworthy according to the TL-2 impact conditions published in the NCHRP Report No. 350 impact safety standards. Photographs of the TTI low-height, sloped concrete end treatment are provided in Figure 16

In 2013, TTI researchers modified the sloped concrete end treatment by removing the seven steel drop pins that were used to anchor the end section [4]. TTI then subjected the free-standing sloped concrete end treatment to two full-scale crash tests using the MASH TL-2 impact safety standards with a small car and a pickup truck, as summarized in Table 3 [16]. Following the completion of the full-scale crash testing program, the modified, sloped concrete end treatment was deemed crashworthy according to the MASH TL-2 impact safety standards.

Table 3. TTI Crash Tests on Low-Height, Sloped Concrete End Treatment

Reference	Vehicle Type	Crash Test Designation No.	Target Impact Angle (degrees)	Target Impact Speed (mph)	Location of Impact
1998 TTI [3]	Small Car	350 2-30	0	43.5	End of Terminal
		350 2-32	15	43.5	End of Terminal
		350 2-34	15	43.5	Critical Impact Point
	Pickup Truck	350 2-31	0	43.5	End of Terminal
		350 2-33	15	43.5	End of Terminal
		350 2-35	20	43.5	Beginning of Length of Need
		350 2-39	20	43.5	Mid Length of Terminal
2013 TTI [4]	Small Car	MASH 2-34	15	44	Critical Impact Point
	Pickup Truck	MASH 2-35	25	44	Beginning of Length of Need

End View

Isometric View

Small Car Vehicle

Figure 16. Low-Height, Sloped Concrete End Treatment [3]

2.5.2 TL-2 Low-Profile, Concrete Bridge Railing with Sloped End Treatment

In 2002, MwRSF researchers completed a Midwest Pooled Fund Program (MPFP) study to develop, test, and evaluate a low-height, reinforced concrete bridge railing to meet TL-2 impact safety standards published in NCHRP Report No. 350 [1-2]. The 20-in. tall bridge railing was configured with a top width of 14 in. and base width of 11 in., as depicted in Figure 17. The bridge railing utilized a rectangular shape as the upper beam and a narrow, lower vertical wall to support the beam. Overall, the bridge railing generally appeared to be an upside-down "L" shape with the top section extending forward from the vertical wall, which was intended to reduce wheel climb during impact events. The concrete bridge rail was subjected to one full-scale crash test with 2000P pickup truck and resulted in satisfactory safety performance according to the TL-2 criteria found in NCHRP Report No. 350.

For the original sloped end treatment, the 20-in. tall reinforced-concrete bridge railing was configured to slope downward to the roadway surface using the same vertical slope that was utilized for the TTI sloped concrete end treatment [3-4]. The original reinforced-concrete, sloped end treatment was 15 ft long with an upstream height of 4 in. and width of 14 in., as shown in Figure 17. Using the noted configuration and geometry, MwRSF researchers deemed it unnecessary to conduct additional crash testing on the reinforced-concrete, sloped end treatment beyond that testing already conducted by TTI researchers [3-4].

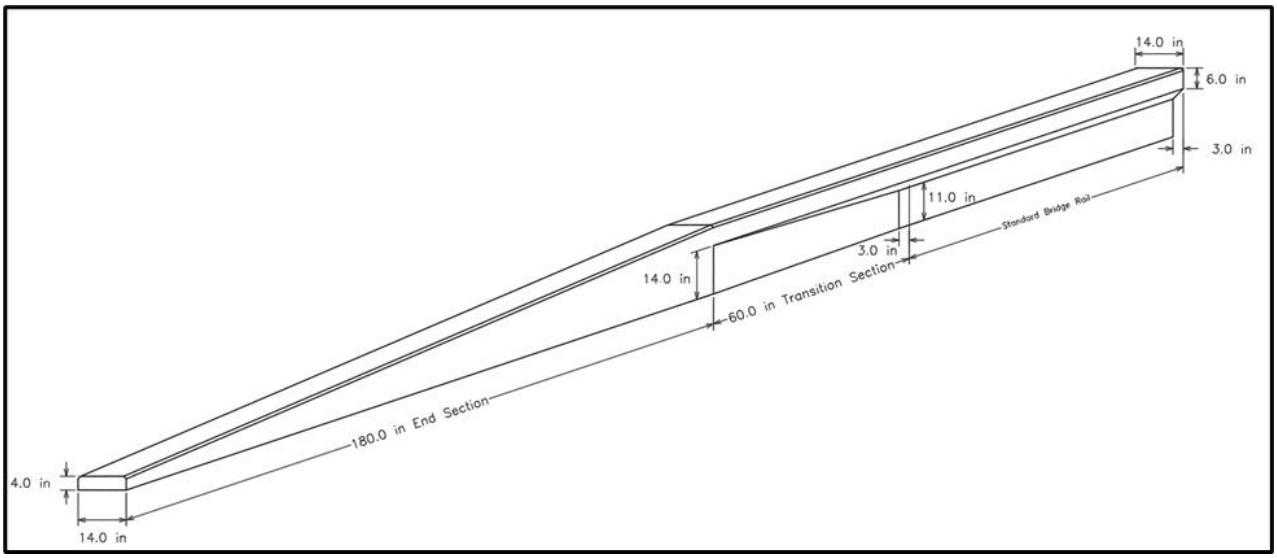

Figure 17. Original MPFP Bridge Rail with Sloped Concrete End Treatment [2]

2.5.3 USDA-FS-NTDP TL-1 Low-Profile, Concrete Bridge Railing with Modified Sloped End Treatment

During this study, the geometry and steel reinforcement for the MPFP NCHRP Report No. 350 TL-2 low-height, reinforced concrete bridge railing with sloped concrete end section [2] were modified. Those general changes to the bridge railing and sloped end treatment are provided in advance within Figure 18. The width of the bridge railing was reduced by 4 in., while the longitudinal and vertical steel reinforcement was also modified. Due to minor modifications made

to the bridge rail, no full-scale or component crash testing was required when considering that the system would only need to meet MASH TL-1 and configured with a 20-in. top rail height. The width of the end treatment was also reduced by 4 in., and the steel reinforcement was modified slightly. Since the changes to the end treatment were minor, no full-scale crash testing was deemed necessary.

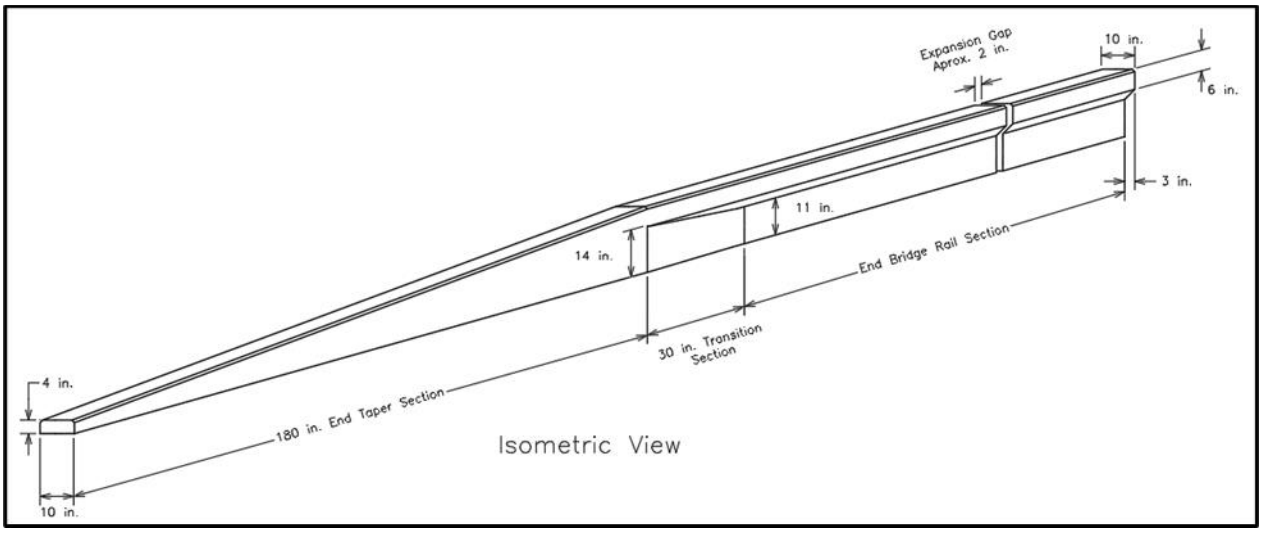

Figure 18. USDA-FS-NTDP Modified Bridge Railing with Sloped Concrete End Treatment

3 THEORETICAL ANALYSIS OF NDOR CONCRETE BRIDGE RAIL

3.1 Analysis of NDOR Concrete Bridge Rail

To begin analysis of the NDOR barrier, the yield-line and punching shear capacities were determined using the equations outlined in the AASHTO *BDS* [6]. Using equation A13.3.1-1, the yield-line capacity of the barrier was determined to be 44.2 kips. This equation has been summarized below as Equation 3.1 [6]. Figure 19 provides the analytical model that was used to represent the yield-line failure mechanism.

$$R_w = \left(\frac{2}{2L_c - L_t}\right) \cdot \left(8M_b + 8M_w + \frac{M_c L_c^2}{H}\right) \quad (3.1)$$

where R_w is the total transverse resistance of the railing, L_c is the critical length of yield-line failure, M_b is the additional flexural resistance of the beam in addition to M_w if any, at the top of the wall, M_c is the flexural resistance of the cantilevered walls about an axis parallel to the longitudinal axis of the bridge, M_w is the flexural resistance of the wall about its vertical axis, and H is the height of the wall. It should be noted that while multiple yield-line shapes can be used to evaluate capacity, a triangular yield-line mechanism was adopted to maintain consistency with the 9th edition *BDS*.

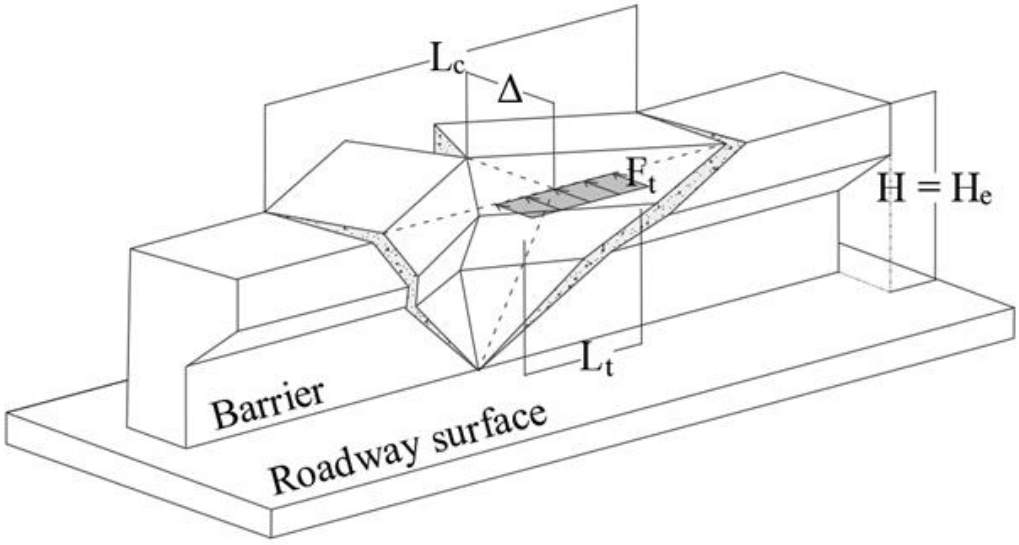

Figure 19. Analytical Model of Triangular Yield-line Failure Mode

After the barrier's yield-line capacity was determined, the punching shear capacity was evaluated. Guidance regarding punching shear in the AASHTO design manual allows for several different punching shear scenarios to be utilized, each of which result in slightly different punching shear capacities. Equation 5.13.2.5.4-1 is the first instance in AASHTO, and accounts for punching shear occurring from a beam loading a concrete ledge. Equation 5.13.3.6.3-1 can also be used, and accounts for punching shear on a two-way slab. Lastly, Equation A13.4.3.2-3 is defined in AASHTO and accounts for punching shear occurring in a post and beam scenario. For the three punching shear scenarios outlined in the AASHTO bridge design manual, the scenario leading to

the most conservative punching shear strength was utilized. In the case of this barrier system, treating the bridge rail as a two-way slab provided a punching shear capacity of 137.5 kips. The two-way slab punching shear equation has been summarized below as Equation 3.2 [6].

$$V_n = \left(0.063 + \frac{0.126}{\beta_c}\right)\sqrt{f_c'} \cdot b_o \cdot d_v \leq 0.126\sqrt{f_c'} \cdot b_o \cdot d_v \quad (3.2)$$

where β_c is the ratio of the long side to the short side of the shear patch, b_o is the perimeter of the critical section, and d_v is the effective shear depth. Figure 20 outlines the lengths which make up the b_o dimension on the NCHRP TL-2 barrier. After analyzing the barrier using AASHTO's guidance for two-way slab punching shear, a barrier capacity of 147.2 kips was obtained for the interior barrier section.

Figure 20 provides the analytical model that was used to represent the two-way slab punching shear failure. Table 4 summarizes the two limit states evaluated to determine the strength of the NDOR barrier. From the table, it can be observed that the yield-line capacity is the limiting failure mechanism. For a more in-depth explanation of the methodologies used to obtain these two limit state values see Appendix A and Appendix B.

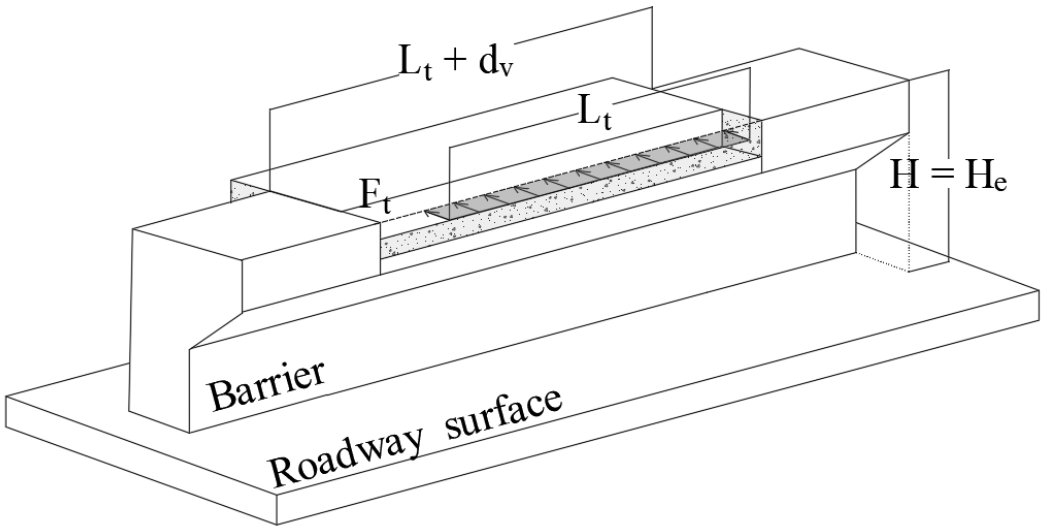

Figure 20. Analytical Model of Two-Way Slab Punching Shear

Table 4. Summary of NDOR Low-Height Concrete Barrier Limit States Capacities

Limit State	Value (kips)
Punching Shear	137.5
Yield-line	44.2

4 MODIFICATIONS MADE TO NDOR CONCRETE BRIDGE RAIL

4.1 Height and Strength Considerations

To determine which modifications should be made to the NDOR bridge rail to meet MASH TL-1 criteria, the design parameters, shown in Table 5 [17] and Equations 4.1 through 4.9 were compared to the height and lateral capacity of the NDOR bridge railing. It should be noted that the outlined design parameters reflect the recommendations currently under consideration under NCHRP Project22-41 to update Section 13 of the *BDS* to reflect MASH test conditions rather than prior design guidance given in AASHTO, which was developed to represent NCHRP 350 test conditions.

The height of the barrier was considered first. Upon comparing the NDOR bridge rail's 20-in. height to the minimum allowable MASH TL-1 height shown in Table 5, it was determined that no height modifications were required. The lateral strength needed for TL-2 impacts was also obtained from Table 5. Comparing the necessary lateral resistance for TL-2 impacts from Table 5 to the actual lateral capacity of 44.2 kips in the NDOR bridge rail, it was determined that the capacity of bridge rail could be reduced to only handle TL-1 impact loads. Ideally, the barrier modifications would optimize the design to handle exactly TL-1 impact scenarios. However, no full-scale crash testing was to be performed to verify any modifications made to the design of the bridge rail. Therefore, instead of targeting the TL-1 strength, the 35-kip capacity for TL-2 was targeted.

Table 5. MASH Design Parameters for Bridge Railings

Design Parameter	**Railing Test Level**					
	TL-1	**TL-2**	**TL-3**	**TL-4**	**TL-5**	**TL-6**
Minimum Barrier Height, H (in.)	20	24	30	36	42	90[1]
Design lateral impact load, F_t (kips)	17	35	70	*Eqn. 4.1*	*Eqn.4.2*	350
Design vertical impact load F_v (kips)	4.5	4.5	4.5	*Eqn. 4.3*	*Eqn.4.4*	NA[2]
Design longitudinal impact load, F_l (kips)	4.5	9	18	*Eqn. 4.5*	*Eqn. 4.6*	*Eqn. 4.6*
Height of Lateral load application, H_e (in.)	18	20	19	*Eqn. 4.7*	*Eqn.4.8*	64
Longitudinal Distribution of lateral and longitudinal loads, L_t or L_l (ft)	4	4	4	*Eqn. 4.9*	10	10
Longitudinal distribution over vertical loads, L_v (ft)	18	18	18	18	40	40

[1] Simulation study performed by Whitfield [18] suggest that a height as low as 50 in. may be adequate for TL-6, but in lieu of full-scale crash testing or further simulation, the existing height of 90 in. is recommended.
[2] Minimum barrier height of 90 in. prevents vehicle roll onto barrier. Thus, vertical forces arise from friction only and should be considered negligible.

$$F_{t,TL-4} = \begin{cases} 2H - 4 \text{ kips} & 36 \text{ in.} \leq H \leq 42 \text{ in.} \\ 0.15H + 74 \text{ kips} & 42 \text{ in.} < H \end{cases} \quad (4.1)$$

$$F_{t,TL-5} = \begin{cases} 17.2H - 560 \text{ kips} & 42 \text{ in.} \leq H \leq 48 \text{ in.} \\ 5.7H - 8 \text{ kips} & 48 \text{ in.} < H \leq 54 \text{ in.} \\ 0.2H + 289 \text{ kips} & 54 \text{ in.} < H \end{cases} \quad (4.2)$$

$$F_{v,TL-4} = \begin{cases} 101 - 1.75H \text{ kips} & 36 \text{ in.} \leq H \leq 45 \text{ in.} \\ 32.7 - 0.23H \text{ kips} & 45 \text{ in.} < H \end{cases} \quad (4.3)$$

$$F_{v,TL-5} = \begin{cases} 496 - 8H \text{ kips} & 42 \text{ in.} \leq H \leq 54 \text{ in.} \\ 97.4 - 0.62H \text{ kips} & 54 \text{ in.} < H \end{cases} \quad (4.4)$$

$$F_{L,TL-4} = \begin{cases} 0.867H - 9.6 \text{ kips} & 36 \text{ in.} \leq H \leq 42 \text{ in.} \\ 0.007H + 26.5 \text{ kips} & 42 \text{ in.} < H \end{cases} \quad (4.5)$$

$$F_{L,TL-5} = \begin{cases} 0.308H + 60.6 \text{ kips} & 42 \text{ in.} \leq H \leq 54 \text{ in.} \\ 79.6 - 0.044H \text{ kips} & 54 \text{ in.} < H \end{cases} \quad (4.6)$$

$$H_{e,TL-4} = \begin{cases} 1.33H - 27 \text{ in.} & 36 \text{ in.} \leq H \leq 40 \text{ in.} \\ 0.15H + 24.3 \text{ in.} & 40 \text{ in.} < H \end{cases} \quad (4.7)$$

$$H_{e,TL-5} = \begin{cases} 1.33H - 27 \text{ in.} & 36 \text{ in.} \leq H \leq 40 \text{ in.} \\ 0.15H + 24.3 \text{ in.} & 40 \text{ in.} < H \end{cases} \quad (4.8)$$

$$L_{t,TL-4} = \begin{cases} 4 \text{ ft} & 36 \text{ in.} \leq H < 39 \text{ in.} \\ 5 \text{ ft} & 39 \text{ in.} \leq H \leq 42 \text{ in.} \\ 0.09H + 1.2 \text{ ft} & 42 \text{ in.} < H \end{cases} \quad (4.9)$$

4.2 Modifications to NDOR Concrete Bridge Rail

To lower the capacity of the barrier, the top and bottom thickness were reduced by 4 in., resulting in top and bottom barrier thicknesses of 10 in. and 7 in., respectively. Additionally, the spacing of the No. 3 vertical steel along the length of the deck was increased from 18 to 24 in. The configuration of the longitudinal bars in the barrier was modified from seven No. 3 bars to eight No. 3 bars. After modification, the yield-line and punching shear capacities of the barrier were determined to be 35.1 kips and 77.4 kips, respectively. The capacities of both the NDOR and USDA-FS-NTDP barrier are shown in Table 6, and Figures 22 through 27 show the reinforcement of the modified bridge rail at an interior section.

In addition to modifying the NDOR bridge rail barrier shape, an end section was reconfigured for the bridge rail. At expansion gap locations (i.e., end sections), the same top and bottom thicknesses, as used for interior sections of the modified bridge rail, were used. The spacing of the vertical reinforcement was 6 in., and all the reinforcement utilized No. 3 bars. The yield-line and punching shear capacities for the modified end section were determined to be 41.0 and 67.8 kips, respectively, as tabulated in Table 6, and Figure 23 shows the reinforcement details of the modified bridge rail at an end section.

A reinforced-concrete, sloped end treatment was also reconfigured for the bridge railing system. The USDA-FS-NTDP modified end treatment was 11 in thick and had an upstream and downstream height of 4 and 20 in. respectively, which was sloped over a 15 ft length. Design drawings of the end treatment have been provided in Figures 23 through 26.

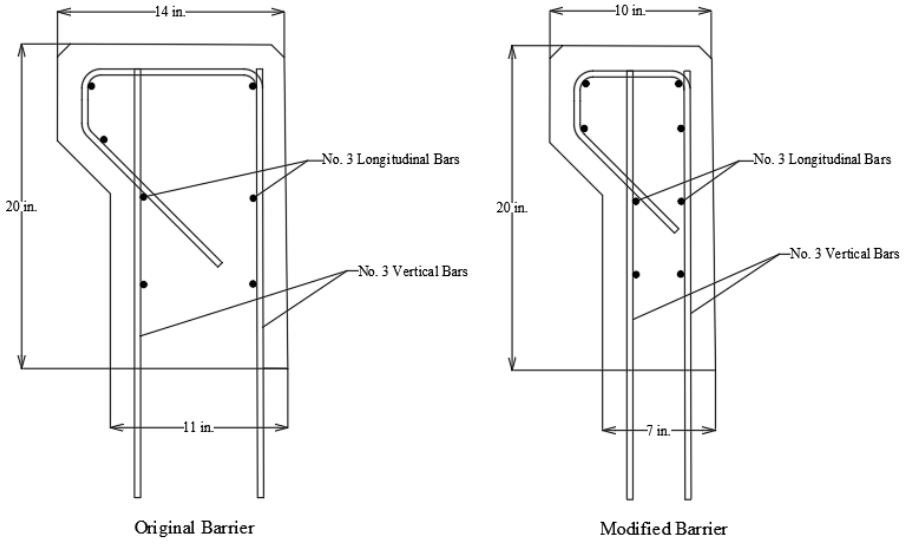

Figure 21. Comparison of NDOR Bridge Rail and USDA-FS-NTDP Bridge Rail Designs

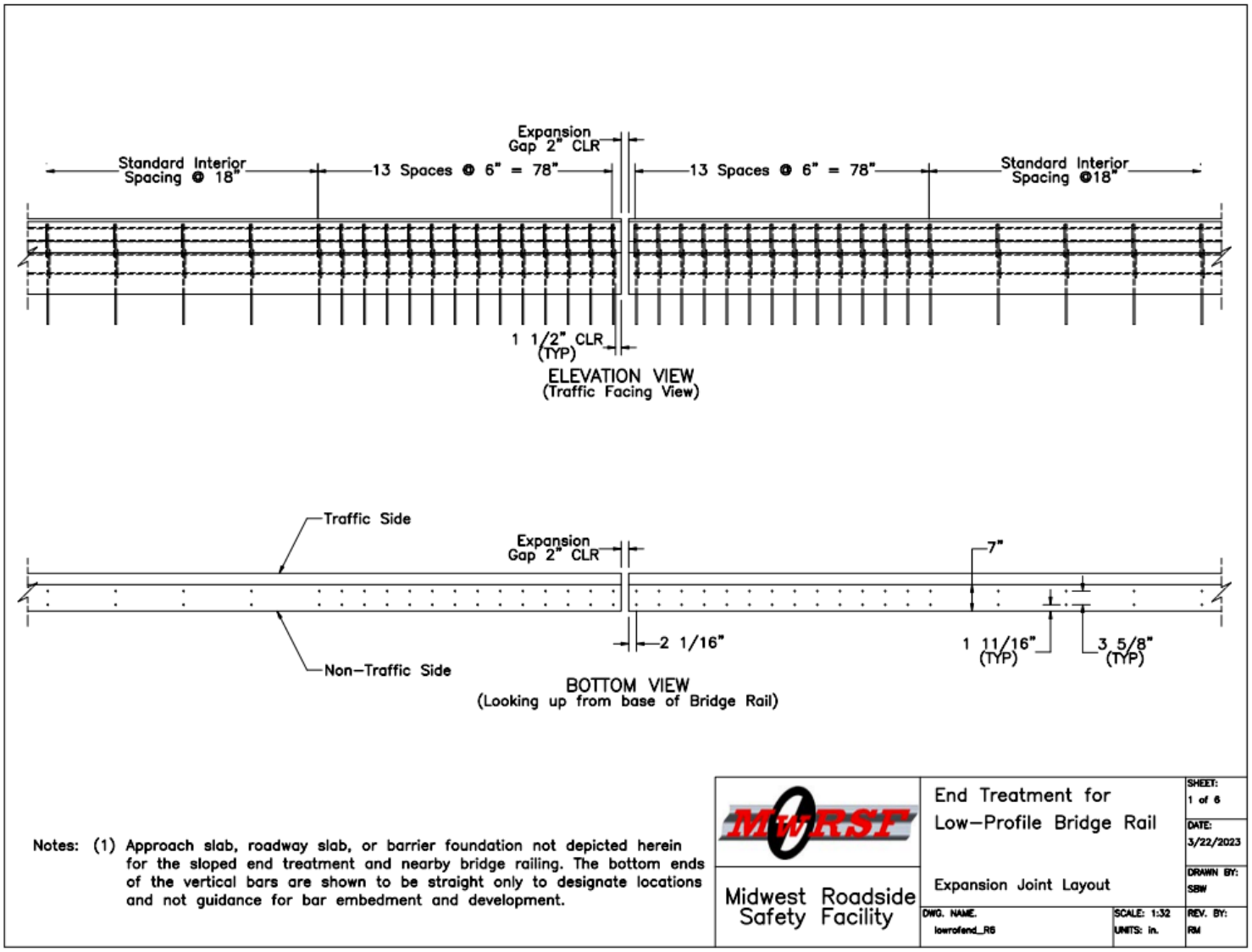

Figure 22. Modified NDOR Bridge Railing System, Expansion Joint Layout

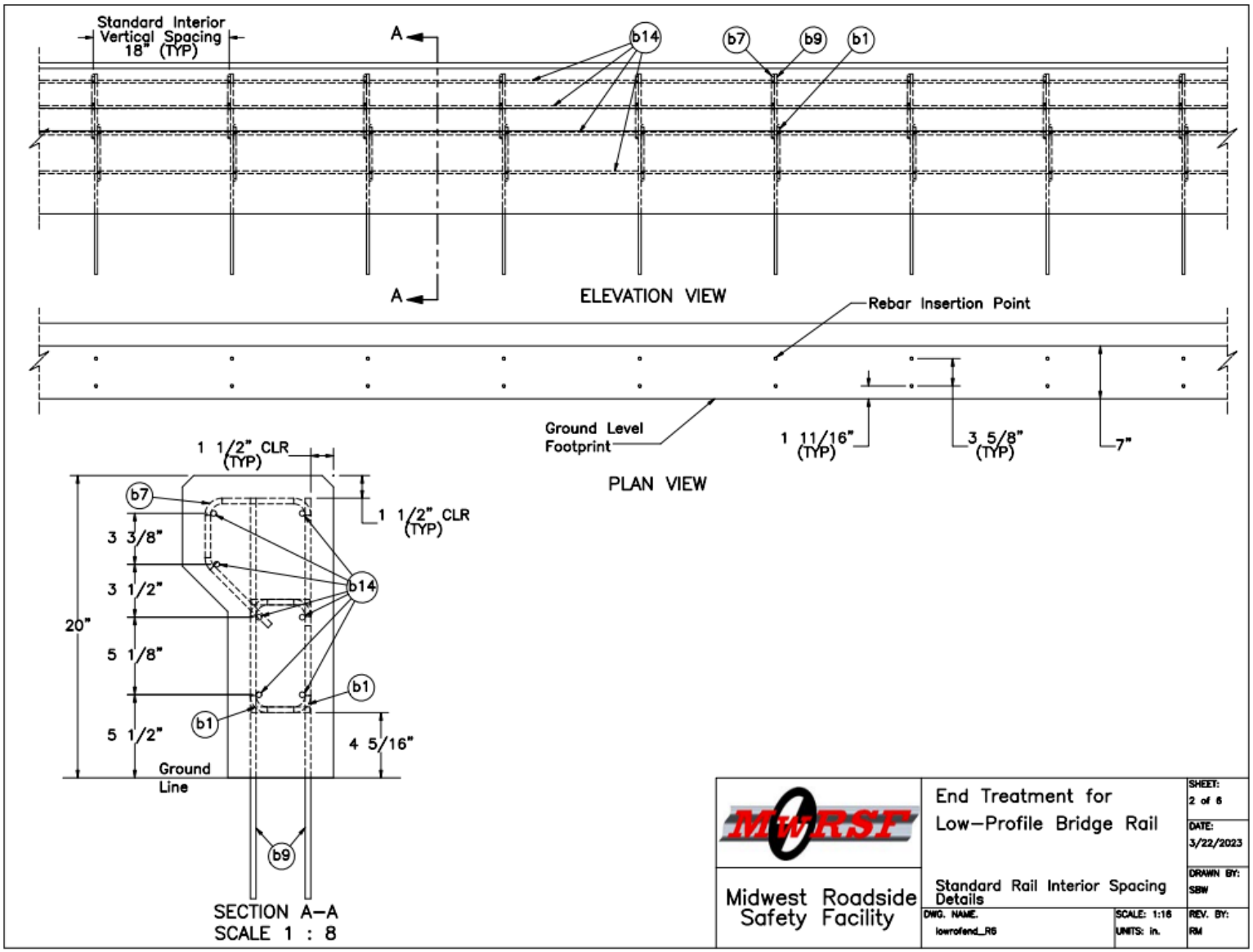

Figure 23. Modified NDOR Bridge Railing System, Standard Rail Interior Spacing Details

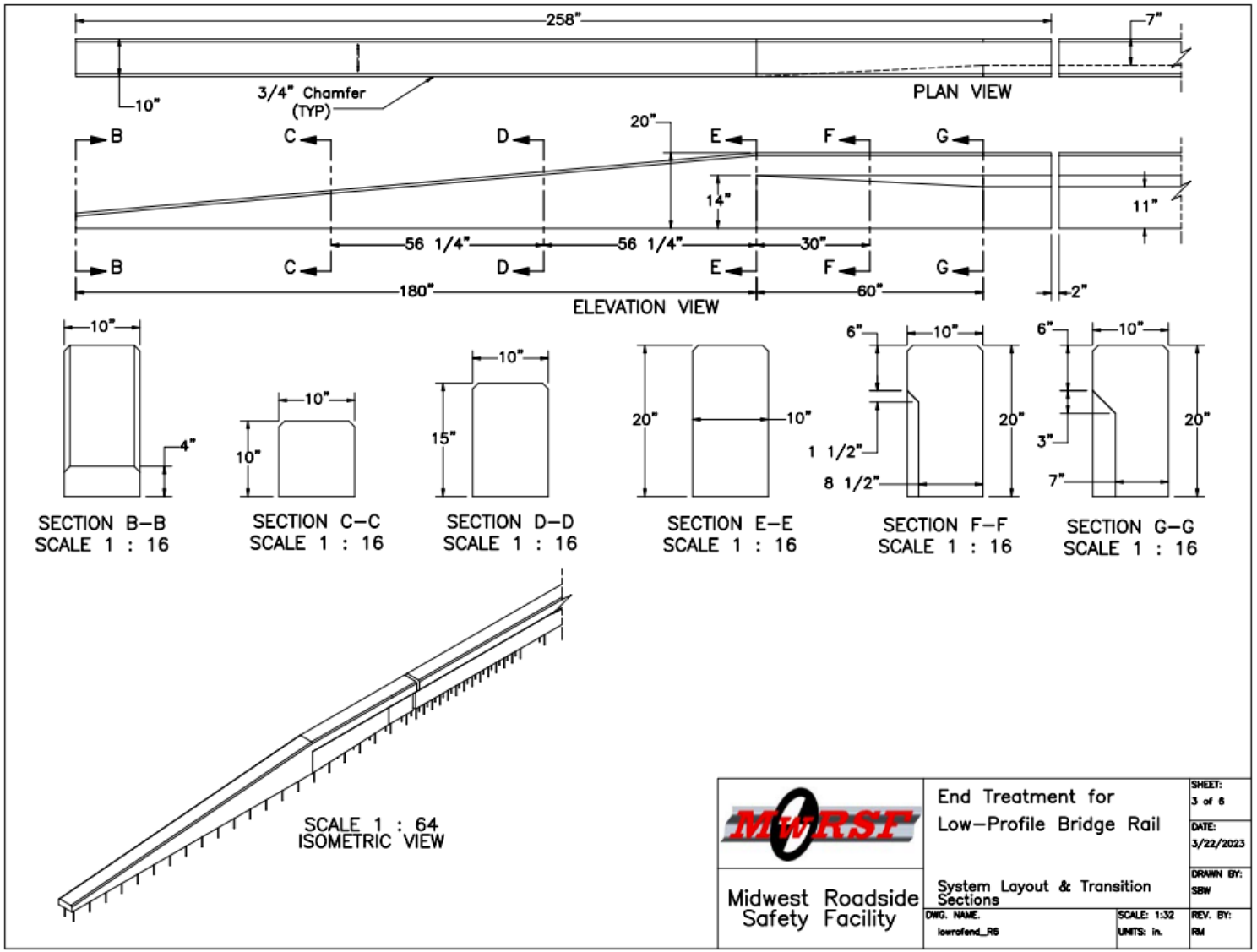

Figure 24. Modified NDOR Bridge Railing System, System Layout and Transition Sections

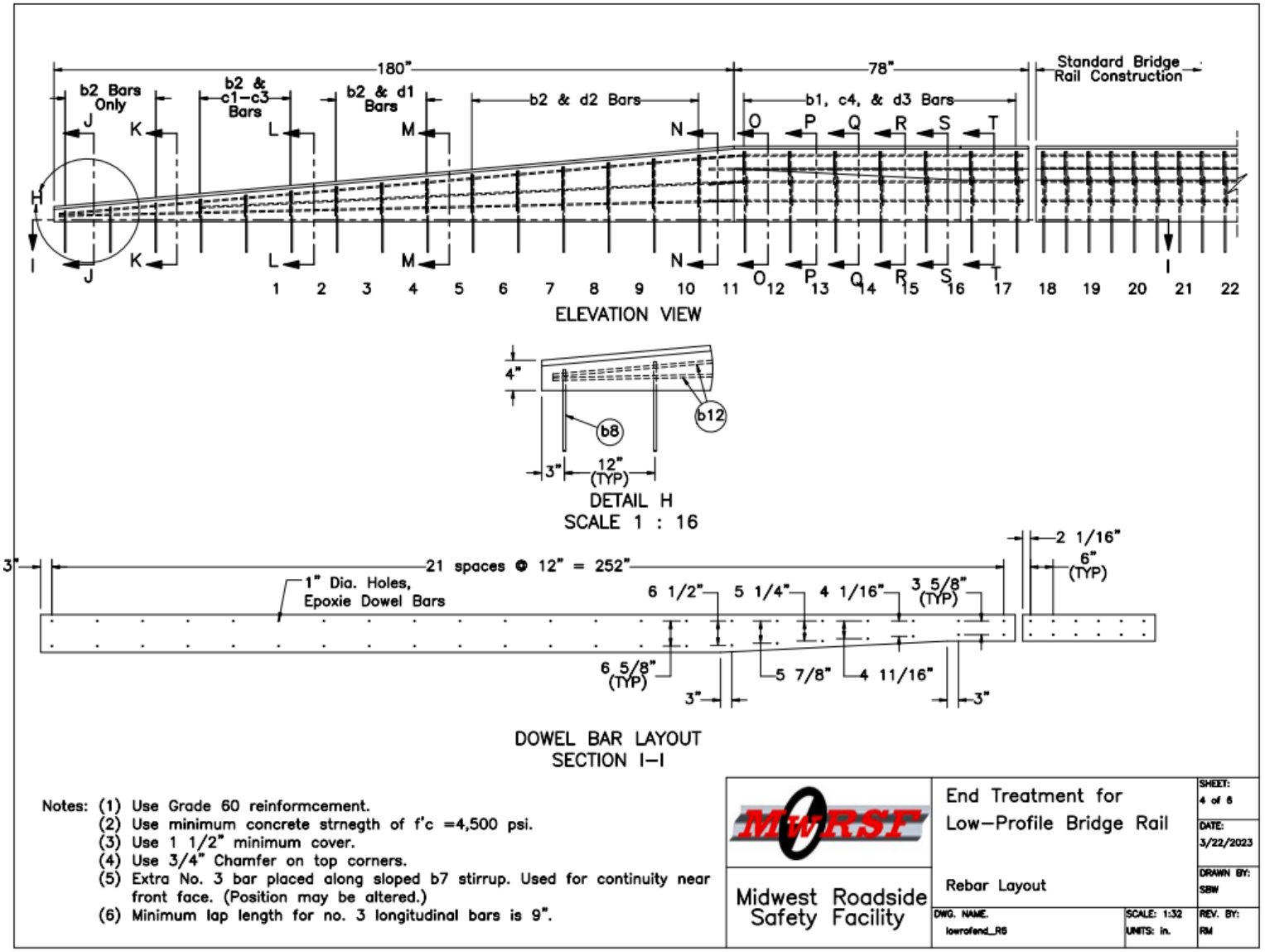

Figure 25. Modified NDOR Bridge Railing System, Rebar Layout

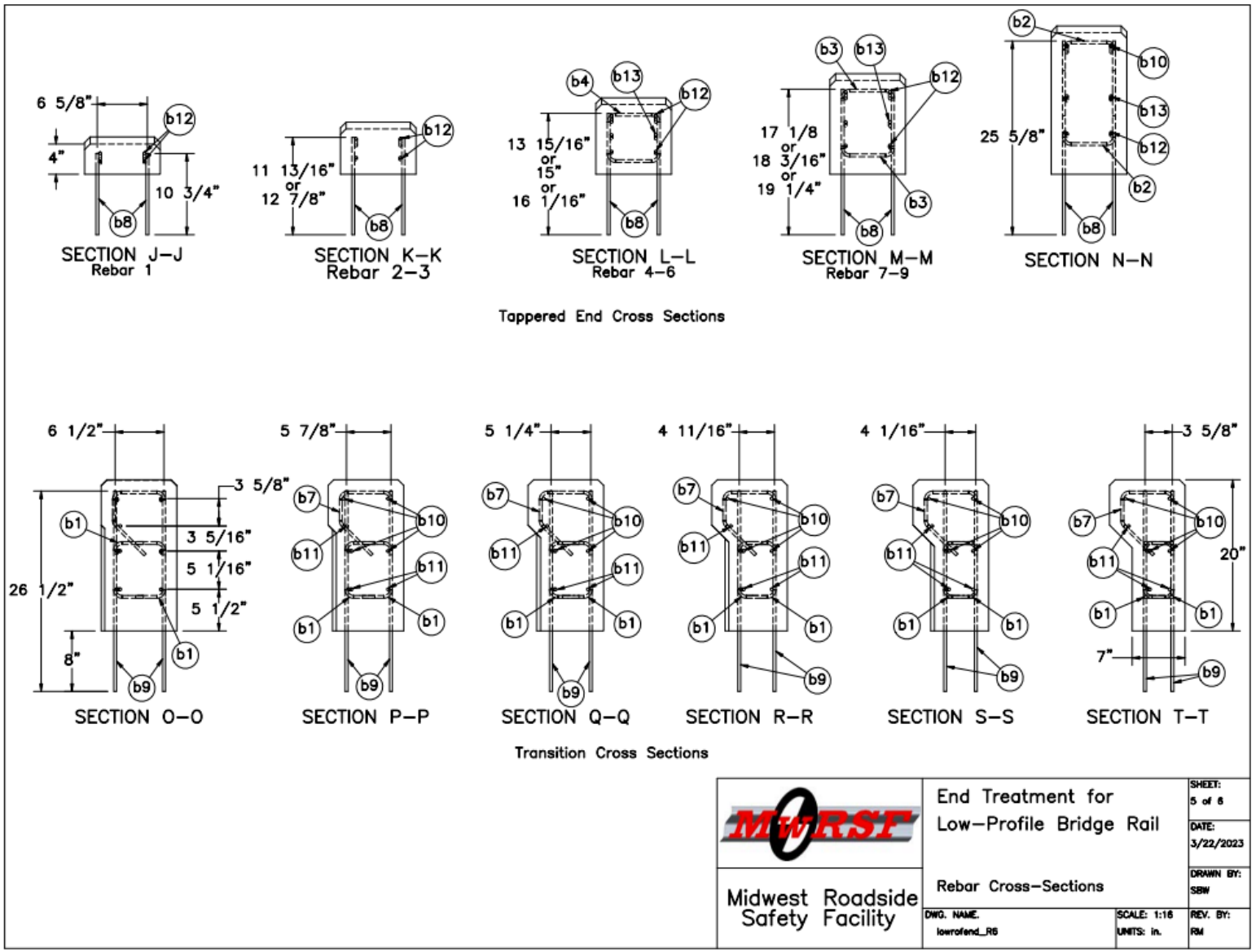

Figure 26. Modified NDOR Bridge Railing System, Rebar Cross-Sections

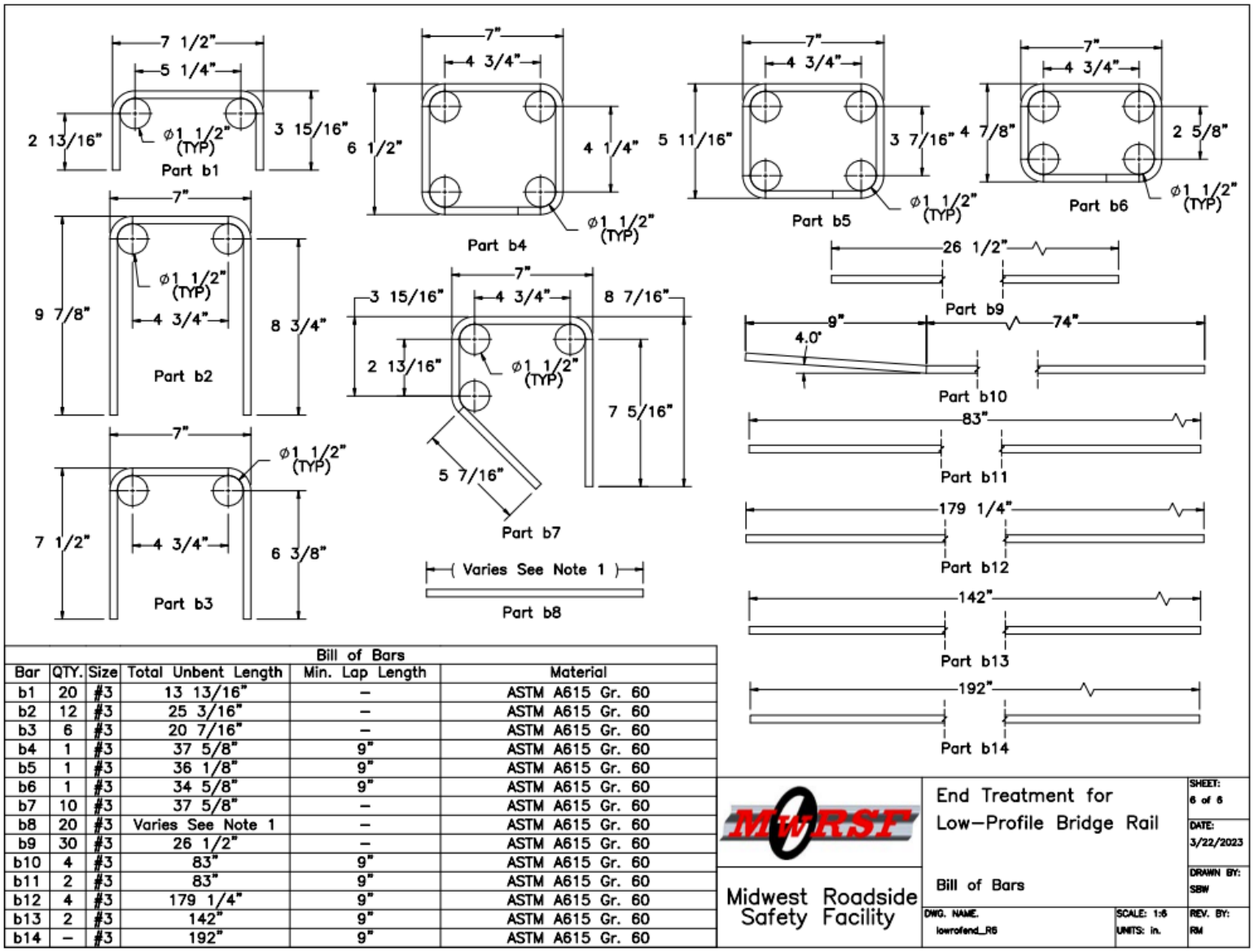

Bill of Bars

Bar	QTY.	Size	Total Unbent Length	Min. Lap Length	Material
b1	20	#3	13 13/16"	–	ASTM A615 Gr. 60
b2	12	#3	25 3/16"	–	ASTM A615 Gr. 60
b3	6	#3	20 7/16"	–	ASTM A615 Gr. 60
b4	1	#3	37 5/8"	9"	ASTM A615 Gr. 60
b5	1	#3	36 1/8"	9"	ASTM A615 Gr. 60
b6	1	#3	34 5/8"	9"	ASTM A615 Gr. 60
b7	10	#3	37 5/8"	–	ASTM A615 Gr. 60
b8	20	#3	Varies See Note 1	–	ASTM A615 Gr. 60
b9	30	#3	26 1/2"	–	ASTM A615 Gr. 60
b10	4	#3	83"	9"	ASTM A615 Gr. 60
b11	2	#3	83"	9"	ASTM A615 Gr. 60
b12	4	#3	179 1/4"	9"	ASTM A615 Gr. 60
b13	2	#3	142"	9"	ASTM A615 Gr. 60
b14	–	#3	192"	9"	ASTM A615 Gr. 60

MwRSF
Midwest Roadside Safety Facility

End Treatment for Low–Profile Bridge Rail

Bill of Bars

DWG. NAME. lowrofend_R6
SCALE: 1:6
UNITS: in.
SHEET: 6 of 6
DATE: 3/22/2023
DRAWN BY: SBW
REV. BY: RM

Figure 27. Modified NDOR Bridge Railing System, Bill of Bars

4.3 Discussion of Results

Table 6 summarizes the punching shear and yield-line capacities of the NDOR and USDA-FS-NTDP barrier shapes. At the interior region of the USDA-FS-NTDP, the controlling limit state occurs due to yield-line failure. The resulting 35.1-kip lateral capacity was slightly higher than the targeted 35-kip strength necessary for resisting TL-2 lateral impacts. From Table 6, it can also be observed that the modified barrier shape at an end region was also controlled by yield-line failure over punching shear. At the end region, the controlling lateral capacity of the barrier was 41.0 kips, which was above the targeted 35-kip lateral capacity, while still remaining relatively close to the targeted capacity. In summary, the bridge rail modifications to the NDOR Bridge Rail reduced the lateral capacities at the interior and end regions to be slightly higher than the targeted 35-kip lateral capacity, resulting in a design deemed adequate for use under MASH TL-1 impact conditions.

Table 6. Comparison of NDOR and USDA-FS-NTDP Bridge Rail Capacities

Limit State	Barrier Version		
	NDOR Bridge Rail	USDA-FS-NTDP Barrier, Interior Region	USDA-FS-NTDP Barrier, End Region
Yield-line (kips)	44.2	35.1	41.0
Punching Shear (kips)	137.5	77.4	67.8

5 CONCRETE DECK AND RAIL REINFORCEMENT DESIGN

5.1 Bridge Rail to Deck Connection Details

The connection between the USDA-FS-NTDP bridge rail and deck was also investigated during this project. Two separate connection designs were developed to accommodate the range of deck thicknesses. The first connection was designed to accommodate thinner decks with only a single reinforcing mat of steel, while the second connection was designed for thicker decks configured with two steel mats. The design for connecting the USDA-FS-NTDP bridge rail to a single mat deck is shown in Figure 28(a). In this connection, the No. 3 vertical bars in the rail were bent at the ends into L-shaped hooks, which then tied into the sides of the transverse steel in the deck. An example of the design for the USDA-FS-NTDP bridge rail connection to a double mat deck is shown in Figure 28(b). In this connection, the No. 3 vertical bars in the rail were bent at the ends into L-shaped hooks, which then tied into the sides of the transverse steel on the bottom mat.

5.2 Deck Reinforcement Patterns

Longitudinal and transverse reinforcement details were also developed for the single and double mat decks. In the single mat configuration, the longitudinal bars were placed above the transverse steel in order to prevent upward prying action resulting from errant vehicles impacting the bridge rail. As seen in Figure 28(a), the two exterior most spacings of the longitudinal bars are specified as 3½ and 3 in. These specific spacings were designated for the longitudinal bars to provide tie-in locations for the transverse steel in the deck and for the vertical bars in the USDA-FS-NTDP bridge rail. Spacing on the longitudinal bars used for tie-in locations were given a variable spacing of "X" as it is expected that the design engineer will complete the final configuration constructing the deck.

In the double mat deck, the longitudinal bars were placed beneath transverse steel in the top mat and above the transverse steel in the bottom mat. Spacing of the longitudinal bars directly beneath the USDA-FS-NTDP bridge rail was dictated primarily by the locations in which the longitudinal bars would allow for easy tie-in locations to the transverse steel in the deck. Beyond this location, the spacing of the longitudinal bars were given a variable spacing of "X" for both the top and bottom mats of steel as it is expected that the design engineer will complete the final configuration constructing the deck. In the example design drawing of the double mat, the top mat of transverse steel utilized a U-shaped hook, which then tied into the transverse steel in the bottom mat. The U-shaped hook was implemented to address development length concerns of the transverse steel in the deck.

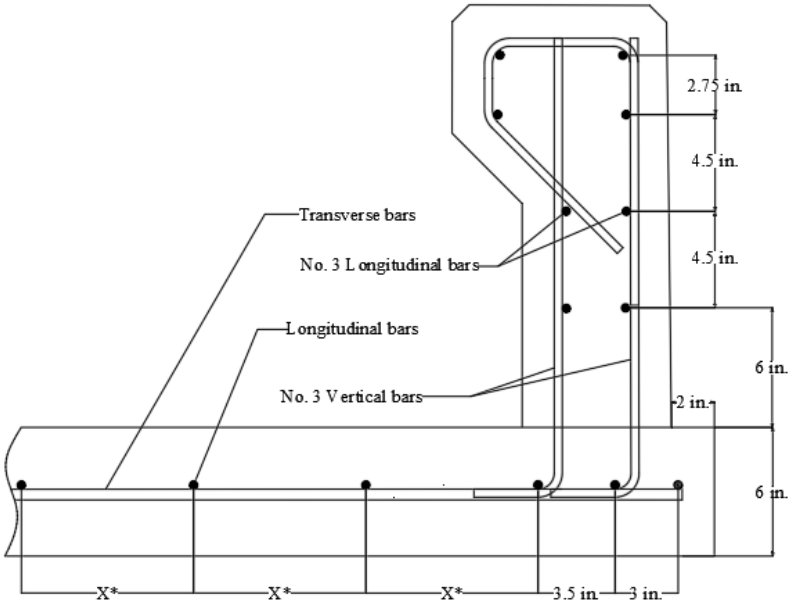

(a) Single Mat Deck

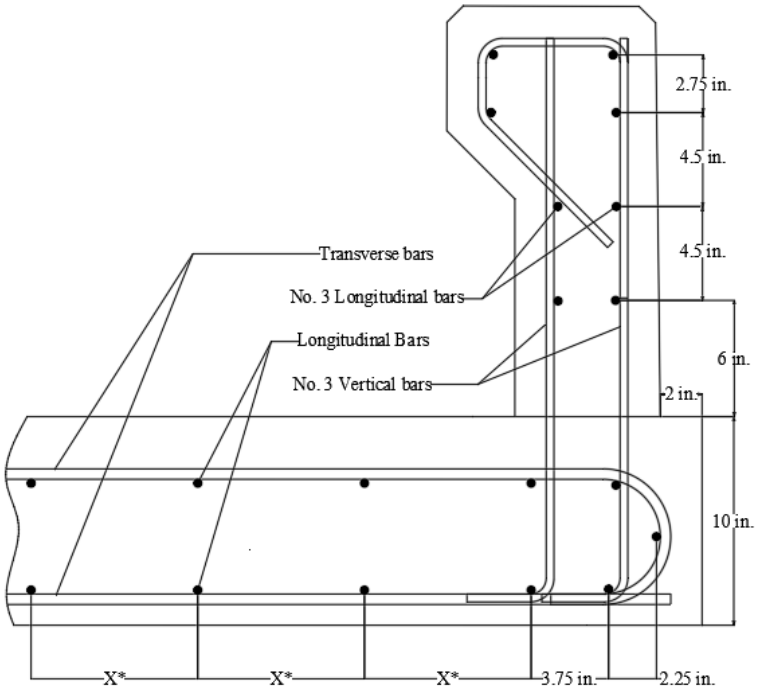

(b) Double Mat Deck

Figure 28. Reinforcement Details for USDA-FS-NTDP on (a) Single Mat Deck and (b) Double Mat Deck

5.2.1 U-Shaped Hook Geometry

Double mat decks can have a wide range of deck thicknesses. Therefore, accommodations to the hook geometry were made such that an increase or decrease in deck thickness would still allow the hook to tie into the bottom mat of transverse steel. For the scope of this project, double mat decks were limited to a range of 7 to 10 in. and were examined at 1-in. increments. To aid in the design of the U-shaped hooks required for different deck thickness, Chapter 25 of the ACI 318 manual was consulted [19]. The ACI 318 manual specifies that for a No. 4 or No. 5 bar, the minimum bend diameter of a U-shaped hook must be 3 and 3¾ in., respectively. Due to the required minimum bend diameter for the No. 4 and 5 bars analyzed for the double mat decks, some deck thicknesses were too small to fit the standard hooks into the deck when oriented vertically. In these instances, the hook was rotated about its cross-sectional end. In instances where the minimum bend diameter was smaller than the vertical space available in the deck, the hook was simply bent to match the size of the vertical space available in the deck. The different required bend diameters for the No. 4 and 5 bars are summarized in Table 7. Figure 29 shows an example of a rotated U-shaped hook bar

Table 7. U-Shaped Hook Geometry for Double Mat Decks

Deck Thickness (in.)	Largest allowable inside bend diameter for a given deck thickness			
	Available space for diameter bend using a 0-degree turn (in.)	Required bend diameter (in.) and turn angle, Φ (degrees)	Available space for diameter bend using a 0-degree turn (in.)	Required bend diameter (in.) and turn angle, Φ (degrees)
10	5.5	5.5 @ 0	5.25	5.25 @ 0
9	4.5	4.5 @ 0	4.25	4.25 @ 0
8	3.5	3.5 @ 0	3.25	3.75 @ 30
7	2.5	3 @ 24	2.25	3.75 @ 53

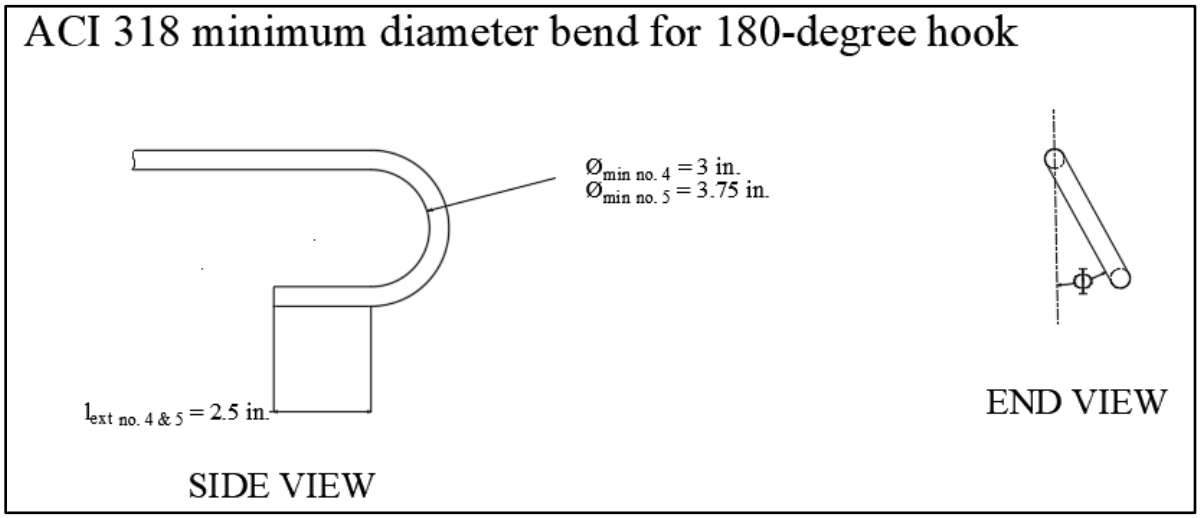

Figure 29. Transverse Bar Hook Geometry

5.2.2 Deck Bar Development Length

Given the relatively narrow bottom barrier width and the small deck offset, there was concern regarding the bridge rail's ability to expect full development from the No. 4 and 5 straight transverse deck bars at design section 1-1. To investigate this potential issue, the development lengths required for a No. 4 and 5 straight bars were determined utilizing Equation 3 from the ACI 318 design manual [19].

$$l_d = \left(\frac{3}{40} \frac{f_y}{\lambda \sqrt{f_c'}} \frac{\Psi_t \Psi_e \Psi_s \Psi_g}{\left(\frac{c_b + K_{tr}}{d_b} \right)} \right) d_b \qquad \text{Equation 3}$$

where f_y is the yield stress, λ is the lightweight modification factor, Ψ_t is the casting position factor, Ψ_e is the epoxy modification factor, Ψ_s is the size modification factor, Ψ_g is the reinforcement grade modification factor, c_b is the minimum clear cover factor, K_{tr} is the confinement term, and d_b is the bar diameter.

No. 4 and No. 5 bars were evaluated based on the literature review that was conducted, which indicated that these bar sizes would be reasonable in concrete decks used to support TL-1 bridge rail systems. The resulting development lengths of the No. 4 and 5 bars were determined as 12.1 and 16.1 in., respectively. Given the modified 7-in. bottom barrier width and the barrier position relative to the deck edge, only 7½ in. of transverse bar length was available for development length. Therefore, insufficient development length would be available to fully utilize the reinforcement at section 1-1 in the deck. Figure 30 provides a side by side comparison of the available space in the deck to develop a No. 4 straight bar versus the actual length needed to develop the No. 4 straight bar. Figure 31 provides a side by side comparison of the available space in the deck to develop a No. 5 straight bar versus the actual length needed to develop the No. 5 straight bar

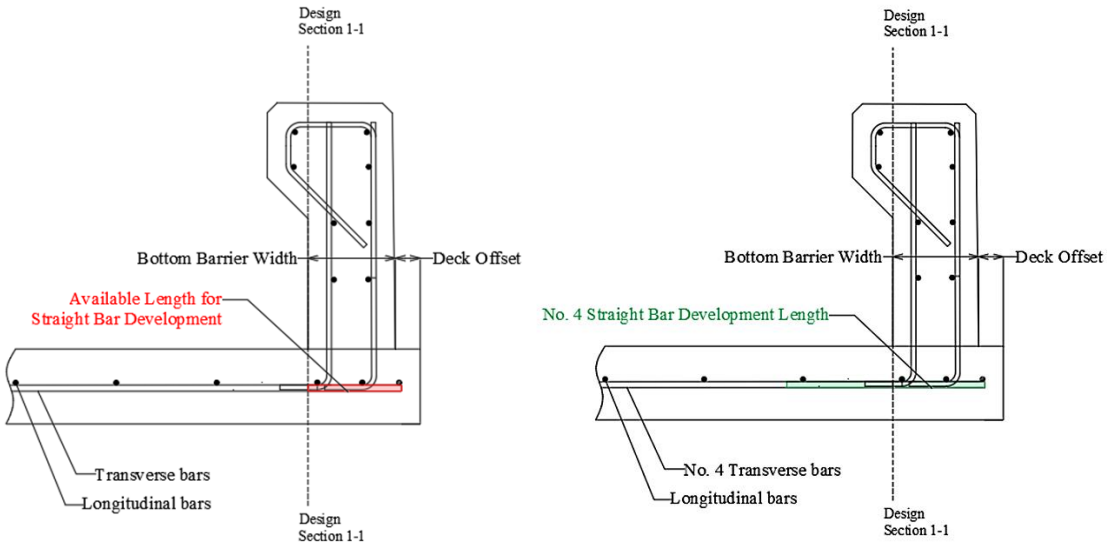

Figure 30. Comparison on No. 4 Bar Available Development Length to Actual Development Length

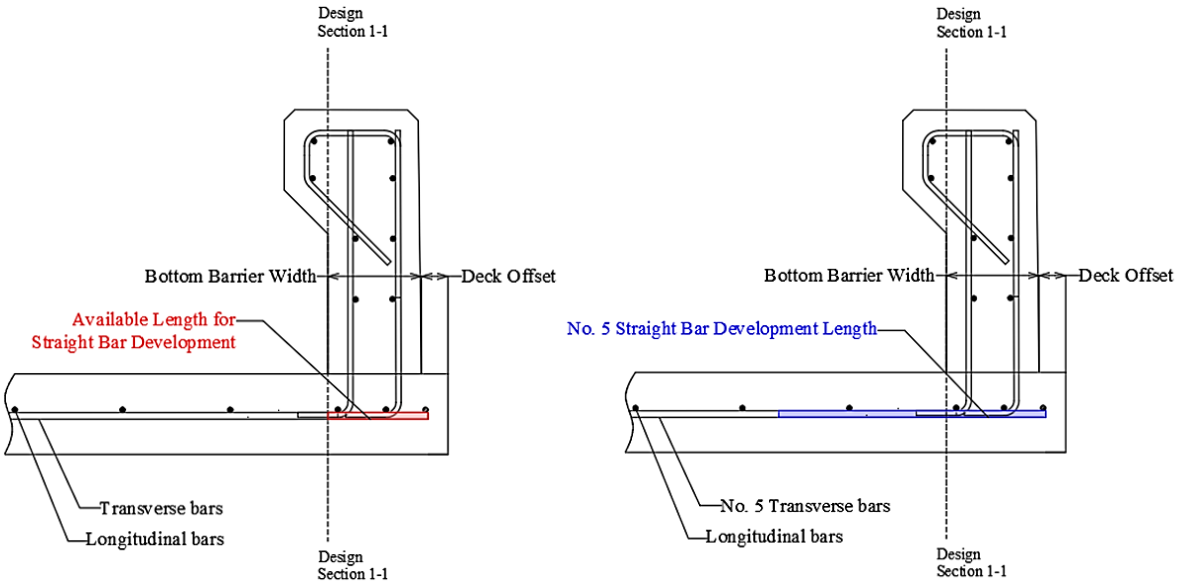

Figure 31. Comparison on No. 5 Rebar Available Development Length to Actual Development Length

6 CONCRETE DECK DESIGN CASES

6.1 Summary of Design Cases 1, 2, and 3

After modifying the barrier, several different deck overhang configurations were developed using the design parameters gathered during the literature review. These deck overhang configurations with the USDA-FS-NTDP bridge rail were evaluated using Design Cases 1, 2, and 3 from AASHTO LFRD Bridge Design [6]. Some of the major details which distinguish these design cases from one another are summarized in Table 8, including: (1) the type of loading; (2) the limit state used to assess the deck overhang; and (3) the sections of the deck overhang analyzed for each design case. Figures 32 through 36 show isometric views of a generic bridge rail and deck overhangs being exposed to Case 1 through 3 loading conditions. The equations used to evaluate loading of each design case are further discussed in Appendix C.

Design Cases 1 and 2 were used to analyze the deck overhang and bridge rail under "extreme event" loading scenarios, as shown in Table 8, whereas Design Case 3 analyzed a strength limit state scenario. Extreme event loading scenarios refer to loading in which an errant vehicle impacts the barrier. Design Cases 1 and 2 share additional similarities where the deck overhang sections are both analyzed for strength at design sections 1-1 and 2-2. For the purposes of this project, section 1-1 was considered to be located at the lower traffic-side face of the bridge rail, and section 2-2 was located at the centerline of the exterior most girder. Design Cases 1 and 2 differ from one another in the direction of vehicle impact loading to the bridge rail. In Design Case 1, the errant vehicle inflicts a lateral load into the traffic-side face of the barrier. In Design Case 2, the errant vehicle inflicts a vertical load onto the non-traffic side face top edge of the bridge rail. For Design Cases 1 and 2, the dead load from the deck overhang, deck surfacing, and bridge railing, are also evaluated in addition to the collision force loading at design sections 1-1 and 2-2. In contrast to Design Cases 1 and 2, the loading in Design Case 3 is used to assess a strength limit state scenario. As opposed to representing vehicle impact scenarios, Design Case 3 is used to evaluate a scenario in which vehicles are stalled toward the edge of the cantilever section of a bridge deck. To represent the loading of stalled vehicles at the deck edge, a uniform 1-kip/ft line load is applied 1 ft away from interior most face of the bridge rail. The applied loads considered in Design Case 3 are the dead loads from the bridge deck, any surfacing, and the bridge rail, plus the live loads from the stalled vehicles, as shown in Table 8. Additionally, only section 2-2 is analyzed for strength in Design Case 3. Further discussion of Deck Design Cases 1, 2, and 3 are provided in Appendix C.

Table 8. Deck Loading Design Cases 1, 2, and 3

Design Case	Applied Loads	Limit State	Design Location(s)
1	Horizontal Collision Force	Extreme Event	1-1, 2-2
2	Vertical Collision Force	Extreme Event	1-1, 2-2
3	Dead and Live Loads	Strength	2-2

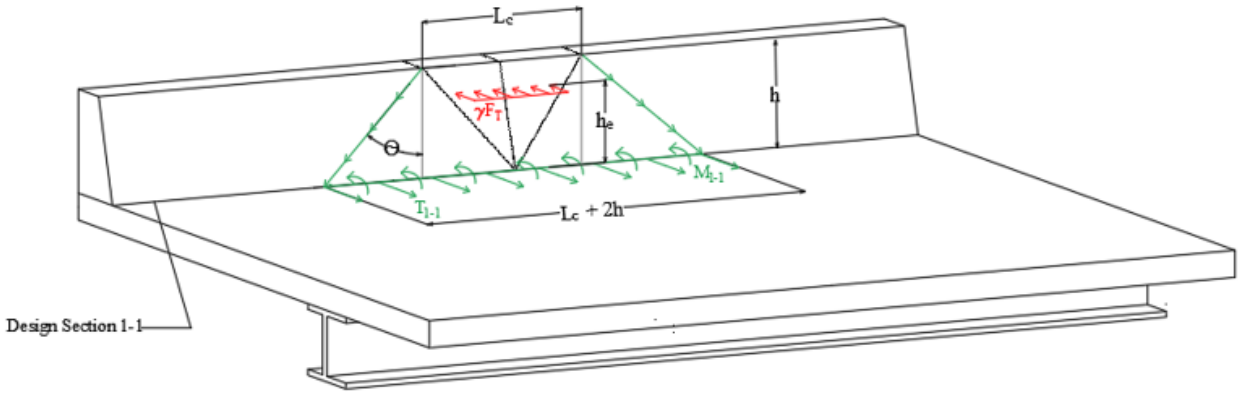

Figure 32. Generic Bridge Rail Deck Loading - Design Case 1, Section 1-1

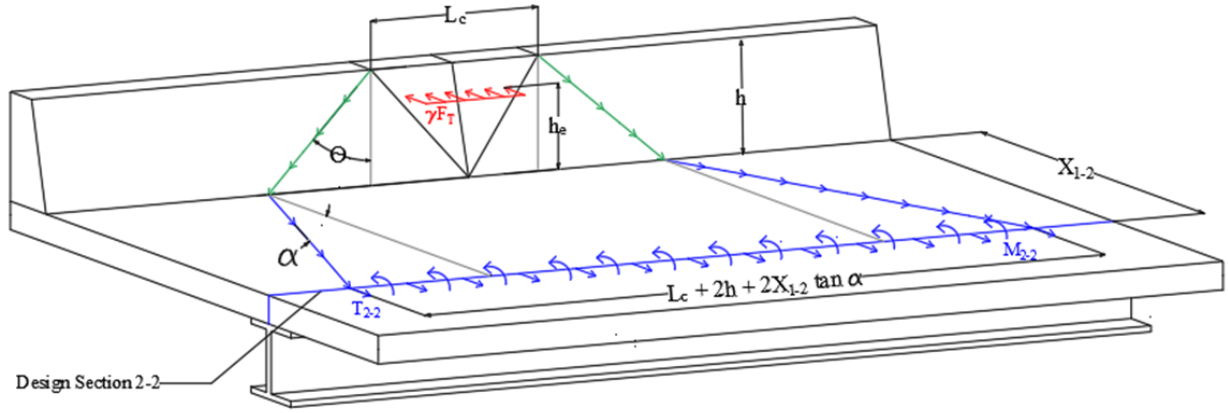

Figure 33. Generic Bridge Rail Deck Loading – Design Case 1, Section 2-2

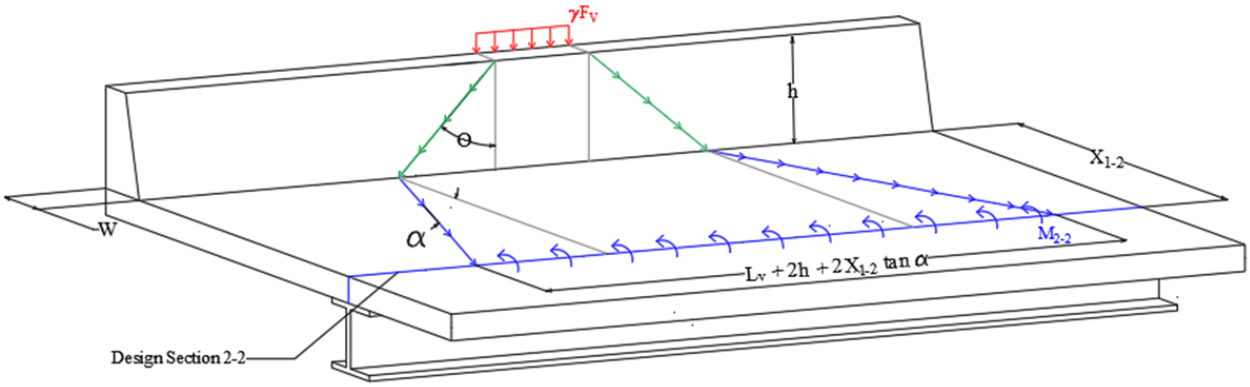

Figure 34. Generic Bridge Rail Deck Loading - Design Case 2, Section 1-1

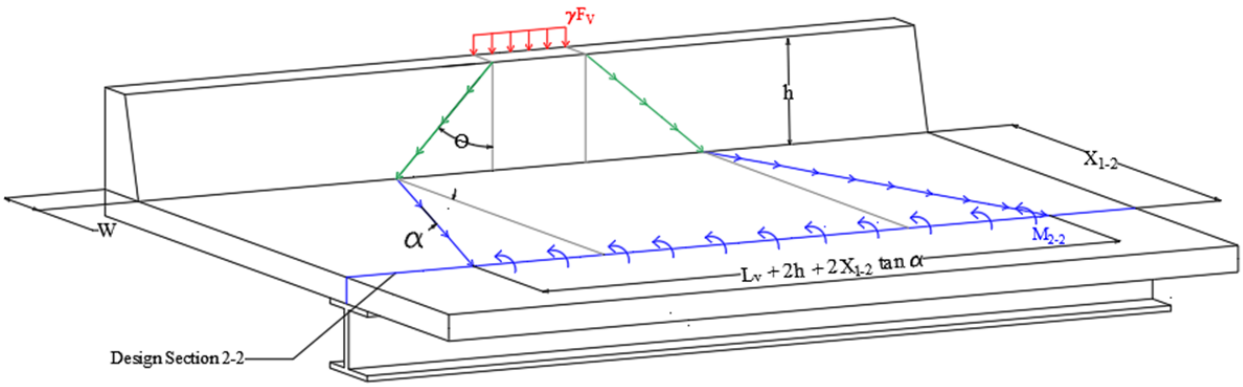

Figure 35. Generic Bridge Rail Deck L

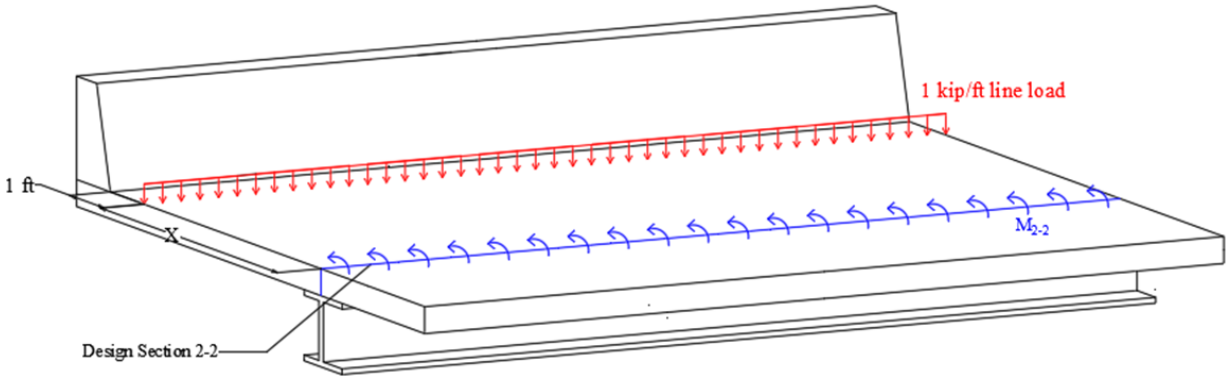

Figure 36. Generic Bridge Rail Deck Loading – Design Case 3, Section 2-2

6.2 Recommended Spacing for Transverse Deck Reinforcement

After analyzing the different bridge deck and rail configurations with Design Cases 1, 2, and 3, recommended spacing of the transverse reinforcement used in each deck and rail configuration were determined. The recommended transverse rebar spacings for the different deck configurations are summarized in Tables 9 through 14, where each table corresponds to a specific deck thickness. Within each table, cantilever lengths ranging from 1 to 5 ft are listed with a corresponding transverse bar spacing shown for an interior and end section for No. 4 and No. 5 bars. The transverse deck spacing column shows two values. The first value is the spacing that is most practical based on the recommended vertical reinforcement in the bridge rail, and the second value, in parentheses, indicates the maximum possible spacing that a given deck could handle. It should be noted that due to the practical transverse deck spacing values in the tables corresponding to the recommended vertical reinforcement in the barrier, any further alterations that change the vertical reinforcement spacing would invalidate the practicality of the results. In these tables, some of the vertical spacing values are bolded. The bold text are instances in which the provided spacing will not result in adequate development length of the transverse deck bars at the edge of the deck if straight bars are utilized. Lastly, note that that the spacing shown in the tables is based on a single mat which utilizes a top clear cover of 2.5 in. and double mat deck whose top and bottom clear covers are 2.5 in. and 1 in., respectively.

Table 9. 6-in. Single-Mat Deck Configurations

Cantilever Length	Section	Controlling Design Case	Transverse Deck Spacing (in.)	
			#4 Bars	#5 Bars
1 ft	Interior	1	**9 (10)**	**9 (16)**
	End	1	**3 (3)**	**3 (5)**
2 ft	Interior	1	**9 (9)**	**9 (14)**
	End	1	**3 (3)**	**3 (5)**
3 ft	Interior	1	**6 (8)**	**9 (13)**
	End	1	**3 (3)**	**3 (5)**
4 ft	Interior	3	3 (4)	6 (6)
	End	2	NA **(2)**	**3 (4)**
5 ft	Interior	3	NA (2)	3 (3)
	End	2	NA **(2)**	**3 (3)**

(1) Numbers in parentheses indicate largest transverse bar spacing for deck.
(2) Deck spacing set up for end and interior barrier vertical bar spacing of 6 in. and 18 in., respectively. NA indicates no spacing will work with current barrier's vertical bar spacing.
(3) Top and bottom clear cover are 2½ and 1 in., respectively.
(4) Bolded numbers indicate decks that need headed or hooked transverse bars to achieve full-development length.
(5) Longitudinal deck bars were not used in deck analysis.

Table 10. 6.5-in. Single Mat Deck Configurations

Cantilever Length	Section	Controlling Design Case	Transverse Deck Spacing (in.)	
			#4 Bars	#5 Bars
1 ft	Interior	1	**9 (12)**	**18 (18)**
	End	1	**3 (4)**	**6 (6)**
2 ft	Interior	1	**9 (11)**	**9 (17)**
	End	1	**3 (4)**	**6 (6)**
3 ft	Interior	1	**9 (10)**	**9 (15)**
	End	1	**3 (4)**	**3 (6)**
4 ft	Interior	3	3 (5)	6 **(8)**
	End	2	**3 (3)**	**3 (5)**
5 ft	Interior	3	3 (3)	3 (4)
	End	2	NA **(2)**	**3 (4)**

(1) Number in parentheses indicate largest transverse bar spacing for deck.
(2) Deck spacing set up for end and interior barrier vertical bar spacing of 6 in. and 18 in., respectively. NA indicates no spacing will work with current barrier's vertical bar spacing.
(3) Top and bottom clear cover are 2½ and 1 in., respectively.
(4) Bolded numbers indicate decks that need headed or hooked transverse bars to achieve full-development length.
(5) Longitudinal deck bars were not used in deck analysis.

Table 11. 7-in. Double-Mat Deck Configurations

Cantilever Length	Section	Controlling Design Case	Transverse Deck Spacing (in.)	
			#4 Bars	#5 Bars
1 ft	Interior	1	**18 (20)**	**18 (31)**
	End	1	**6 (6)**	**6 (10)**
2 ft	Interior	1	**18 (18)**	**18 (28)**
	End	1	**6 (6)**	**6 (9)**
3 ft	Interior	1	9 **(15)**	**18 (24)**
	End	1	**6 (6)**	**6 (9)**
4 ft	Interior	3	6 (6)	9 (10)
	End	2	**3 (5)**	**6 (8)**
5 ft	Interior	3	3 (4)	6 (6)
	End	2	**3 (3)**	**6 (6)**

(1) Number in parentheses indicate largest transverse bar spacing for deck.
(2) Deck spacing set up for end and interior barrier vertical bar spacing of 6 in. and 18 in., respectively. NA indicates no spacing will work with current barrier's vertical bar spacing.
(3) Top and bottom clear cover are 2½ and 1 in., respectively.
(4) Bolded numbers indicate decks that need headed or hooked transverse bars to achieve full-development length.
(5) Longitudinal deck bars were not used in deck analysis.

Table 12. 8-in. Double-Mat Deck Configurations

Cantilever Length	Section	Controlling Design Case	Transverse Deck Spacing (in.)	
			#4 Bars	#5 Bars
1 ft	Interior	1	**18 (23)**	**18 (36)**
	End	1	**6 (8)**	**6 (12)**
2 ft	Interior	1	**18 (21)**	**18 (33)**
	End	1	**6 (7)**	**6 (12)**
3 ft	Interior	1	**18 (18)**	**18 (28)**
	End	1	**6 (7)**	**6 (12)**
4 ft	Interior	3	9 (9)	9 (14)
	End	2	**6 (7)**	**6 (11)**
5 ft	Interior	3	3 (5)	6 (8)
	End	2	3 **(5)**	**6 (7)**

(1) Number in parentheses indicate largest transverse bar spacing for deck.
(2) Deck spacing set up for end and interior barrier vertical bar spacing of 6 in. and 18 in., respectively. NA indicates no spacing will work with current barrier's vertical bar spacing.
(3) Top and bottom clear cover are 2½ and 1 in., respectively.
(4) Bolded numbers indicate decks that need headed or hooked transverse bars to achieve full-development length.
(5) Longitudinal deck bars were not used in deck analysis.

Table 13. 9-in. Double-Mat Deck Configurations

Cantilever Length	Section	Controlling Design Case	Transverse Deck Spacing (in.)	
			#4 Bars	#5 Bars
1 ft	Interior	1	**18 (26)**	**18 (41)**
	End	1	**6 (9)**	**6 (14)**
2 ft	Interior	1	**18 (24)**	**18 (36)**
	End	1	**6 (9)**	**6 (14)**
3 ft	Interior	1	**18 (21)**	**18 (33)**
	End	1	**6 (9)**	**6 (14)**
4 ft	Interior	3	9 (10)	9 (16)
	End	2	**6 (8)**	**6 (13)**
5 ft	Interior	3	6 (6)	9 (10)
	End	2	**6 (6)**	**6 (9)**

(1) Number in parentheses indicate largest transverse bar spacing for deck.
(2) Deck spacing set up for end and interior barrier vertical bar spacing of 6 in. and 18 in., respectively. NA indicates no spacing will work with current barrier's vertical bar spacing.
(3) Top and bottom clear cover are 2½ and 1 in., respectively.
(4) Numbers with asterisks indicate decks that need headed or hooked transverse bars to achieve full-development length.
(5) Longitudinal deck bars were not used in deck analysis.

Table 14. 10-in. Double-Mat Deck Configurations

Cantilever Length	Section	Controlling Design Case	Transverse Deck Spacing (in.)	
			#4 Bars	#5 Bars
1 ft	Interior	1	**18 (29)**	18 **(45)**
	End	1	**6 (10)**	6 **(16)**
2 ft	Interior	1	**18 (26)**	18 **(42)**
	End	1	**6 (10)**	6 **(16)**
3 ft	Interior	1	**18 (23)**	18 **(37)**
	End	1	**6 (10)**	6 **(16)**
4 ft	Interior	3	9 (12)	18 (19)
	End	2	**6 (9)**	6 **(15)**
5 ft	Interior	3	6 (7)	9 (12)
	End	2	**6 (7)**	6 **(11)**

(1) Number in parentheses indicate largest transverse bar spacing for deck.
(2) Deck spacing set up for end and interior barrier vertical bar spacing of 6 in. and 18 in., respectively. NA indicates no spacing will work with current barrier's vertical bar spacing.
(3) Top and bottom clear cover are 2½ and 1 in. respectively.
(4) Numbers with asterisks indicate decks that need headed or hooked transverse bars to achieve full-development length.
Longitudinal deck bars were not used in deck analysis.

7 SUMMARY, CONCLUSIONS, AND RECOMENDATIONS

In this project, the previously-designed, low-height, NCHRP 350 TL-2 bridge railing system was adapted to accommodate only MASH TL-1 impact events by reducing the bridge railing's width and modifying the reinforcement in the barrier. The new bridge railing's strength was evaluated using the yield-line and punching shear equations outlined in the AASHTO LRFD BDS. Next, the barrier's connection details were modified such that it could be attached to bridge deck overhangs. Using a range of typical deck thicknesses and overhang lengths, multiple bridge rail and deck configurations were assessed for strength using Design Cases 1, 2, and 3.

Based on this evaluation, it is recommended that the modifications to the bridge railing discussed in Chapter 4 of this report be adopted for use. Additionally, when installing the USDA-FS-NTDP bridge rail onto the edge of a cantilever deck, it is recommended that the transverse deck bar spacings shown in Tables 9 through 14 be followed in order that the vertical reinforcement in the bridge rail can easily tie into transverse deck steel. Values shown in red text, indicate that development length of straight transverse deck bars will be a concern. When red text is shown, it is recommended that a headed or hooked end bar be utilized to in place of the straight bars to decrease bar development length. If neither of those solutions are viable, adding more straight transverse bars to the deck is another option to account for development length concerns.

Lastly, the USDA-FS-NTDP bridge deck and rail also features a sloped end treatment. As discussed previously, the sloped end treatment was configured based on prior research performed by MwRSF and TTI personnel.

8 REFERENCES

1. Ross, H.E., Sicking, D.L., Zimmer, R.A., and Michie, J.D., *Recommended Procedures for the Safety Performance Evaluation of Highway Features*, National Cooperative Highway Research Program (NCHRP) Report 350, Transportation Research Board, Washington, D.C., 1993.

2. Polivka, K.A., Faller, R.K., Sicking, D.L., Rohde, J.R., Reid, J.D., and Holloway, J.C., *Development of a Low-Profile Bridge Rail for Test Level 2 Applications*, Final Report for the Midwest States' Regional Pooled Fund Program, Nebraska Department of Roads, Report No. SPR-3(017), Performing Organization Report No. TRP-03-109-02, Sponsoring Agency Code: RPFP-01-06, Midwest Roadside Safety Facility, University of Nebraska-Lincoln, August 20, 2002.

3. Beason, L.W., Menges, W.L., Ivey, D.L., *Development of a High-Speed Low-Profile End Treatment*, Final Report to the Texas Department of Transportation, Transportation Planning Division, Transportation Research Report No. FHWA/TX-98/1403-S, Project No.: 0-1403, The Texas A&M University System, College Station, Texas, April 1998.

4. Beason, L.W., Brackin, M.S., Bligh, R.P., Menges, W.L., Development and Testing of Non-Pinned Low-Profile End Treatment, Final Report to Texas Department of Transportation, Research and Technology Implementation Office, Transportation NO. FHWA/TX-13/9-1002-12-7, Project No.: 9-1002-12-7, Texas Department of Transportation, Research and Technology Implementation Office, Austin, Texas, October 2013a.

5. *Manual for Assessing Safety Hardware (MASH), Second Edition*, American Association of State Highway and Transportation Officials (AASHTO), Washington, D.C., 2016.

6. *AASHTO LRFD Bridge Design Specifications, 9th Edition*, American Association of State Highway and Transportation Officials (AASHTO), Washington, D.C., 2020.

7. *Bridge Office Policies and Procedures (BOPP)*, Nebraska Department of Roads Bridge Division, Lincoln, Nebraska, 2016.

8. *Sponsor Communications and MwRSF-UNL Research Proposal and Agreement*, United States Department of Agriculture – Forest Service (USDA-FS) and National Technology and Development Program (NTDP), 2022-2021.

9. Polivka, K.A., Faller, R.K., Rohde, J.R., Reid, J.D., Sicking, D.L., and Holloway, J.C., *Safety Performance Evaluation of the Nebraska Open Bridge Rail on an Inverted Tee Bridge Deck*, Final Report to the Nebraska Department of Roads, Project No. TRP-03-133-04, Midwest Roadside Safety Facility, University of Nebraska-Lincoln, January 21, 2004.

10. Rosenbaugh, S.K., DeLone, J.A., Faller R.K., and Bielenberg, R.W., *Development and Testing of a Bridge Rail for Low-Volume Roads*, Final Report for the Nebraska Department of Transportation, Transportation Report No. TRP-03-407-20, Sponsoring Agency Code: RPFP-SG-05, Midwest Roadside Facility, University of Nebraska-Lincoln, September 3, 2020.

11. Rosenbaugh, S.K., Benner, C.D., Faller, R.K., Bielenberg, R.W., Reid, J.D., and Sicking, D.L., *Development of a TL-1 Timber, Curb-Type, Bridge Railing for Use on Transverse, Nail-Laminated, Timber Bridges*, Final Report to the West Virginia Department of Transportation, Transportation Research Report No. TRP 03 211 09, Project No.: WV-09-2007-B1, Sponsor Agency Code: SPR-3(017) Supplement #53, Midwest Roadside Safety Facility, University of Nebraska Lincoln, May 6, 2009.

12. Mongiardini, M, Rosenbaugh, S.K., Faller, R.K., Reid, J.D., Bielenberg, R.W., and Sicking, D.L., *Design and Testing of Two Bridge Railings for Transverse, Nail-Laminated, Timber Deck Bridges*, Paper No. 11-2936, Transportation Research Record No. 2262, Journal of the Transportation Research Board, TRB AFB20 Committee on Roadside Safety Design, Transportation Research Board, Washington D.C., January 2011.

13. Williams, W.F., Bligh, R.B., and Menges, W.L., *MASH Test 3-11 of the TXDOT Single Slope Bridge Rail (Type SSTR) on Pan-Formed Bridge Deck* Technical Report for Texas Department of Transportation, Transportation Report No. FHWA/TX-11/9-1102-3, Project No. 9-1002, Texas A&M Transportation Institute, The Texas A&M University System, March 2011.

14. Williams, W.F., Menges, W.L., Schroeder, W.J.L., Griffith, B.L., Wegenast, S.A., and Kuhn, D.L., *MASH Test 4-12 on T2P Retrofit Bridge Rail*, Technical Report for Texas Department of Transportation, Transportation Report No. FHWA/TX-21/0-7086-R5, Project No. 0-7086, Texas A&M Transportation Institute The Texas A&M University System, August 2021.

15. Arrington, D.R., Bligh, D.P., and Menges, W.L., *MASH Test 3-11 on the 5-inch Barrier Anchors*, Test Report for Texas Department of Transportation, Transportation Research Report No. FHWA/TX-12/9-1002-7, Project No. 9-1002, Texas Transportation Institute Proving Ground, The Texas A&M University System, December 2011.

16. *Manual for Assessing Safety Hardware (MASH), First Edition*, American Association of State Highway and Transportation Officials (AASHTO), Washington, D.C., 2009.

17. Steelman, J.S., *MASH Railing Load Requirement for Bridge Deck Overhang*, Interim Report, Midwest Roadside Safety Facility, University of Nebraska-Lincoln, January 6, 2021, In Progress.

18. Whitfield, D.L., *Investigation of a Tractor-Tank Trailer Roadside Containment Barrier*, Thesis, University of Nebraska-Lincoln, November 29, 2018

19. ACI 318 Building Code Requirements for Structural Concrete (ACI 318-19), Nineteenth Edition, Farmington Hills, MI 48331, 2019.

9 APPENDICIES

Appendix A. Yield -Line Failure Methodology

To determine the capacity of the NDOR Bridge Rail and modified barriers for this project, the barriers' yield line capacity was determined using Section A13 of the AASHTO LRFD Bridge Design Specifications. Equations A13.3.1-1 and A13.3.1-3 provide the barrier's yield-line capacity at interior and end regions, respectively. The equations from AASHTO are provided as:

$$R_w = \left(\frac{2}{2L_c - L_t}\right) \cdot \left(8M_b + 8M_w + \frac{M_c L_c^2}{H}\right) \qquad Eq: A13.3.1-1$$

$$R_w = \left(\frac{2}{2L_c - L_t}\right) \cdot \left(M_b + M_w + \frac{M_c L_c^2}{H}\right) \qquad Eq: A13.3.1-3$$

where R_w is the total transverse resistance of the railing, L_c is the critical length of yield line failure, M_b is the additional flexural resistance of the beam in addition to M_w if any, at the top of the wall, M_c is the flexural resistance of the cantilevered walls about an axis parallel to the longitudinal axis of the bridge, M_w is the flexural resistance of the wall about its vertical axis, and H is the height of the wall. To determine the value of L_c, AASHTO provides equations A13.3.1-2 and A13.3.1-4 for the interior and end segment yield-line lengths, respectively. These equations are shown as:

$$L_c = \frac{L_t}{2} + \sqrt{\left(\frac{L_t}{2}\right)^2 \cdot \frac{8H(M_b + M_w)}{M_c}} \qquad Eq: A13.3.1-2$$

$$L_c = \frac{L_t}{2} + \sqrt{\left(\frac{L_t}{2}\right)^2 \cdot \frac{H(M_b + M_w)}{M_c}} \qquad Eq: A13.3.1-2$$

where L_t is the longitudinal length of distribution of impact force. In addition to these equations, AASHTO provides the drawings in Figure A-1. The left image shows yield line failure at an interior segment, while the right image shows a yield-line mechanism at an end section of a barrier.

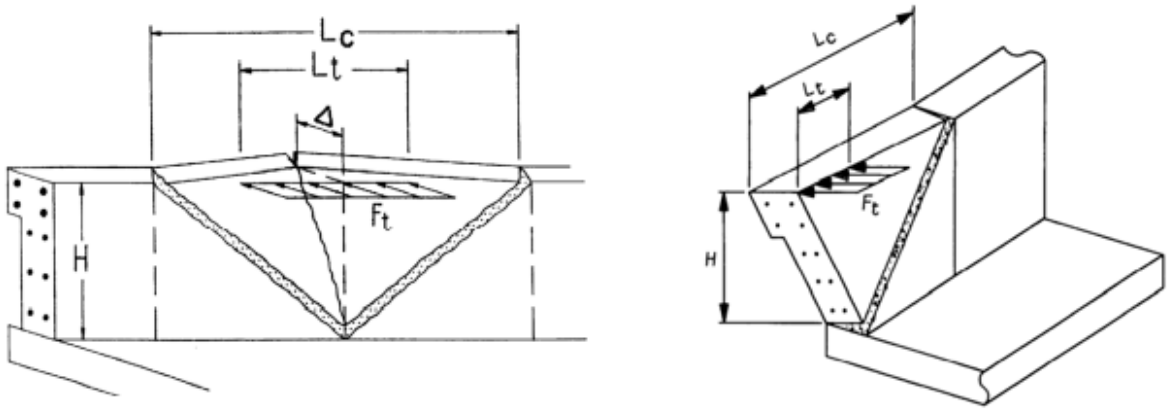

Figure A-1. Barrier Yield-Line Failure at Interior and End Sections

Note the yield-line failure shape resembles a tringle. While other yield-line failure shapes can be utilized to assess a barrier's yield-line capacity, the most current version of AASHTO uses equations which reflect a triangular yield-line failure. To remain consistent with AASHTO, a triangular yield-line shape was used to determine the NDOR and USDA-FS-NTDP Bridge Rail capacities.

Determination of M_b, M_w, and M_c

Due to the non-uniform shape of the bridge rail in question determining which portions of the bridge contributed to the M_b, the M_w, and M_c capacities required engineering judgement. After discussion with the design team, the regions for these three barrier capacities were divided into the configurations shown in Figure A-2(a) and (b) for the NDOR and USDA-FS-NTDP Bridge Rail shapes, respectively. In both figures, the design drawing on the left shows the areas of the barriers used to determine the M_b and M_w capacities of the bridge rail, and the right-hand images show the areas used to find the barrier's M_c capacity. The right-hand images show that the capacity of M_c has been divided into $M_{c\ Top}$ and $M_{c\ Bottom}$. Dividing the capacity for M_c into two sections was necessary to account for the two different barrier thicknesses. After dividing M_c into two sections, both capacities were determined and the lesser of the two values was utilized as M_c. The orange triangle in Figure A-2(a) and (b) shows the portion of the bridge that was not considered when assessing the barrier strength. Removing this section of the bridge rail allowed for a simplified analysis that provided a more conservative strength estimate. After establishing which portions of the barrier contributed toward the capacities of M_b, M_w, and M_c, the resultant capacities are provided in Table A-1.

After determining the values of M_b, M_w, and M_c, the NDOR bridge rail's yield-line capacity was found to be 43.3 kips. The USDA-FS-NTDP bridge rail's yield-line capacity at interior and end regions was also determined as 35.1 kips and 41.0 kips, respectively. It should also be noted that after utilizing AASHTO equations A13.3.1-1 and A13.3.1-3 to find the yield-line capacities, no additional modifications factors to the strength were given. Therefore, these capacities reflect the nominal yield-line strengths of the NDOR and USDA-FS-NTDP Bridge Rail.

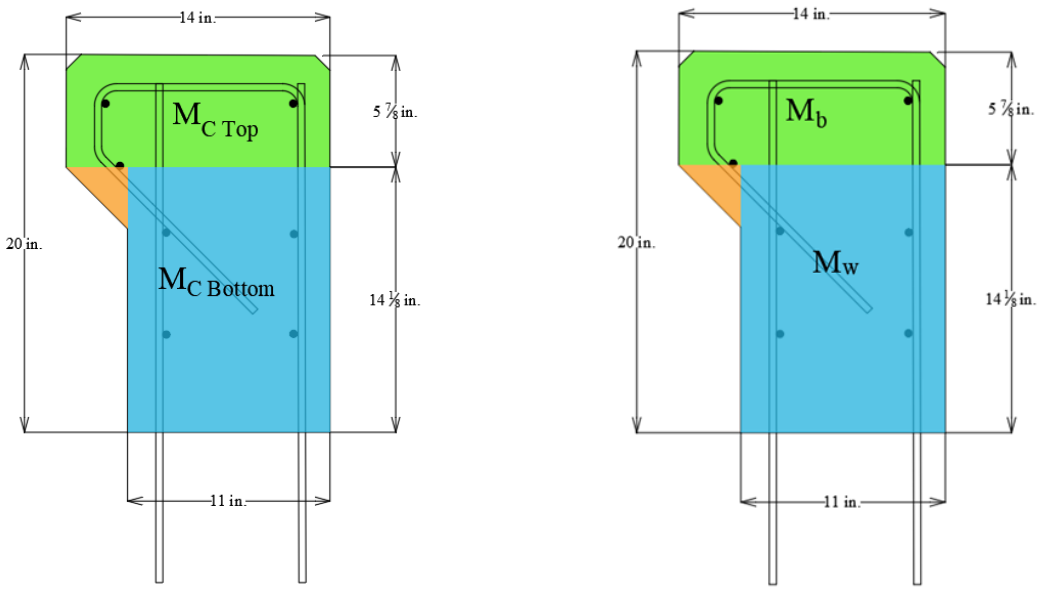

(a) Division of M_b, M_w, and M_c in NDOR Bridge Rail

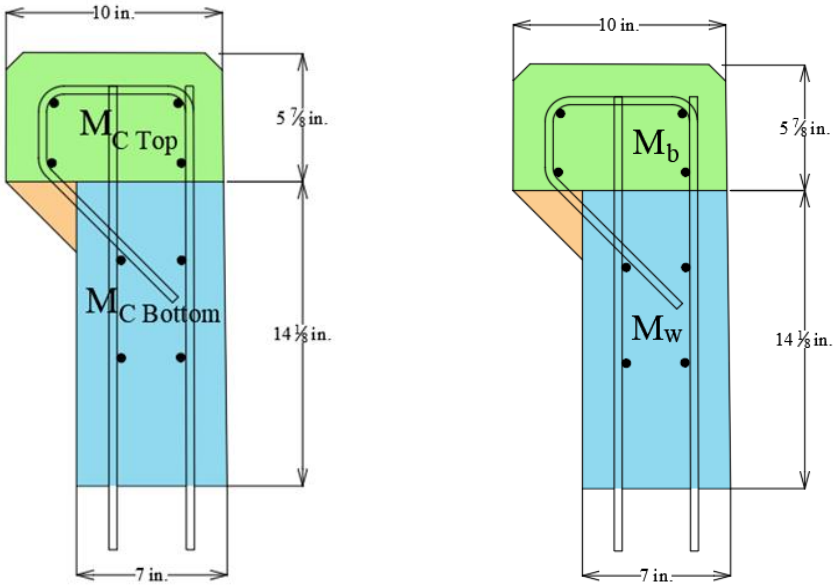

(b) M_b, M_w, and M_c in MT-USFS Bridge Rail

Figure A-2. Division of M_w, M_b, and M_c for (a) NDOR and (b) USDA-FS-NTDP Bridge Rail

Table A-1. Capacities of M_b, M_w, and M_c for NDOR and USDA-FS-NTDP Bridge Rails

Barrier Version	M_w (kip-ft)	M_w (kip-ft)	M_c (kip-ft/ft)
NDOR			
USDA-FS-NTDP Interior	9.6	7.2	2.5
USDA-FS-NTDP End			

Appendix B. Punching Shear Failure

Punching shear was another limit state evaluated to assess the strength of the NDOR and USDA-FS-NTDP bridge rail for this project. Similar to the yield-line limit state, failure due to punching shear also occurs due to lateral loading in the barrier system. Most typically this limit state controls barriers that have thin walls. While the NDOR and USDA-FS-NTDP bridge rails had thicker walls, their capacities were still determined for completeness.

To begin, the punching shear analysis utilized the AASHTO LRFD BDS. Guidance provided in AASHTO allows for three different punching shear scenarios to be considered, each of which yield a slightly different capacity estimate. To ensure the most conservative punching shear capacity was considered and selected in the analysis of the NDOR barrier, all scenarios outlined in AASHTO were analyzed. After determining which of the three punching shear scenarios provided the most conservative design for the NDOR bridge rail, that same punching shear scenario was used to evaluate the capacity of the USDA-FS-NTDP barrier shape.

Section 5 is the first instance in AASHTO which accounts for punching shear. This instance of punching shear occurs due to loading of a beam ledge. Figure B-1 provides the image used by AASHTO to depict this scenario. The left-hand image provides a side view, and the image on the right provides a top view.

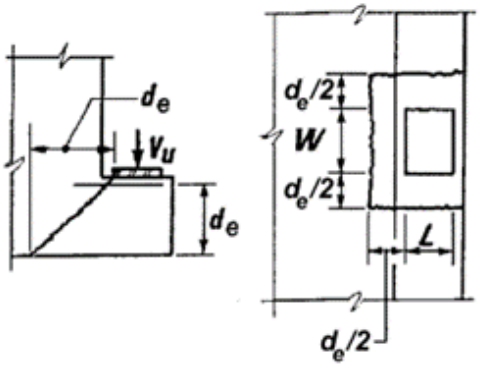

Figure B-1. Beam on a Ledge Punching Shear

AASHTO equations 5.13.2.5.4-1 and 5.13.2.5.4-2 represent the barrier's interior and end punching shear capacities for a beam-ledge scenario:

$$V_n = 0.125\sqrt{f_c'}(W + 2L + d_e) \cdot d_e \qquad Eq: 5.13.2.5.4 - 1$$

$$V_n = 0.125\sqrt{f_c'}(W + L + d_e) \cdot d_e \qquad Eq: 5.13.2.5.4 - 2$$

where V_n is the nominal punching shear resistance, f'_c is the specified strength of concrete at 28 days, W is the width of the bearing plate or pad, L is the length of the bearing pad, and d_e is the effective depth from extreme compression fiber to centroid of tensile force.

For the purposes of barrier analysis, the bearing plate shown in Figure B-1 was replaced with the section of the car that would impact the barrier during a MASH TL-1 impact event. Figure

B-2 illustrates how the beam on a ledge punching shear case was represented on the NDOR barrier system during analysis. Using AASHTO's beam on ledge punching shear equation resulted in a barrier capacity of 242.0 kips for the interior section of the barrier. This value, as well as the values obtained from the remaining punching shear analyses, are summarized in Table B-1. Table B-1 also provides all relevant dimensions used to determine the punching shear capacities.

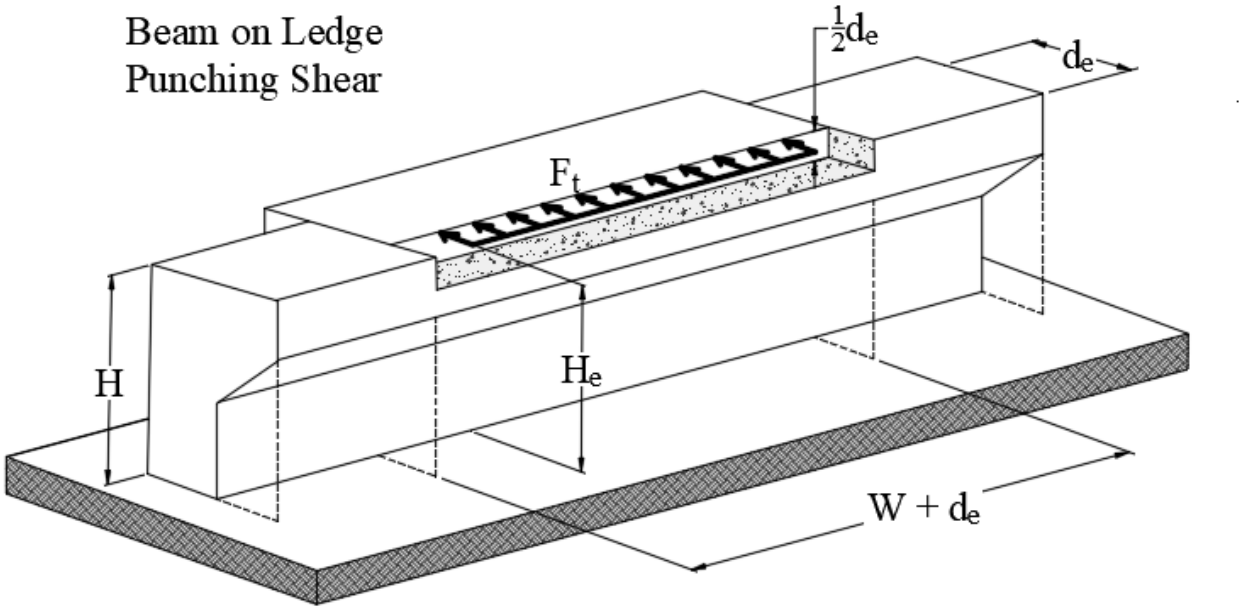

Figure B-2. Beam on a Ledge Punching Shear

Another punching shear scenario provided in AASHTO occurs on a two-way slab. Equation 5.13.3.6.3 was used to determine the two-way slab punching shear capacity in the barrier:

$$V_n = \left(0.063 + \frac{0.126}{\beta_c}\right)\sqrt{f_c'} \cdot b_o \cdot d_v \leq 0.126\sqrt{f_c'} \cdot b_o \cdot d_v \qquad Eq: 5.13.3.6.3 - 3$$

where β_c is the ratio of the long side to the short side of the shear patch, b_o is the perimeter of the critical section, and d_v is the effective shear depth. Figure B-3 outlines the lengths which make up the b_o dimension on the NCHRP TL-2 barrier. After analyzing the barrier using AASHTO's guidance for two-way slab punching shear, a barrier capacity of 147.2 kips was obtained for the interior barrier section.

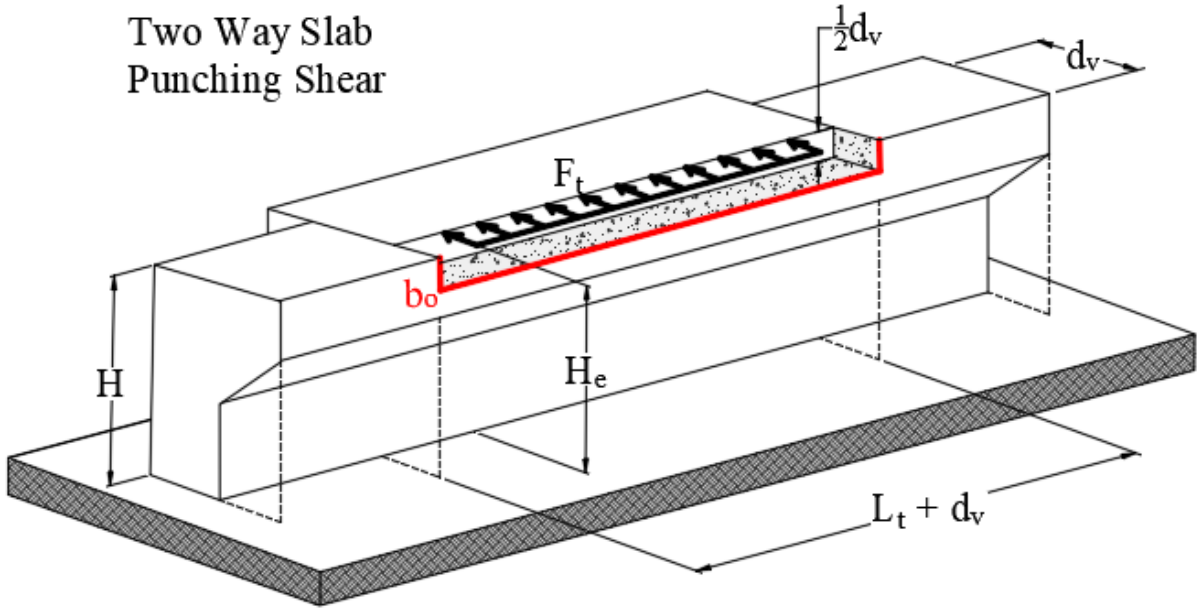

Figure B-3. Two -Way Slab Punching Shear

The last punching shear scenario occurs on a post-and-beam railing system, described in Section A13.4.3.2 in the AASHTO manual and depicted in Figure B-4. In this figure, the top image shows a top view of punching shear at an interior region and the bottom image shows the punching shear from the side.

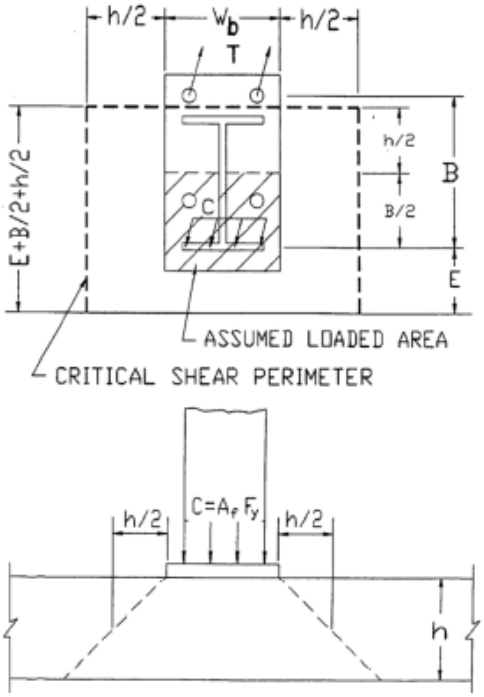

Figure B-4. Post and Beam Punching Shear

AASHTO provided post-and-beam punching shear equation A13.4.3.2-3:

$$V_n = v_c \cdot \left[W_b + h + 2\left(E + \frac{B}{2} + \frac{h}{2}\right)\right] \cdot h \qquad Eq: A13.4.3.2-4$$

where W_b is the width of the base plate, E is the distance from the edge of slab to the centroid of the compressive stress resultant in the post, B is the distance between centroids of the tensile and compressive stress resultants in the post, h is given as the depth of the slab, and v_c is the nominal shear resistance provided by the tensile stresses in concrete which is given as:

$$\left(0.0633 + \frac{0.1265}{\beta_c}\right) \cdot \sqrt{f_c'} \leq 0.1265 \cdot \sqrt{f_c'} \qquad A13.4.3.2-5$$

While the post and beam punching shear provided by AASHTO included the variables E and B in equation A13.4.3.2-3, these variables were not needed during the barrier analysis as there would be no tensile region formed in the barrier during an impact. This assumption, along with all other variables used to find the barrier's capacity for the given scenario, are shown in Figure B-5. The resulting capacity of the barrier in a post-and-beam punching shear scenario was determined to be 175.1 kips.

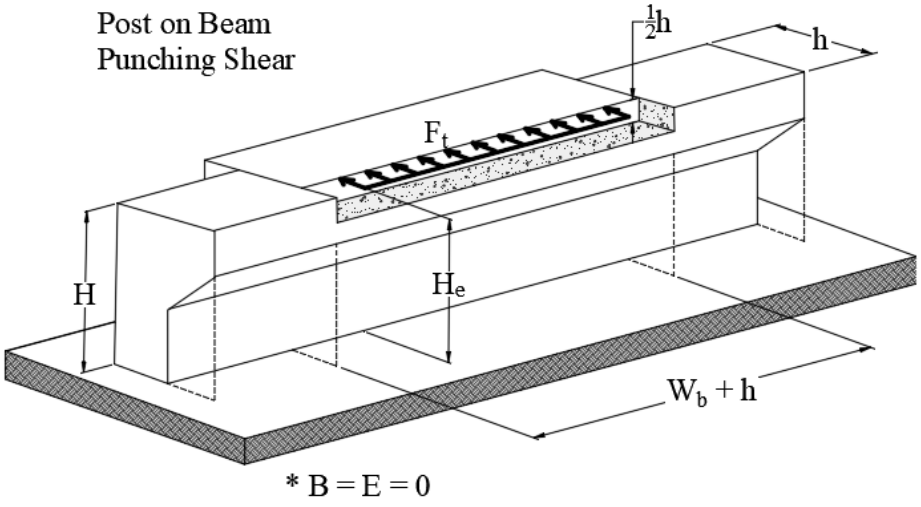

Figure B-5. Post and Beam Punching Shear

Table B-1. Summary of Barrier Punching Shear Capacities at Interior Region

Variable Descriptions	Beam on Ledge	Two-Way Slab	Post and Beam
Length of Shear Patch	60.5 in.	60.5 in.	62 in.
Height of Shear Patch	6.25 in.	6.25 in.	7 in.
Depth of Shear Patch	12.5 in.	12.5 in.	14 in.
Critical Perimeter, b_o	73 in.	73 in.	69 in.
Length to Width Ratio, β_c	NA	9.7	8.9
Reduction Factor	0.125	0.076	0.16
Punching Shear Capacity, V_n	242.0 kips	147.2 kips	175.1 kips

Appendix C. Description of Deck Design Cases 1, 2, and 3

This appendix provides additional discussion of the Design Cases used to analyze the strength of the bridge rail and deck overhang configurations. Figures C-1 through C-10 depict the moment and tensile demands that occur at design sections 1-1 and 2-2 as a result of the dynamic impact loading from Design Cases 1 and 2, and the static loading from Design Case 3. For Design Cases 1 and 2, an isometric view of a generic barrier being loaded according to the appropriate dynamic load is shown in Figures C-1 through C-2 and C-5 through C-6, respectively. Figures C-1 and C-5 show the demand that develops from the design case loading at section 1-1, and Figures C-2 and C-6 provide the demand that develops from the design case loading at section 2-2. The equations utilized to obtain the demands at sections 1-1 and 2-2 are provided for each of these Design Cases, along with the design assumptions of the distribution angles and safety factors used in the equations. It should be noted that while the equations associated with the generic bridge deck and rail drawings account for the dead loads of the deck overhang and bridge rail, the forces from the dead weight loads are not shown in the bridge deck and rail drawings. Figures C-3 through C-4 and C-7 through C-8 for Design Cases 1 and 2, respectively, are side view drawings of the bridge deck and rail system specific to this project. These drawings include the loading specific to each design case in addition to the dead weights that contribute to the moment demand at sections 1-1 and 2-2. For each load, the moment arm developed to transfer the load out to design sections 1-1 and 2-2 are shown in red dimensions.

Because Design Case 3 does not analyze the deck overhang strength at section 1-1, Figures C-9 and C-10 show the same generic bridge deck and rail drawing and side view drawings used to describe Design Cases 1 and 2, followed by the equations and design assumptions used to determine the demand at section 2-2 for Design Case 3.

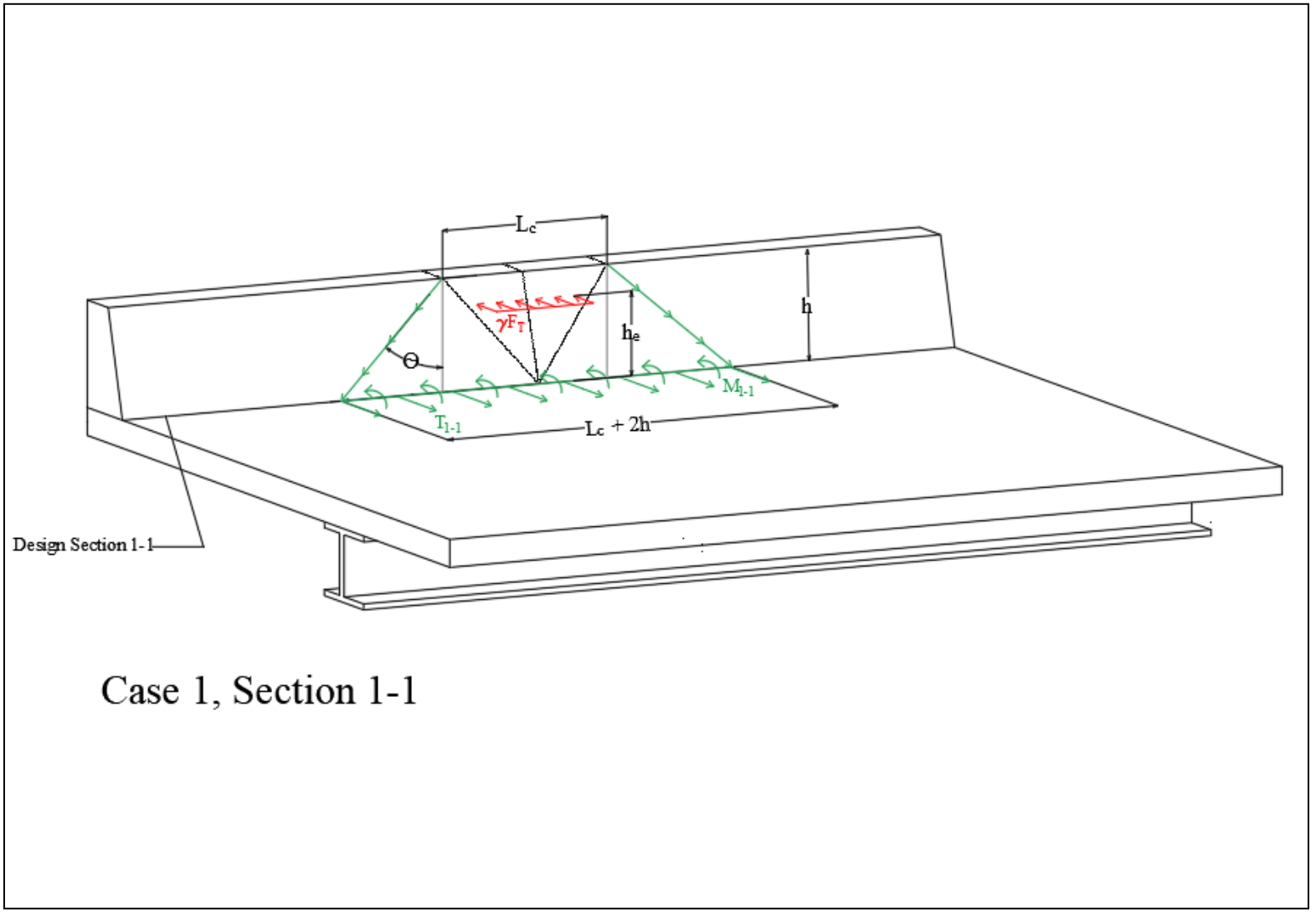

Figure C-1. Generic Bridge Rail for Load Design Case 1, Section 1-1

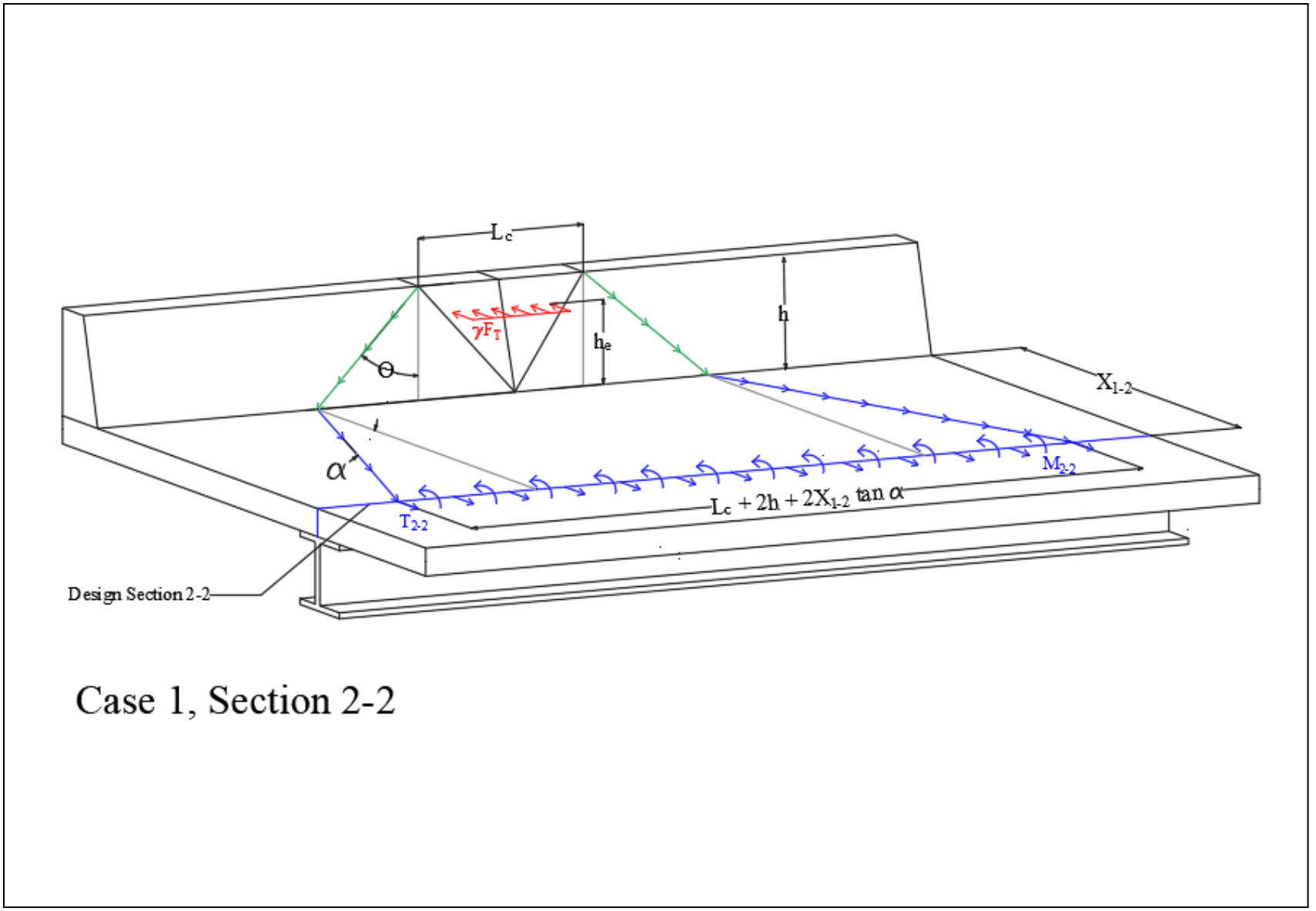

Figure C-2. Generic Bridge Rail for Load Case 1, Section 2-2

Deck Design Case 1 Equations

$$M_{2-2} = min.\left\{\begin{matrix}\frac{\gamma\, F_T H_e}{L_c+2H+2(X_{1-2})tan\alpha} \\ Mc\end{matrix}\right\} + \gamma\left(M_{barrierweight}\right) + \gamma\left(M_{slabweight}\right) \quad \text{Eq: C-1}$$

$$T_{2-2} = \frac{\gamma F_t}{L_c+2H+2(X_{1-2})tan\alpha} \quad \text{Eq: C-2}$$

Description of Variables and Design Assumptions

$X_{1\text{-}2}$ is the distance between critical sections 1-1 and 2-2

Slab distribution angle, α, taken as 45°

Barrier distribution angle, θ, taken as 45°

Load factors, γ, taken as 1

Resistance factor, ϕ, taken as 1

F_t taken as 35 kips

H_e taken as 20 in.

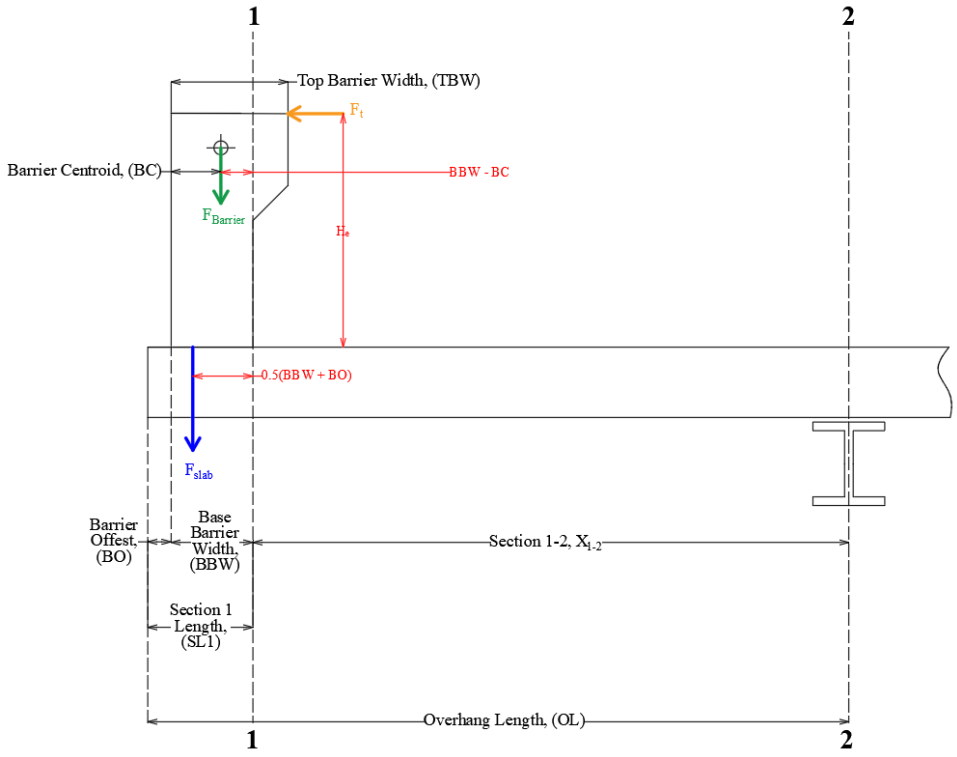

Figure C-3. Side View of Design Case 1, Section 1-1 Impact

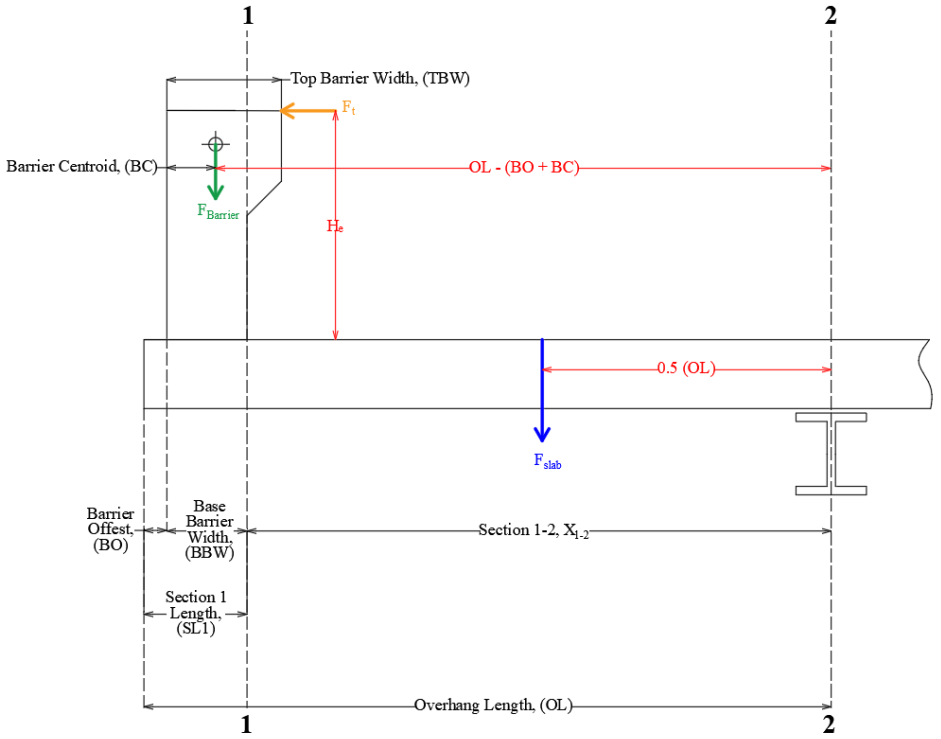

Figure C-4. Side View of Design Case 1, Section 2-2 Impact

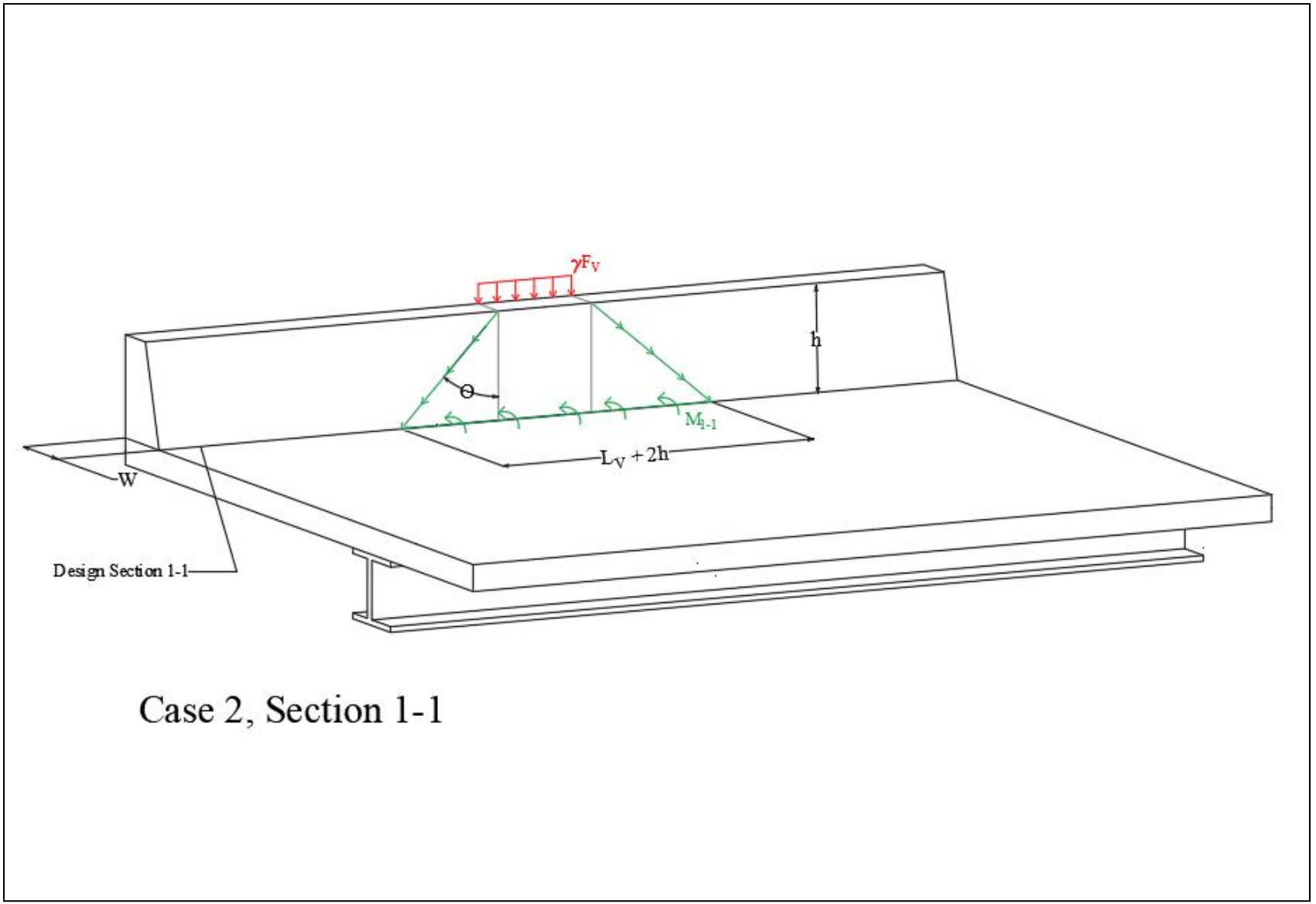

Figure C-5. Generic Bridge Rail for Load Case 2, Section 1-1

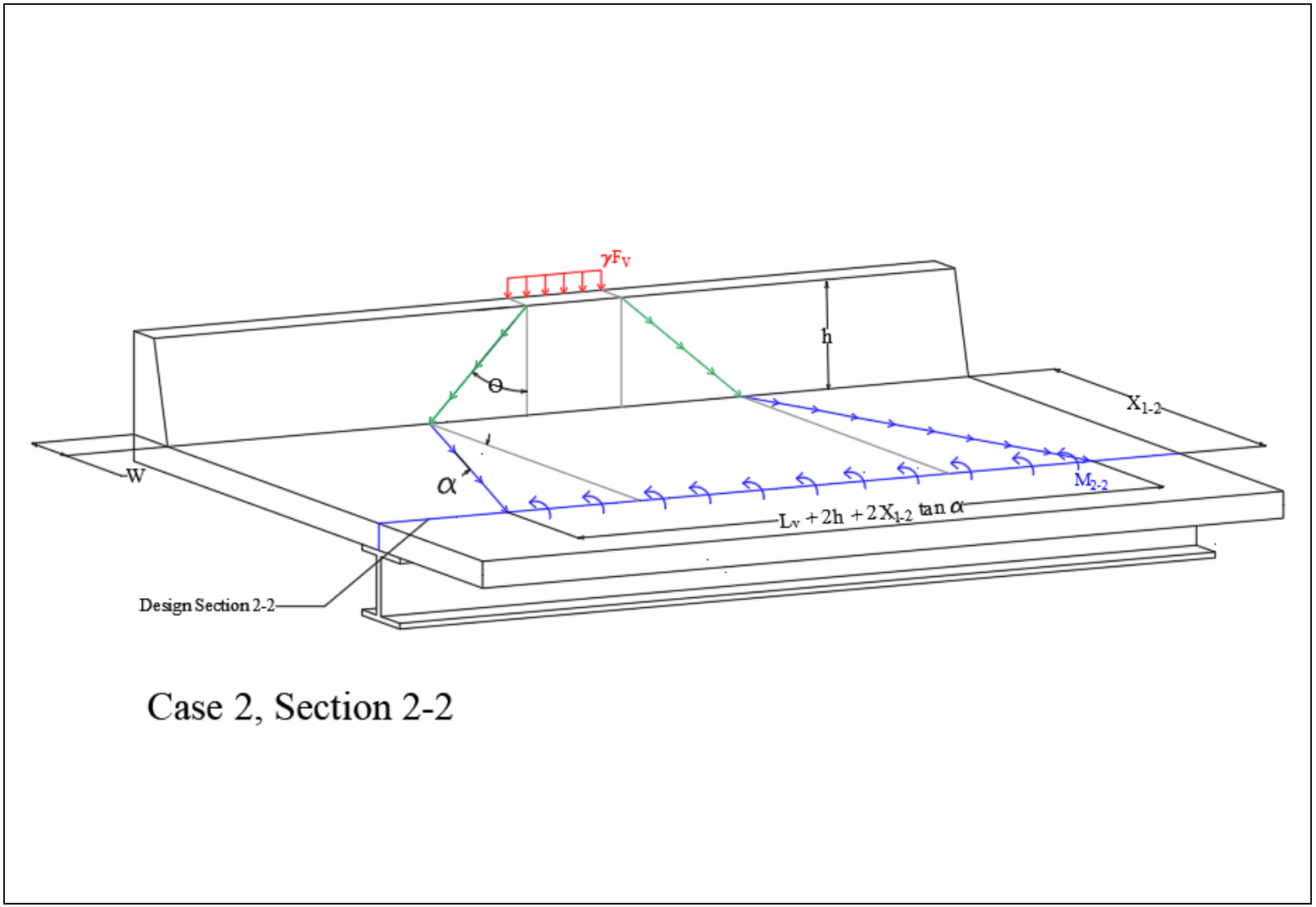

Figure C-6. Generic Bridge Rail for Load Case 2, Section 2-2

Deck Design Case 2 Equations

$$M_{1-1} = \frac{\gamma F_V W}{L_v + 2H} + \gamma\left(M_{barrierweight}\right) + \gamma\left(M_{slabweight}\right) \quad \text{Eq: C-3}$$

$$M_{2-2} = \frac{\gamma F_V (X_{1-2} + W)}{L_c + 2H + 2(X_{1-2})tan\alpha} + \gamma\left(M_{barrierweight}\right) + \gamma\left(M_{slabweight}\right) \quad \text{Eq: C-4}$$

Description of Variables and Design Assumptions

$X_{1\text{-}2}$ is the distance between critical sections 1-1 and 2-2

Slab distribution angle, α, taken as 45°

Barrier distribution angle, θ, taken as 45°

Load factors, γ, taken as 1

Resistance factor, ϕ, taken as 1

F_t taken as 35 kips

H_e taken as 20 in.

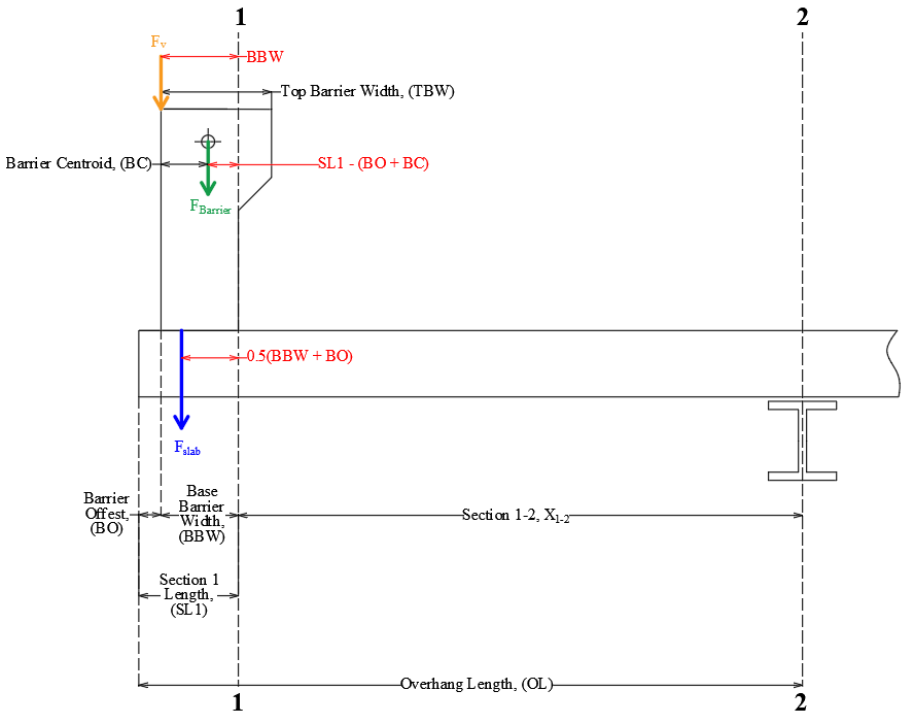

Figure C-7. Side View of Design Case 2, Section 1-1 Impact

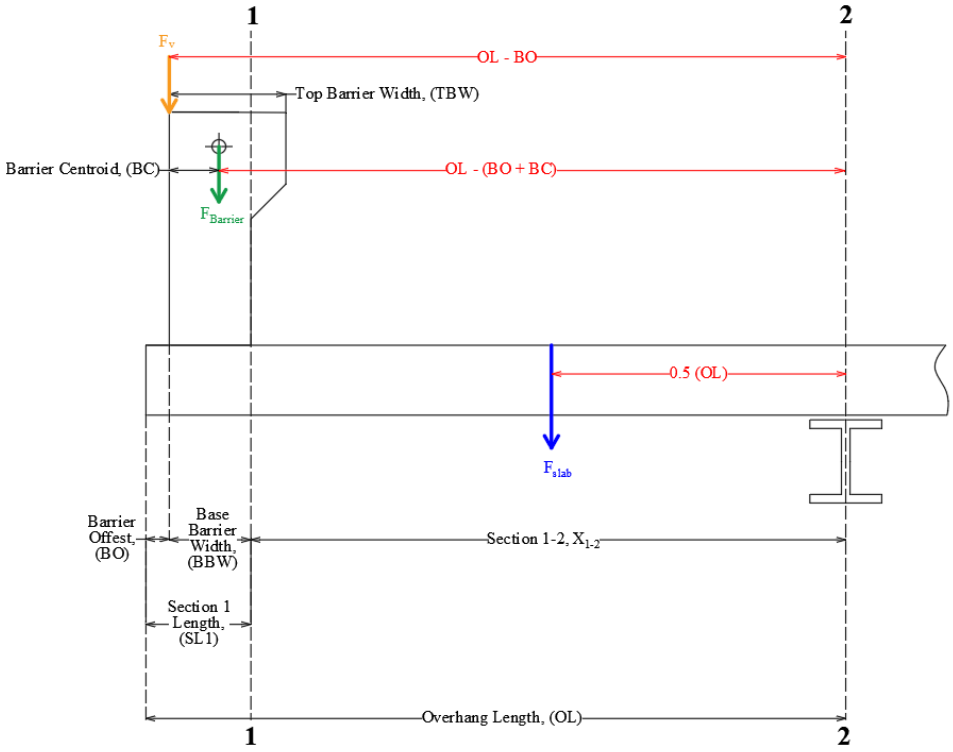

Figure C-8. Side View of Design Case 2, Section 2-2 Impact

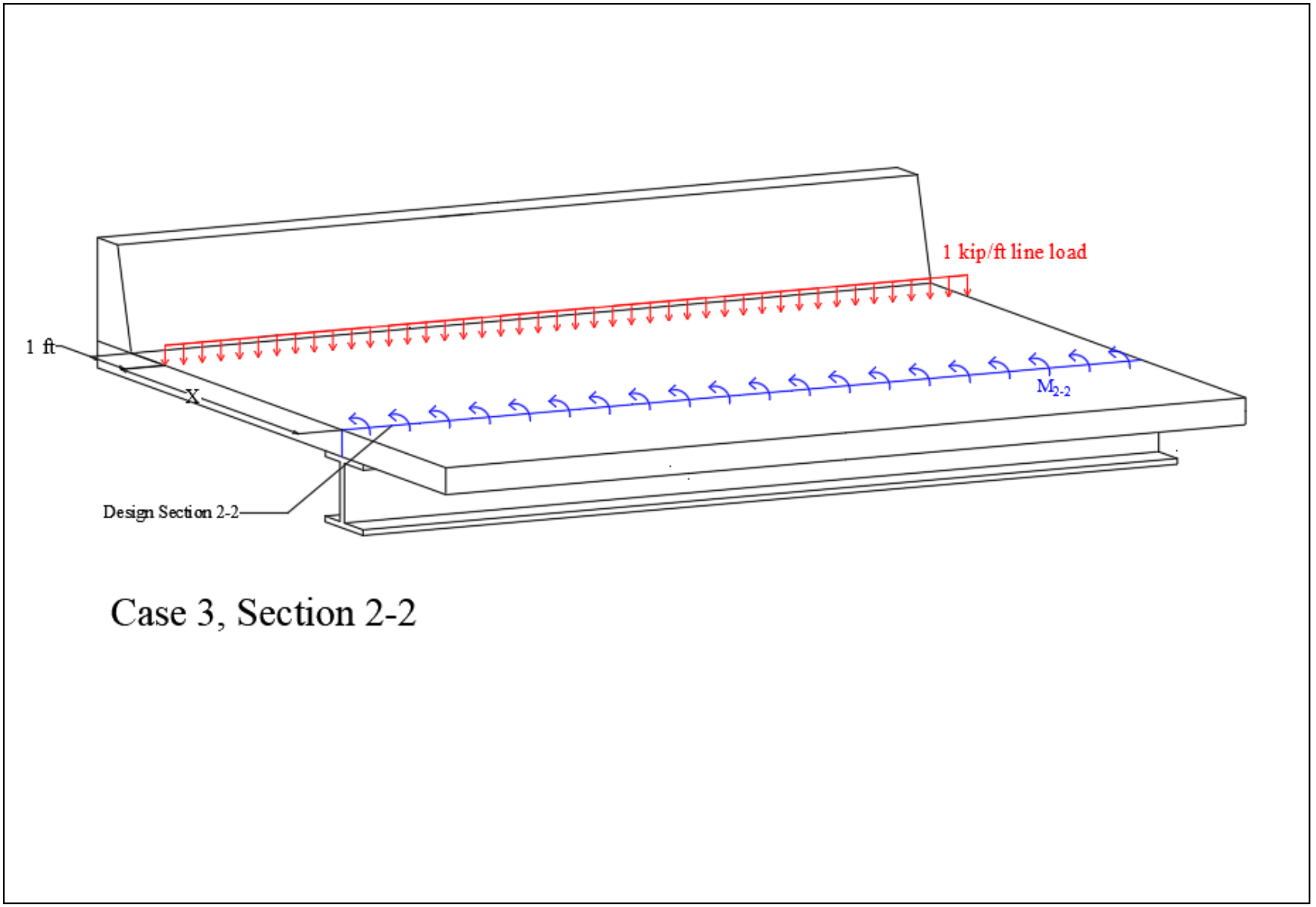

Figure C-9. Generic Bridge Rail for Load Case 3, Section 2-2

Deck Design Case 3 Equation

$$M_{2-2} = (1.75)(I.M.)(1\ kip/ft)(X) + (1.25)M_{barrierweight} + (1.25)M_{slabweight} \qquad \text{Eq: C-5}$$

Description of Variables and Design Assumptions

Load factors, γ, not taken as 1

$\gamma_{\text{1 kip per ft line load}} = 1.75$

$\gamma_{\text{barrierwieght}} = 1.25$

$\gamma_{\text{slabweight}} = 1.25$

I.M. = 1.33

Resistance factor, ϕ, taken as 0.9

X = distance from 1 kip load to section 2-2

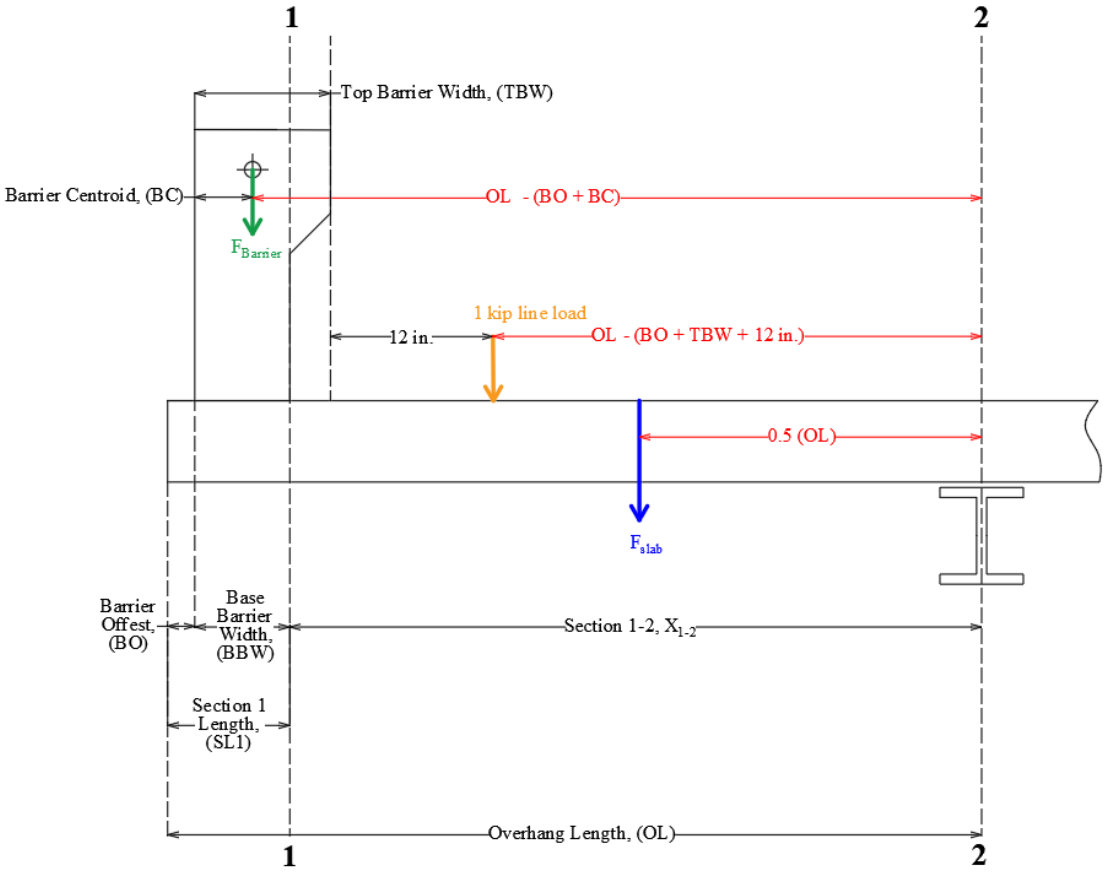

Figure C-10. Side View of Design Case 2, Section 2-2 Live Load

Design Case 3 Wheel Load Design

Typically, Design Case 3 is analyzed with a 1-kip per ft uniform line load placed 1 ft from the base of the bridge rail. However according to AASHTO Section 3.6.1.3.4, if (1) the bridge deck overhang has a cantilever length measuring less than or equal to 6 ft, measured from the centerline of the exterior girder to the deck edge and (2) the bridge being analyzed is considered to be structurally continuous, an alternative method of analysis can be used to assess the bridge rail and deck's adequacy towards Design Case 3 loading scenarios. In this alternative method of analysis, the uniform line load is replaced with (1) two tandem wheels, each weighing 12½ kips and spaced 4 ft apart from one another and (2) a single 16-kip wheel on a HS-25 truck. These two wheel-load scenarios are analyzed independent from one another, and both must result in a deck which can handle either loading. Figure C-11 shows the wheel load configurations for a HS-25 truck and tandem wheel load.

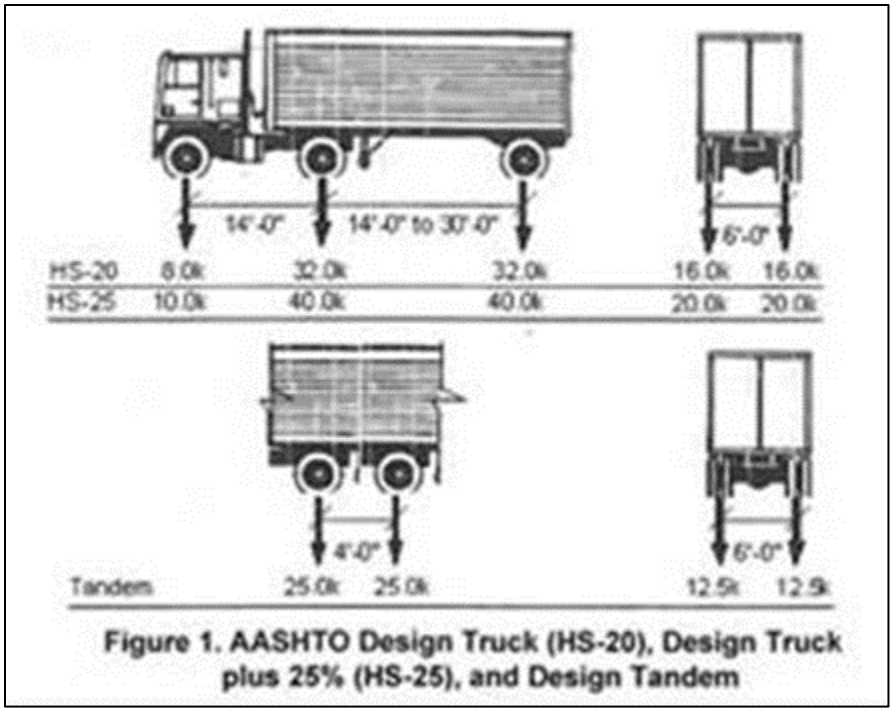

Figure C-11. AASHTO Design HS-25 Truck and Tandem Vehicles

Utilizing wheel loads in place of a uniform line load to assess the strength of the bridge deck and rail was considered for Design Case 3, but the design team decided to analyze the deck and rail configurations using the uniform line load. This decision was made due to the large demands that the wheel loads would inflict on design section 2-2 on the bridge deck overhang, which would lead to overly conservative and unrealistic deck designs. Figure C-12 highlights the large discrepancy in demand developed at section 2-2 when using wheel loading over the uniform line load. This figure depicts a plot of the moment demand versus the X dimension, which is the distance from the centerline of the exterior girder to the location of the uniform line load. As X increases, the discrepancy in demand between the wheel loading at interior and end sections relative to the demand of the uniform line load increases significantly.

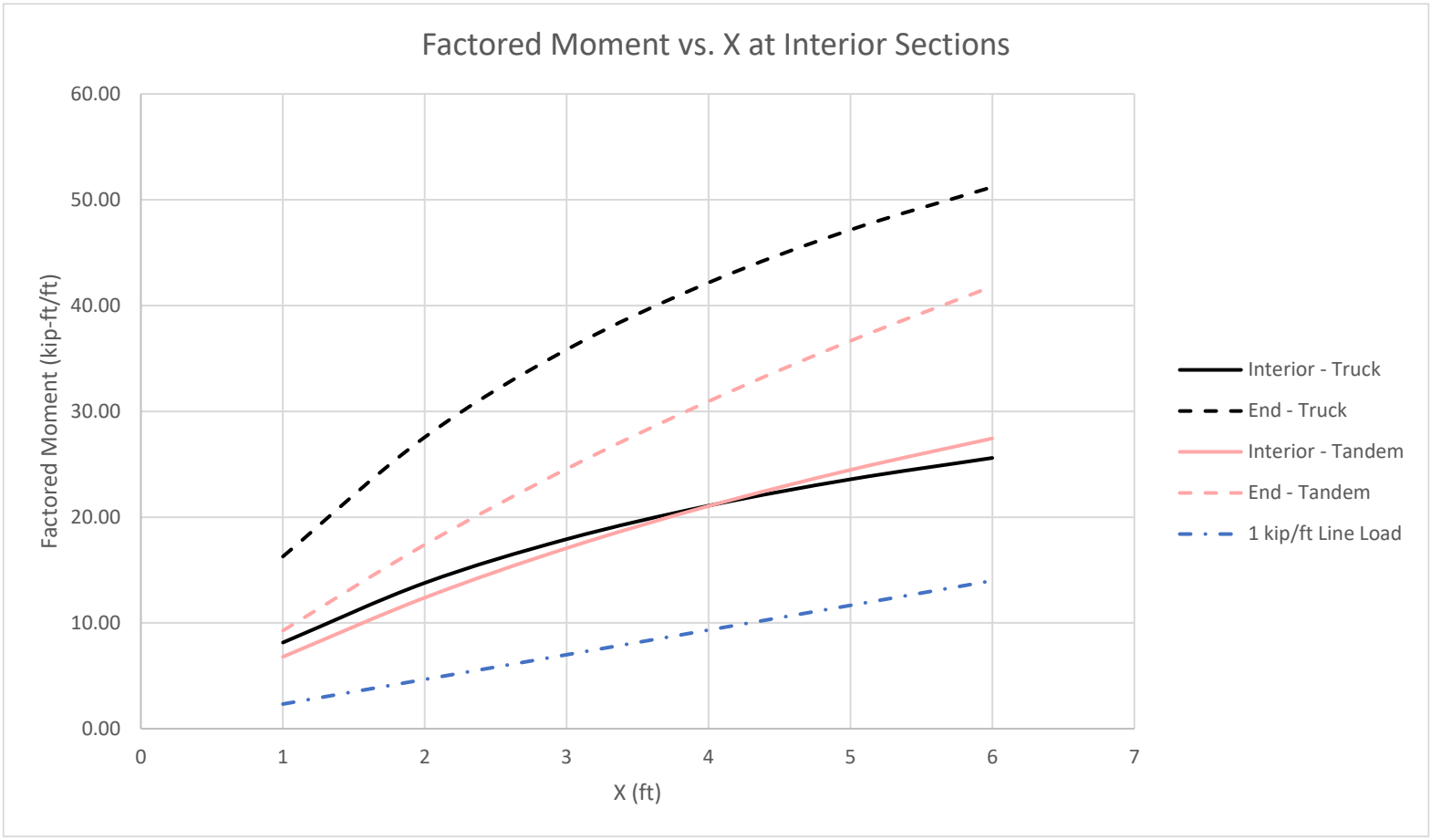

Figure C-12. Factored Moment vs. Design Case 3 Moment Arm

While the alternative wheel loading scenario used to evaluate Design Case 3 was not utilized for this project, the equations used to assess wheel load demands are shown in Equations D-1 through D-6. Under each equation, a brief description of the variables is provided, as well as documentation of the recommended design assumptions. Plan views of the different wheel load scenarios are shown in Figure C-13 and Figure C-13 to clarify where the different wheel loads are placed on the overhang section of the bridge deck and how the load from said wheel loads is distributed to design section 2-2.

Deck Design Case 3 Equations for Interior Truck and Tandem Wheel Loads

$$M_{wheel} = \frac{(X)(Wheel\ Loads)(I.M.)(L.L.)}{Effective\ Slab\ Width} \quad \text{Eq: D-1}$$

$$Effective\ Truck\ Slab\ Width\ (in.) = (45 + 10X) \cdot \frac{1}{12} \quad \text{Eq: D-2}$$

$$Effective\ Tandem\ Slab\ Width\ (in.) = (45 + 10X) \cdot \frac{1}{12} + 4' \quad \text{Eq: D-3}$$

X = Distance from exterior girder to centerline of wheel load(s) in ft

I. M. = Impact Factor = 1.33

L. L. = Live Load Impact Factor = 1.75

Deck Design Case 3 Equations for End Truck and Tandem Wheel Loads

$$M_{wheel} = \frac{(X)(Wheel\ Loads)(I.M.)(L.L.)}{Effective\ Slab\ Width} \quad \text{Eq: D-4}$$

$$Effective\ Truck\ Slab\ Width\ (in.) = \frac{(45+10X)}{2} \cdot \frac{1}{12} \quad \text{Eq: D-5}$$

$$Effective\ Truck\ Slab\ Width\ (in.) = \frac{(45+10X)}{2} \cdot \frac{1}{12} + 4\ ft \quad \text{Eq: D-6}$$

X = Distance from exterior girder centerline to wheel loads(s)in ft

I. M. = 1.33

L. L. = 1.75

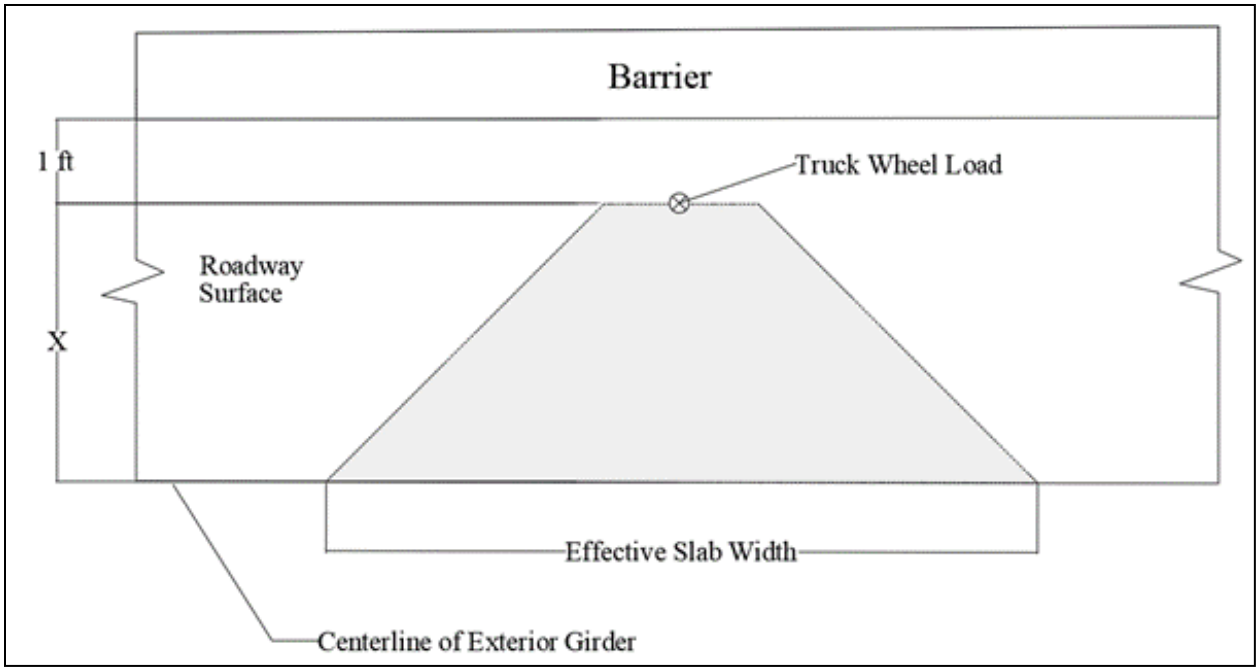

(a) Truck Wheel Load at Interior Section

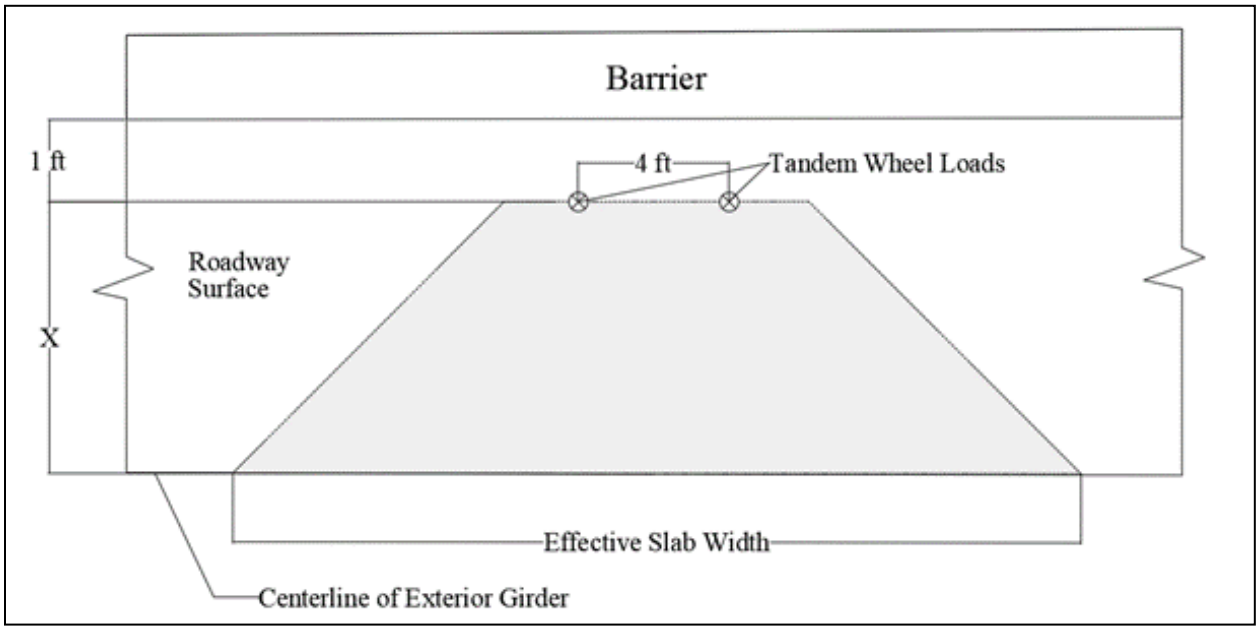

(b) Tandem Wheel Load at Interior Section

Figure C-13. Design Case 3 Wheel Loading at Interior Section

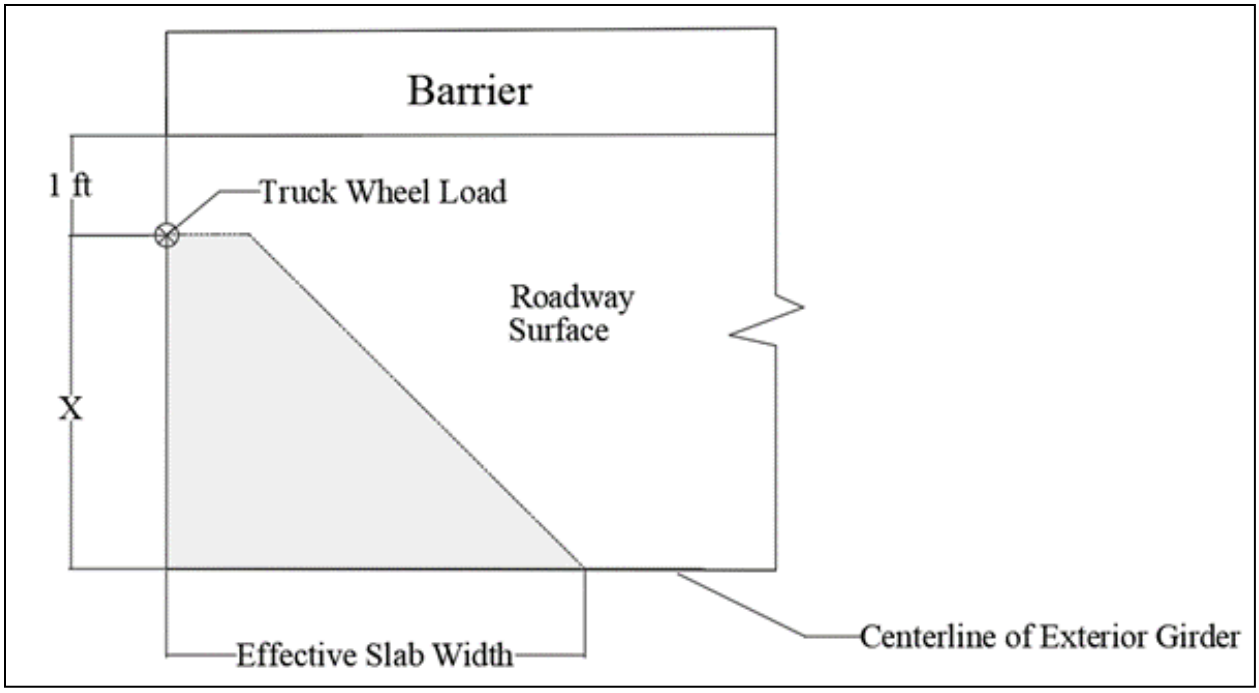

(a) Truck Wheel Load at End Section

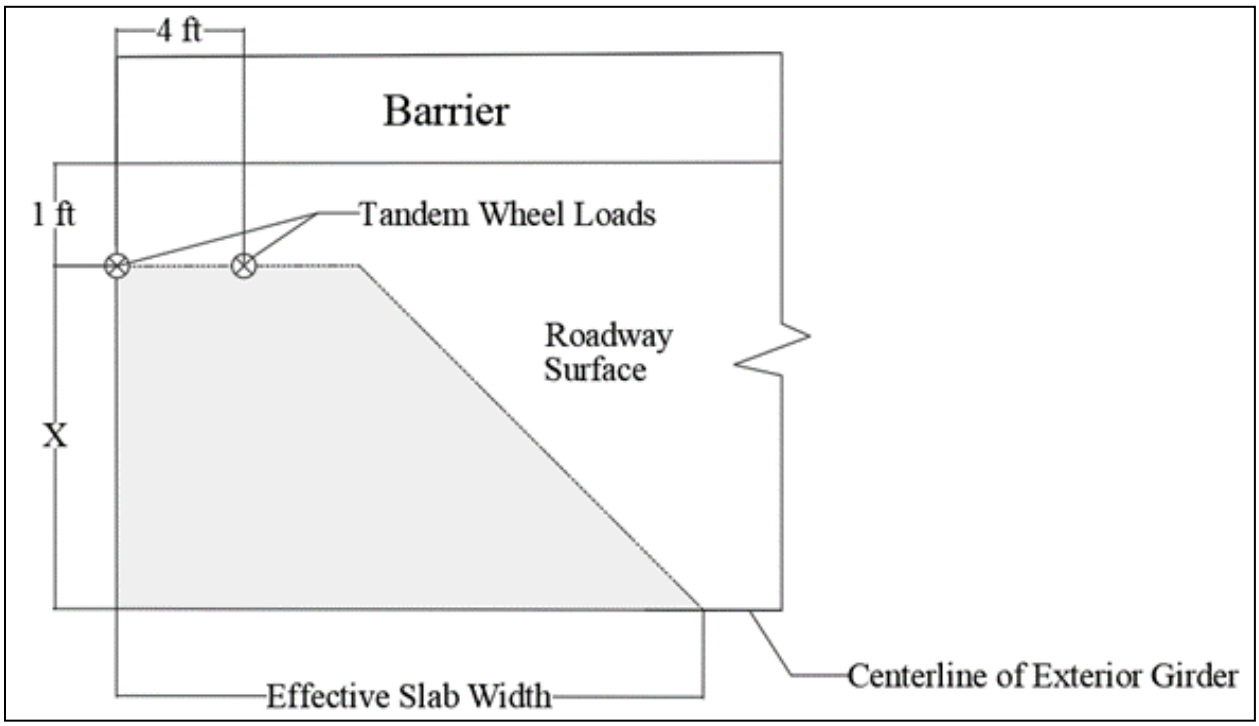

(b) Tandem Wheel Load at End Section

Figure C-14. Design Case 3 Wheel Loading at End Section

END OF DOCUMENT